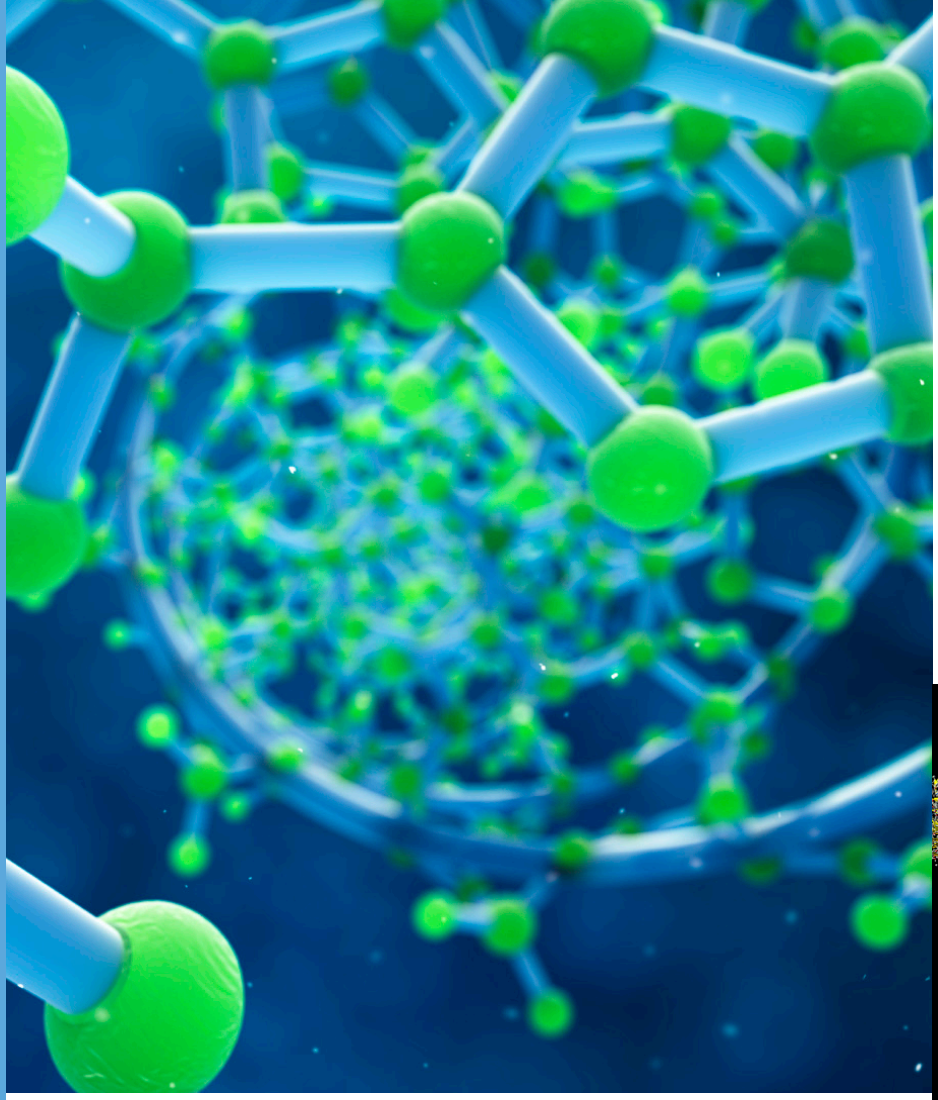

SCIENCE • TECHNOLOGY • RESEARCH HIGHLIGHTS • VISIONS

Dissertation
33

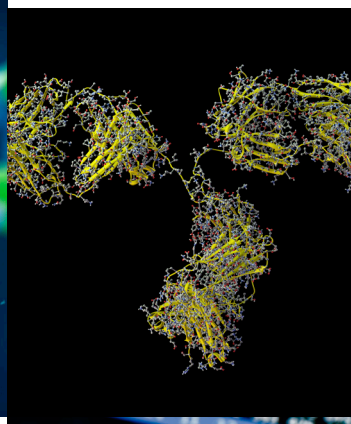

Biofunctionalised surfaces for molecular sensing

Sanna Auer

VTT

VTT SCIENCE 33

Biofunctionalised surfaces for molecular sensing

Sanna Auer

Thesis for the degree of Doctor of Philosophy to be presented with due permission for public examination and criticism in Festia Building, Auditorium Pieni Sali 1, at Tampere University of Technology (Korkeakoulunkatu 8, 33720 Tampere), on the 14th of June, 2013, at 12 noon.

ISBN 978-951-38-8001-9 (Soft back ed.)
ISBN 978-951-38-8002-6 (URL: http://www.vtt.fi/publications/index.jsp)

VTT Science 33

ISSN-L 2242-119X
ISSN 2242-119X (Print)
ISSN 2242-1203 (Online)

JULKAISIJA – UTGIVARE – PUBLISHER

VTT
PL 1000 (Tekniikantie 4 A, Espoo)
02044 VTT
Puh. 020 722 111, faksi 020 722 7001

VTT
PB 1000 (Teknikvägen 4 A, Esbo)
FI-02044 VTT
Tfn +358 20 722 111, telefax +358 20 722 7001

VTT Technical Research Centre of Finland
P.O. Box 1000 (Tekniikantie 4 A, Espoo)
FI-02044 VTT, Finland
Tel. +358 20 722 111, fax + 358 20 722 7001

Kopijyvä Oy, Kuopio 2013

Biofunctionalised surfaces for molecular sensing

Biofunktionalisoidut pinnat molekyylien määrityksessä. **Sanna Auer.**
Espoo 2013. VTT Science 33. 76 p. + app. 46 p.

Abstract

In many application fields, like in biosensors, the sensing biomolecules are immobilized on solid surfaces to enable measuring of very small concentrations of molecules to be analysed. Such application fields are, for example, diagnostics, detection of abused drugs, environmental monitoring of toxins and tissue engineering.

This thesis studies the immobilization of biomolecules (antibodies and Fab'-fragments, avidins and oligonucleotide sequences) on gold surfaces in biosensors. In order to achieve high nanomolar sensitivity even in difficult sample matrices, the effect of the sensing molecule immobilization type and concentration within these biomolecular surfaces were studied in detail. The suitability of these surfaces for neuronal stem cell attachment was also one of the topics. Real-time label-free detection was performed with surface plasmon resonance (SPR). The molecular surfaces in this study were constructed of biomolecules and repellent molecules, which formed self-assembled monolayers on gold. The molecules were immobilized on surfaces via reactive thiol- or disulphide groups. On surfaces assembled of proteins, the non-specific binding was minimized by hydrophilic polymer molecules and on surfaces assembled of oligonucleotides by means of lipoate molecules embedded on the surface in between the biomolecules, respectively.

With these highly sensitive biomolecular surfaces, a nanomolar detection of small sized molecules such as the 3,4-methylenedioxymethamphetamine (MDMA) drug was achieved. MDMA was analysed from a difficult sample matrix of diluted saliva. Improved orientation of surface immobilized Fab'-fragments leading to a higher sensitivity was shown with surfaces constructed of cys-tagged avidins: Fab'-fragments immobilized via thiol-biotinylation to a surface constructed of cys-tagged avidins bound almost ten times the amount of antigen when compared to a conventional surface constructed of non-oriented wild-type avidins. Polymer molecules embedded in between the biomolecules efficiently reduced non-specific binding. Selective neuronal cell attachment was also shown with polymer and neuronal-specific antibody molecules physisorbed on cell culture plates. Only the differentiated neuronal cells attached to surfaces physisorbed with neuronal-specific antibodies, while the non-differentiated neurospheres did not.

Selective surfaces were also developed for oligonucleotide sequences. Lipoate-based molecules efficiently reduced the non-specific binding of proteins and non-complementary DNA. A nanomolar detection range was achieved for single-stranded, breast cancer-specific polymerase chain reaction (PCR) products. First, the shorter single-stranded PCR-products were analysed and a nanomolar detection range was achieved in buffer. In the following study, the DNA-surfaces were

analysed in the presence of diluted serum. Even in diluted serum matrix, nanomolar concentrations of longer single- stranded sequences could be analysed due to the efficient blocking of non-specific binding of serum proteins.

It was found that sensitive detection surfaces for biomolecular recognition can be achieved, when optimal function of the biomolecules is ensured by immobilizing the molecules on surfaces in an oriented manner towards the analyte. Efficient reduction of non-specific binding is also important in reaching highly sensitive label-free detection. The surfaces were also found to be effective in selective neuronal stem cell attachment.

Keywords antibody, Fab´-fragment, cysteine tagged avidin, neuronal cells, DNA hybridisation, gold surface, immobilisation, surface plasmon resonance, non-specific binding

Biofunktionalisoidut pinnat molekyylien määrityksessä

Biofunctionalised surfaces for molecular sensing. **Sanna Auer.**
Espoo 2013. VTT Science 33. 76 s. + liitt. 46 s.

Tiivistelmä

Monilla sovellusalueilla, kuten bioantureissa, tietylle analyytille herkät biomolekyylit kiinnitetään kiinteälle pinnalle, mikä mahdollistaa hyvin pienten analyyttipitoisuuksien määrittämisen. Tällaisia sovellusalueita ovat esimerkiksi sairauksien merkkiaineiden määritys, huumausaineiden tai ympäristömyrkkyjen määritys ja kudosteknologia.

Tämä väitöskirja käsittelee biomolekyylien (vasta-aineiden ja Fab´-fragmenttien, avidiinien ja deoksiribonukleiinihappo (DNA) -koettimien) kiinnittämistä kultapinnoille bioantureissa. Tunnistavien molekyylien kiinnittämistapaa ja pitoisuutta biomolekulaarisilla pinnoilla tutkittiin yksityiskohtaisesti nanomolaarisen herkkyyden saavuttamiseksi myös vaikeista lähtömateriaaleista. Lisäksi tutkittiin, miten nämä pinnat soveltuvat kantasoluista erilaistettujen hermosolujen tartuttamiseen. Reaaliaikainen määritys ilman leima-aineita tehtiin pintaplasmoniresonanssin (SPR) avulla. Tutkimuksessa käytetyt itseasettuvat kalvot muodostettiin biomolekyyleistä ja hylkivistä molekyyleistä kultapinnoille. Molekyylit kiinnitettiin pinnoille tioli- tai disulfidiryhmien kautta. Proteiinipinnoilla epäspesifistä sitoutumista vähennettiin hydrofiilisten polymeerien avulla ja DNA-koetinpinnoilla vastaavasti lipoaattipohjaisten molekyylien avulla, jotka oli asetettu pinnoilla biomolekyylien väliin.

Biomolekulaaristen pintarakenteiden avulla pystyttiin mittaamaan myös pienikokoinen 3,4-dimetyleenidioksimetyyliamfetamiini (MDMA) -huumausaine nanomolaarisessa pitoisuudessa. MDMA pystyttiin määrittämään myös laimennetusta sylkinäytteestä. Kysteiinimuokattujen avidiinipintojen avulla pystyttiin parantamaan Fab´-fragmenttien orientaatiota pinnoilla, mikä johti tavoiteltuihin, korkeampiin antigeenivasteisiin. Tioli-ryhmiin biotinyloituja Fab´-fragmentteja pystyttiin kiinnittämään kysteiinimuokattuihin avidiinipintoihin kymmenkertainen määrä verrattuna villityypin ei-orientoituihin avidiinipintoihin. Biomolekyylien väliin pinnoille kiinnitetyt polymeerimolekyylit ehkäisivät tehokkaasti epäspesifistä sitoutumista. Kun hermosolujen kasvatuslevyille kiinnitettiin polymeeriä ja hermosoluille spesifisiä vasta-ainemolekyylejä, levyille saatiin tarttumaan valikoidusti vain kantasoluista erilaistuneita hermosoluja. Kantasoluista erilaistumattomat solut eivät kiinnittyneet vasta-ainepolymeeripinnoille.

Valikoivia pintoja kehitettiin myös DNA-koettimille. Proteiinien ja ei-pariutuvan DNA:n epäspesifinen sitoutuminen DNA-koetinpinnoille pystyttiin ehkäisemään tehokkaasti lipoaattipohjaisten molekyylien avulla. Yksijuosteiset rintasyöpäspesifiset DNA-juosteet pystyttiin tunnistamaan nanomolaarisella herkkyydellä. Ensin tutkittiin lyhyiden yksijuosteisten DNA-näytteiden tunnistusta puskuriliuoksessa saavuttaen nanomolaarinen herkkyys. Seuraavaksi DNA-pintojen toi-

minnallisuutta tutkittiin seerumiin laimennetuilla näytteillä. Myös pidempiä yksijuosteisia DNA-näytteitä pystyttiin määrittämään nanomolaarisina pitoisuuksina seerumilaimennoksesta, koska lipoaattipohjaiset molekyylit estivät tehokkaasti seerumin proteiinien epäspesifisen sitoutumisen pinnoille.

Biomolekyylien määritykseen pystytään tekemään herkästi tunnistavia pintoja, kunhan biomolekyylien optimaalinen toiminta varmistetaan kiinnittämällä biomolekyylit pinnoille siten, että analyytin tunnistavat osat ovat orientoituneet analyyttiä kohden. Myös epäspesifisen sitoutumisen estäminen pinnoille on tärkeää korkean herkkyyden saavuttamiseksi leimavapaissa mittauksissa. Vasta-aine-polymeeripinnat todettiin hyvin toiminnallisiksi myös haluttaessa tartuttaa pinnoille valikoiden vain hermosoluja.

Avainsanat antibody, Fab´-fragment, cysteine tagged avidin, neuronal cells, DNA hybridisation, gold surface, immobilisation, surface plasmon resonance, non-specific binding

Preface

The work described in this thesis was carried out at VTT Technical Research Centre of Finland in the Molecular Sensors team between 2007 and 2011. Vice President R&D Sensors and wireless devices Dr. Arto Maaninen and Technology Manager Dr. Timo Varpula are thanked for providing excellent working facilities and for supporting the finalization of this thesis. Team leader Dr. Kirsi Tappura is gratefully acknowledged for leading the research team. Financial support from the Academy of Finland (OriMab), EU (FP6 program Biognosis No. 016467), Nordic Innovation Centre (Intoxsign, 07135) and VTT is gratefully acknowledged.

I would like to express my deepest gratitude to my supervisor, Dr. Inger Vikholm-Lundin. I thank her for being my mentor, for always finding the encouraging words and for showing me the road ahead. I also wish to thank all my co-authors for their contribution to this work.

Professor Matti Karp is thanked for supporting this thesis. Professors Tero Soukka and Jouko Peltonen are thanked for their careful pre-examination of the thesis and their insightful comments for improving it.

All the members of the Molecular Sensors team are thanked for providing a pleasant working atmosphere during these years. Dr Martin Albers is gratefully acknowledged for his helpful comments on the thesis. Dr. Tony Munter, Hannu Välimäki, Dr. Jan Saijets, Timo Flyktman and Hannu Helle are thanked for their friendship, support and for so many refreshing discussions. Other colleagues from VTT Materials Science are also thanked for their kindness and support. I want to thank all my former group leaders, members, friends and colleagues, especially in Protein Engineering team, but also other closely related teams at VTT Biotechnology; I have so many good memories from those times, and I think the scientist in me started to evolve during those years.

My beloved husband Jouni is thanked for sharing his life with a scientist and for encouraging me, for helping me find the time to concentrate on the writing of this thesis during the recent months, for all possible IT-support over these decades, for making it possible to finalize this doctoral-degree despite our large number of very much loved children. I want to thank my sons Pyry and Aarni for their never-ending interest in certain aspects of mommy´s work and all the nice discussions that have been very educating, especially to me. My twin daughters Anna and Ella have otherwise just kept me very busy, but so immensely happy outside the work! I want to thank my parents – especially my father´s interest towards this work has been a delight. Finally, I would like to encourage my children to explore the wonders of nature and remember always to cherish them.

Academic dissertation

Supervisor	Dr. Inger Vikholm-Lundin VTT Tampere, Finland
Reviewers	Professor Tero Soukka Department of Biotechnology University of Turku, Finland
	Professor Jouko Peltonen Laboratory of Physical Chemistry Åbo Akademi University Turku, Finland
Opponent	Professor Tero Soukka Department of Biotechnology University of Turku, Finland
	Docent Alice Ylikoski PerkinElmer Wallac Turku, Finland

List of publications

This thesis is based on the following original publications, which are referred to in the text by Roman numerals I–V. The publications are included in this thesis as appendices in the printed version.

I Auer, S., Lappalainen, R.S., Skottman, H., Suuronen, R., Narkilahti, S. and Vikholm-Lundin, I. (2010). An antibody surface for selective neuronal cell attachment. Journal of Neuroscience Methods 186: 72–76.

II Vikholm-Lundin, I., Auer, S. and Hellgren, A.-C. (2011). Detection of 3,4-methylenedioxymethamphetamine (MDMA, ecstasy) by displacement of antibodies. Sensors and Actuators B: Chemical 156: 28–34.

III Vikholm-Lundin, I., Auer, S., Paakkunainen, M., Määttä, J.A.E., Munter, T., Leppiniemi, J., Hytönen, V.P. and Tappura, K. (2012). Cysteine-tagged chimeric avidin forms high binding capacity layers directly on gold. Sensors and Actuators B: Chemical 171–172: 440–448.

IV Vikholm-Lundin, I., Auer, S., Munter, T., Fiegl, H. and Apostolidou, S. (2009). Hybridization of binary monolayers of single stranded oligonucleotides and short blocking molecules. Surface Science 603: 620–624.

V Auer, S., Nirschl, M. Schreiter, M. and Vikholm-Lundin, I. (2011). Detection of DNA hybridisation in a diluted serum matrix by surface plasmon resonance and film bulk acoustic resonators. Analytical and Bioanalytical Chemistry 400: 1387–1396.

Author's contributions

Publication I

The author contributed to the planning of the work and conducted the laboratory work on the surfaces for SPR measurements. The author had the main responsibility with R. Lappalainen in writing the publication.

Publication II

The author contributed to the planning of the work, conducted the laboratory work with antibodies, surface functionalisation and SPR measurements. The author participated in writing the publication.

Publication III

The author contributed to the planning of the work and conducted the laboratory work on the biotinylated antibody fragments. The author participated in writing the publication.

Publication IV

The author contributed to the planning of the work, conducted the laboratory work on surface functionalisation and SPR measurements and participated in writing the publication.

Publication V

The author contributed to the planning of the work, conducted the laboratory work on surface functionalisation and SPR measurements and had the main responsibility in writing the publication.

Contents

Appendix V of this publication is not included in the PDF version.
Please order the printed version to get the complete publication.
(http://www.vtt.fi/publications/index.jsp).

List of symbols

2-MEA	Cysteamine-HCl
BAEC	Bovine aortic endothelial cell
CDI	Carbodiimide
C_H	Constant heavy domain of an immunoglobulin molecule
ChiAvd-Cys	Engineered chimeric avidin molecule with C-terminal cysteine-tags
CM	Carboxymethyldextran
Da	Dalton; commonly used unit of a protein mass. 1 Dalton corresponds to a mass of a hydrogen-atom (1.01 g/mol).
DMT-S-S-ssDNA	Referring to thiol-modified oligonucleotides with the thiol-protective dimethoxy-trityl (DMT) -groups from the oligonucleotide synthesis
DNA	Deoxyribonucleic acid
DTT	Dithiothreitol
EDC	1-ethyl-3-(3-dimethylaminopropyl)-carbodiimide
ECM	Extracellular matrix
EDTA	ethylenediaminetetraacetic acid
Fab'	Fragment antigen binding: antigen recognising –fragment (V_HC_H and V_LC_L domains) of an immunoglobulin molecule
FBAR	Film bulk acoustic resonator
Fc	Fragment crystallisable: fragment (C_H2 and C_H3 domains of both heavy chains) of an immunoglobulin molecule
GFP	Green fluorescent protein
GST	Glutathione *S*-transferase
hESC	Human embryonic stem cell
hIgG	Human immunoglobulin subclass G molecule
IDA	Iminodiacetic acid
IgG	Immunoglobulin subclass G molecule
K_A	Affinity constant, unit M^{-1}, is the measure of the affinity of the binding between two molecules – the higher the number, the tighter the binding

K_D	Dissociation constant, unit M, the smaller the number, the tighter the binding and thus lower dissociation.
Lipa-DEA	N,N-bis(2-hydroxyethyl)-α-lipoamide
MDMA	3,4-methylenedioxymethamphetamine, ecstasy
Mw	Molecular weight
NCAM	Neuronal cell adhesion molecule
NHS	N-hydroxysuccinimide
NSB	Non-specific binding
NTA	Nitrilotriacetic acid
OEG	Oligo(ethylene glycol)
PBS	Phosphate buffered saline
PCR	Polymerase chain reaction
PEG	Poly(ethylene glycol)
pTHMMAA	N-[tris(hydroxymethyl)methyl]-acrylamide
QCM	Quartz crystal microbalance
RI	Refractive index
RU	Resonance units
SAM	Self-assembled monolayer
SDS	Sodium dodecyl sulphate
SDS-PAGE	Sodium dodecyl sulphate polyacrylamide gel electrophoresis
SH-ssDNA	Referring to single-stranded oligonucleotides with a free thiol-(-SH) group
SPR	Surface plasmon resonance
S-S	Disulphide-bridge
ssDNA	single-stranded DNA
ssPCR product	single stranded polymerase chain reaction DNA product
wt-Avd	Wild type avidin molecule

.

1. Introduction

According to Turner (Turner et al. 1987), the definition of a biosensor is: “a compact analytical device incorporating a biological or biologically-derived sensing element either integrated within or intimately associated with a physicochemical transducer. The usual aim of a biosensor is to produce either discrete or continuous digital electronic signals which are proportional to a single analyte or a related group of analytes” (Fig. 1). Ideally, biosensors as devices should be portable, rapid and easily and repeatedly usable simple devices not requiring extensive training of the end-user. Interest in the development and research of such sensors has grown in many different research areas, such as the environmental, chemical and medical sciences as well as the military field (Homola 2003, Ronkainen et al. 2010).

Analysis of blood glucose is one of the best known historical and commercial examples of a biosensor based on near electrode-immobilised glucose oxidase enzymes converting glucose to gluconic acid and consuming oxygen in the reaction. Oxygen consumption can be measured by a biosensor and converted into an electrical signal related to the amount of glucose in the blood (Clark and Lyons 1962, Wang 2000). Biosensors can also be used, for example, in the detection of drug abuse, environmental contaminants, disease genes and so on. However, the optimal function of the biomolecules and sensitivity of the sensors are the questions faced in all research areas involving biosensors. Naturally, the cost of the end product and ease of operation by the end-user are also among the factors to be considered. Studies with biosensors are very challenging, combining many different areas of science: chemistry, biology, physics and engineering. However, at their best, biosensors are already important every day tools in modern societies, as exemplified by diabetic patients.

The aim of this thesis has been the development of biomolecular surfaces for sensitive detection of different sized molecules. The performance of the surfaces was also verified at nanomolar detection of analytes in difficult sample matrixes of diluted saliva and serum.

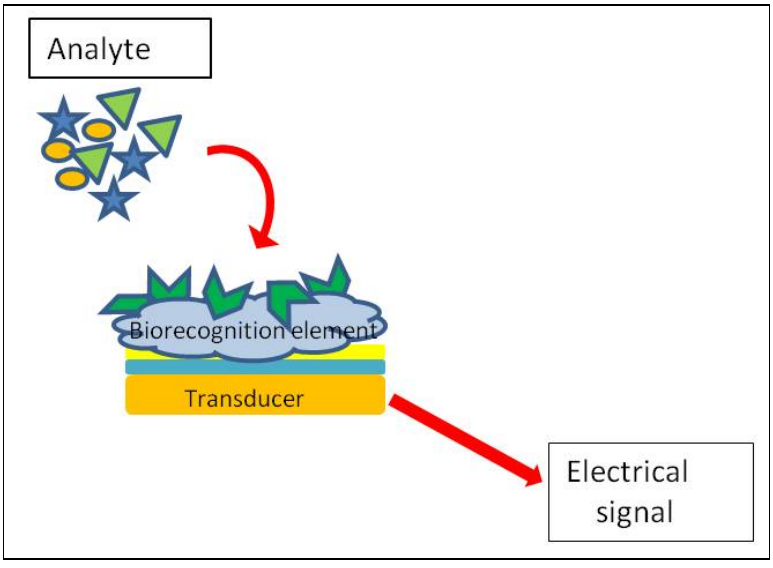

Figure 1. A schematic presentation of a biosensor. Analyte molecules from the sample solution bind to the surface-attached antibody/receptor/DNA-probe molecules (biorecognition element), causing a physico-chemical change, that is transformed into an electrical signal by a transducer.

1.1 The main components of a biosensor

1.1.1 Signal detection

As shown in Fig. 1, the event of analyte binding on the biorecognition element on the sensor surface causes a physicochemical change recognised by the transducer. This measured signal depends on the detection method, and can for example be a change in the refractive index at the surface, as in surface plasmon resonance (SPR). In this thesis, the detection method has been optical SPR, but other detection methods used in biosensors are, for example, electrochemical detection, thermal detection and detection of the change in the resonance frequency (Homola et al. 1999, Ronkainen et al. 2010). Electrochemical detectors can be further devided to conductimetric, amperometric and potentiometric detectors depending on the parameter measured (Ronkainen et al. 2010). Also in optical detectors the optical changes following the analyte interaction can be divided further, depending on whether the detection is based either in a change in the absorbance, emission, polarization, or for example luminescence decay time (Borisov and Wolfbeis 2008). However, the sensitivity in most optical sensors is generally low and thus detection with many of those is based on using molecular labels enhancing the detection signal. Examples of such labelled optical sensors are fluorescence and luminescence detection, which are both very sensitive techniques reaching nano-

molar sensitivity (Borisov and Wolfbeis 2008). Labelling of the biological molecules can, however, modify both the structure of those molecules as well as affect to their function (Cooper 2002, Vashist 2012). There is also other label-free, yet still sensitive, measurement techniques apart from SPR available. These are quartz crystal microbalance (QCM) and film bulk acoustic resonators (FBAR), which both also detect a change in a surface mass, but through a decrease in the resonance frequency. QCM has also been widely used in studies of biomolecular surfaces, but the drawback with QCM is the sensitivity to the visco-elastic properties of the sample, which can be problematic with biomolecules requiring the water-surrounded environment (Katardjiev and Yantchev 2012). On the other hand, QCM can be used also for measuring of larger molecular assemblies that cannot be measured with SPR due to the decay of the SPR evanescent wave, as discussed below. FBAR is a novel, sensitive acoustic technique and might have a promise for wider use in biosensors (Wingqvist et al. 2009). FBARs have a higher operating frequency and smaller volumes compared to QCM and are thus expected to result in higher sensitivity. Low cost mass fabrication and possibility to integrate electronics make FBARs even more appealing new sensor technology (Wingqvist et al. 2009, Wingqvist 2010). The major challenge with all of these three non-labelled techniques is the sensitivity also to the non-specific binding, to which especially the functionalisation of the sensing layers offers solutions.

1.1.2 Layers in biosensors enabling biorecognition

In most detection types the first layer in a biosensor build on top of the transducer is commonly a noble metal, on which the molecules will be assembled to (Ulman 1996). Gold is a standard noble metal in biosensors for many reasons: it is readily available in pure form; it is straightforward to prepare thin films of gold via vapour deposition (sputtering), and it is also a relatively inert metal: it does not react strongly with atmospheric oxygen or with most chemicals (Liedberg et al. 1983, Willander and Al-Hilli 2009). The non-toxicity of gold is also a major benefit when performing studies, especially with cells or biomolecules.

The subsequent layer built on the metal surface comprises the actual sensing molecules, or linking molecules anchoring the sensing molecules. The sensing surfaces are commonly constructed by self-assembly as mixed self-assembled monolayers (SAMs) of biological detecting molecules and molecules that make the surfaces resistant to non-specific binding (Ulman 1996, Love et al. 2005). The molecules minimizing non-specific interactions can be embedded in between the sensing molecules, or can be attached to the first layer via chemical linking groups. In a biosensor, the sensing molecules can be enzymes, antibodies, DNA-probes or even whole cells (Turner et al. 1987). In this thesis, we have studied antibodies and Fab´-fragments and DNA-probes assembled on gold-surfaces.

2. SPR as a measurement technology

SPR is a technique, where the changes of refractive index (RI) are measured at the thin metal-air/water interface with extremely high sensitivity (Otto 1968, Kretschmann and Raether 1971). The most commonly used SPR configuration is the Kretschmann configuration, which employs a thin metal film deposited on glass, which is in optical contact with a prism (Fig. 2). A surface plasmon is a surface charge density wave at a metal surface (Liedberg et al. 1983). "Under conditions of total internal reflection, light incident on the reflecting interface leaks an electric field intensity called an *evanescent wave field* across the interface into the medium of lower refractive index, without actually losing net energy. At a certain combination of angle of incidence and energy (wavelength), the incident light excites plasmons (electron charge density waves) in the gold film. As a result, a characteristic absorption of energy via the evanescent wave field occurs and SPR is seen as a drop in the intensity of the reflected light" (Biacore sensor surface handbook 2008).

In practise, when analyte molecules from the liquid flowing above are bound onto the receptor molecules attached to the sensor gold surface, the binding causes a change in the refractive index at the metal-water interface. This binding is analysed as a change in the SPR resonant angle of the reflected light collected at the optical detection unit. This SPR angle change is proportional to the mass bound onto the surface: the bigger the shift in the resonant angle, the more mass is bound onto the surface and thus a higher resonance signal is generated (Liedberg et al. 1983, Homola et al. 1999, Cooper 2002, Dostalek et al. 2006) (Fig. 2). However, the detection with SPR is limited to a thin region extending to 100–200 nm from the surface, where the electromagnetic field of the reflected light causes an evanescent wave (Liedberg et al. 1983). RI changes beyond this distance, e.g. large molecular assemblies or cells, can thus not be detected by SPR. The most suitable metal for SPR is silver, but in practical biosensor devices the more inert and less toxic gold is commonly used (Homola et al. 1999).

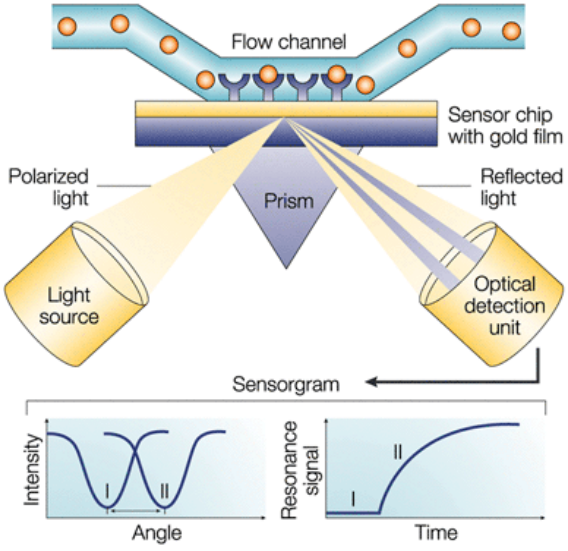

Figure 2. The measuring principle of an SPR biosensor (Kretschmann configuration). The receptor molecules bound onto the sensor surface bind the analyte molecules from the liquid flowing above. This binding causes a change in the refractive index at the metal-water interface, which is analysed as a change in the SPR resonant angle of the reflected light collected at the optical detection unit. This SPR angle change is proportional to the mass bound on the surface; the bigger the shift in the angle (the shift from I to II in the intensity of the angle–curves), the more mass bound on the surface and the higher the resonance signal (resonance signal versus time curve) as shown by the curves in the lower part of the Figure. Image adapted from Cooper 2002.

The major benefits of SPR are a real-time and a direct measurement of the binding events very sensitively without labels. The commercialized SPR sensors, such as Biacore, based on prism coupling have a mass surface density detection limit around 1 pg/mm^2 (Fan et al. 2008, Biacore 2013). SPR sensors are also a generic platform that can be transformed to measure in principle of any desired analyte, when just a specific receptor can be anchored onto the sensor surface. SPR sensors are, however, very sensitive to non-specific binding on the surface. Sample temperature and uneven composition can also cause false changes in the refractive index, leading to misinterpreted signals (Homola 2003). Apart from an accurate amount of the bound substance on the surface in real time, SPR is often used for determining the kinetic and binding constants of antibodies among other biological recognition molecules (Homola et al. 1999, Cooper 2002).

2.1 Binding curves

As is illustrated in Fig. 3, the first phase in the target analyte binding is association phase and in optimal circumstances (concentration, temperature, buffer composition etc.) this phase is fast, and a linear increase in the binding curve can be observed (Homola 2003). In time, the binding reaches equilibrium, as all the accessible binding sites on the surface are occupied, and the binding curve reaches a plateau. This phase is called an equilibrium phase and from this phase the total number of the surface bound molecules can be calculated. With the Biacore SPR instruments 10 resonance units (RU) correspond to a surface coverage of 1 ng/cm^2 (Stenberg et al. 1991, Di Primo and Lebars 2007). Even though binding seems to reach a plateau and equilibrium, the sensor surface is however a dynamic system meaning that there is constantly molecules binding to and dissociating from the surface, depending on the affinity constants and also other external factors (concentration, temperature, buffer composition etc.) affecting to the equilibrium phase of the system. Due to this, as well as sensitivity of SPR, the SPR binding curves do not generally reach a true equilibrium and a plateau within the practical measurement times (5–60 min).

When the surface is washed with a buffer, the dissociation of the molecules from the surface becomes more pronounced. This phase is called as dissociation phase. The equilibrium stage provides information on the affinity of the analyte-ligand interaction, while from the association and dissociation phases, kinetic data (association and dissociation reactions rate constants) can be calculated (Cooper 2002, Homola 2008). In many cases, the surfaces can also be regenerated (regeneration phase) with, for example, a change of pH (with antibodies to very acidic conditions, like pH 2 and with DNA to very basic pH, like 11–12) or an increase in the salt concentration or with surfactants (sodium dodecyl sulphate, SDS). The regeneration conditions are, however, very dependent on the molecules on the surface and how those tolerate these shortly denaturing conditions, causing the total dissociation of the bound molecules, and also how the target molecules on the surface then retain the original and fully functional condition after the regeneration pulse (Cooper 2002, Homola 2008).

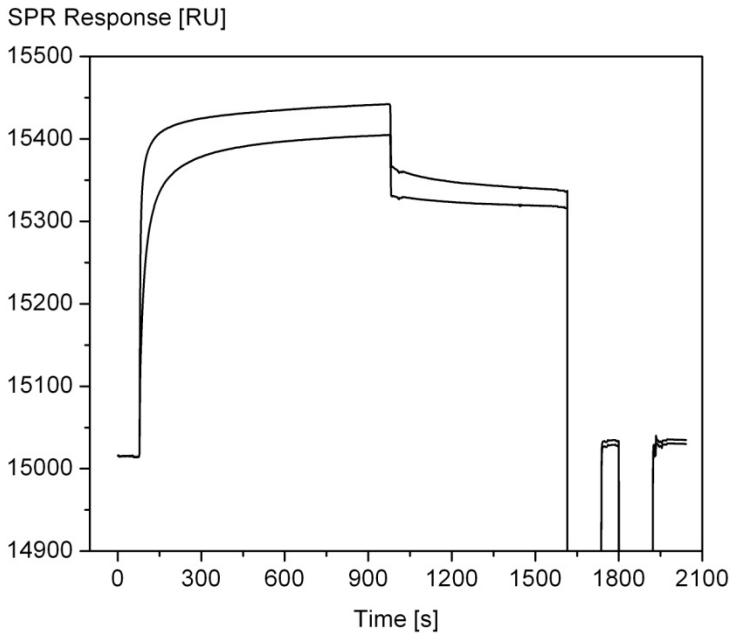

Figure 3. A typical SPR binding curve showing the association (100–1000 s) equilibrium (400–1000 s), dissociation (1000–1600 s) and regeneration (1600–2000 s) phases of the binding. Image modified from Publication V.

The ideal and most straightforward binding situation would be a homogenous binary interaction, where one analyte species interacts with one ligand (Biatechnology handbook 1998). However, in practice the binding situations are seldom ideal, but face heterogeneity, which can arise from several reasons. The ligand and analyte samples can contain polymorphic variants of the molecules having different binding characteristics. Co-operative effects or steric hindrance may complicate the binding reactions and binding kinetics might be interfered due to the impurities in the samples. The immobilization of the ligand is also crucial – if there is variation in ligand presentation on the surface, this might affect to the kinetic characteristics of the binding (Biatechnology handbook 1998, Cooper 2002, Rusmini et al. 2007).

2.2 Assay formats

The most frequently used assay formats in SPR biosensors are direct detection, sandwich assay and inhibition assay (Homola 2003). Detection of medium-to large-sized molecules (> 5 000 Da) is generally done by measuring the analyte straight from the liquid via, for example, antibodies, or fragments of those attached to the surface (Bonroy et al. 2006). In this direct detection format (Fig. 4a), the

resulting refractive index change is directly proportional to the concentration of the analyte. But for analysis of smaller sized molecules (< 5000 Da), which do not cause sufficient RI change themselves, there are other commonly used techniques. In a sandwich assay, the receptor molecules (antibodies) are bound onto the surface (Fig. 4b). Then a small-sized analyte is run on the surface and bound by the surface-attached antibodies. The SPR signal is gained, when a secondary antibody (recognising other epitopic site than the surface bound antibody) binds on the surface-bound analyte.

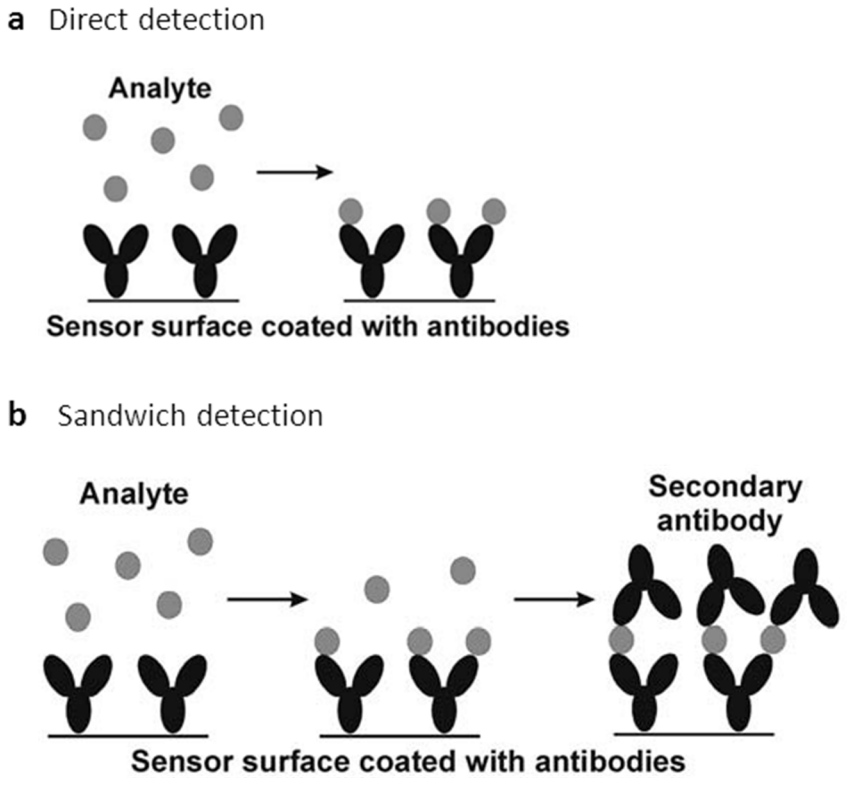

Figure 4. The principles of SPR a) direct detection and b) sandwich detection formats. Direct detection format can be used for analytes > 5000 Da, while sandwich assay format is used for smaller analytes. Sandwich assay is based on the binding of the secondary antibody recognising the analyte bound onto the surface-antibodies. Image adapted from Homola 2003.

Inhibition assay is an example of an indirect assay type. In inhibition assay the unknown amount of the analyte is mixed with a specified concentration of analyte specific antibodies. Then the solution containing known amount of antibodies and unknown amount of analyte is run over the surface with immobilized analyte. Ana-

lyte specific antibodies not complexed with analyte bind on the surface immobilized analyte. The difference in original total and surface bound antibody amounts correlates to the free analyte amount in the liquid (Homola 2003, Dostalek et al. 2006). Yet another assay type, though not as commonly used in SPR detection (Larsson et al. 2006, Klenkar and Liedberg 2008), is a displacement assay. This assay type is based on antibodies having a different affinity to antigenic epitopes, whether they are free in the solution or protein-conjugated and surface bound (Gerdes et al. 1997). Displacement reaction is a good and sensitive assay type for small analyte detection.

3. Molecules for biomolecular sensing

3.1 Antibodies and Fab'-fragments

Antibodies are crucial molecules for our immune system in recognizing harmful invaders (viruses, bacteria, toxins) as well as in activating the immune system to kill or deactivate these invaders (Roitt et al. 1996). The very specific recognition capability of the antigen binding domains and characteristic properties of the Fc-parts of antibodies (Fig. 5) have been used extensively in biotechnological, diagnostic and therapeutic applications. Humans produce five main classes of antibodies (IgG1-4, IgM, IgA1-2,, IgD and IgE). The presence of these different classes depends on the invader (antigen) in question, on the type of the immune reaction (for example allergic or infection), and also on the stage of the infection and whether the antigen has already previously been recognised by the immune system or not (Roitt et al. 1996). Whole antibodies, as well as $F(ab')_2$ and Fab'-fragments of those, have been used in biosensors for some decades already. A biosensor utilising an antibody or a fragment of such is also called an affinity sensor.

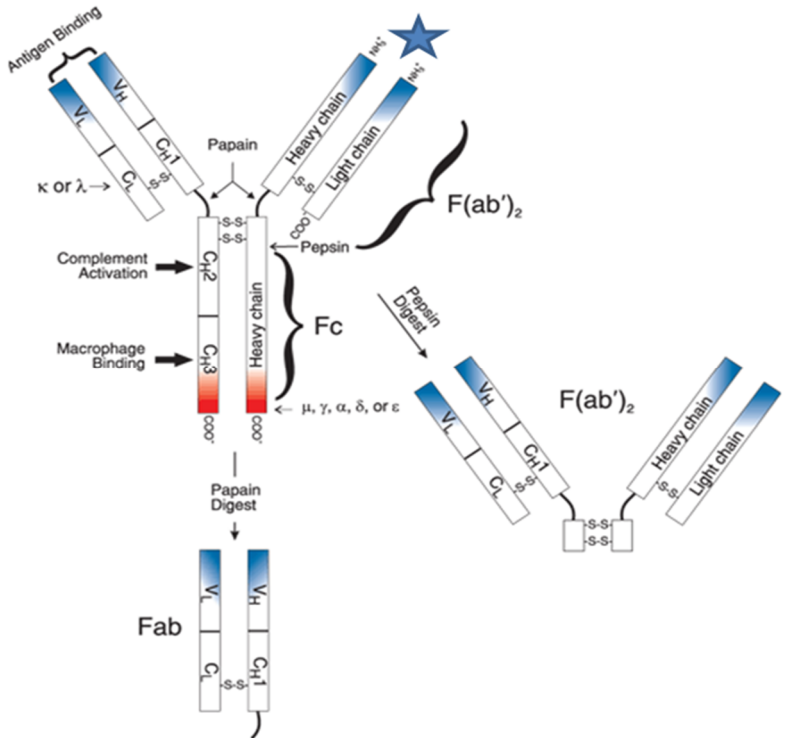

Figure 5. A general presentation of a class IgG1 immunoglobulin molecule showing antigen binding sites, heavy and light chain structure of the molecule, disulphide bridges and enzymatic digestion products. Picture modified from an image at Life Technologies 2013.

Fig. 5 shows a basic structure of an Immunoglobulin (Ig)G1 molecule. Immunoglobulins consist of two identical light and two identical heavy chains linked together via disulphide bridges and also by noncovalent interactions. Light and heavy chains can further be divided into constant and variable regions, forming the basis for the vast heterogeneity of the antigen recognition capability of the antibody arms (Roitt et al. 1996). The hinge region between the constant domains C_H1 (constant heavy) and C_H2 (Fig. 5) ensures the flexibility of the molecule and independent function of the antibody arms. For biosensors too these hinge-region cysteines are essential for site-directed attachment and orientation of the molecules on gold surfaces.

In many applications, such as in affinity sensors, only the antigen recognising domains [$F(ab')_2$ -fragments] are needed and these can be obtained, for example, by enzymatic digestion of an immunoglobulin. There are considerable numbers of antibody engineering studies available for producing only certain parts, like antigen recognising domains, of the immunoglobulins (Filpula 2007, Conroy et al. 2009). Apart from protein engineering one easily available option is also enzymatic

fragmentation of commercial whole mouse IgG1 molecules. Many digestive enzymes, such as peptidases pepsin, papain, ficin and bromelain, have been tested and studied for digestion of immunoglobulins (Nisonoff et al. 1960, Mariani et al. 1991, Jones and Landon 2003). Pepsin (Lee and Ryle 1967), bromelain (Rowan et al. 1990) and ficin (Liener and Friedenson 1970) digest mostly the Fc-part (C_H2 and C_H3 domains) of IgG1 (depending on the host and digestion conditions), leaving the hinge-region and the Fab's intact, while papain (Kamphuis et al. 1985) digests the polypeptide sequences in between the C_H1 and C_H2 domains, leaving the hinge region S-S bridges to the Fc-part (Fig. 5) (Adamczyk et al. 2000, Mariani et al. 1991). However, besides the digestive enzyme, the effect of a subclass (IgG1-4) or the host (mouse, rat, rabbit, sheep), or the digestion conditions (time, pH, temperature) also have a major effect on the enzymatic digestion pattern. In many of the above-mentioned studies, the drawbacks of the enzymatic digestions are faced: partial digestion products, or no digestion at all, microheterogeneity of the digestion products, and even total truncation of the antibodies (Inouye and Ohnaka 2001).

3.2 Avidin-biotin pair

Avidin (Fig. 6a) is a homotetrameric glycoprotein (Mw ~68 kDa) naturally found in chicken egg white, or produced by certain bacteria, such as *Streptomyces avidinii* (Streptavidin) (Green 1975, Green 1990). Streptavidin´s natural function is presumably to hinder growth by binding free biotin. In egg white, avidin is also possibly thought to have an antibiotic role in possible bacterial growth inhibition. Streptavidin is often preferred to positively charged avidin in diagnostic applications, due to its higher isoelectric point and lack of carbohydrates leading to reduced non-specific binding compared to avidin. Avidin and streptavidin are able to bind four molecules of D-biotin (vitamin H, Mw = 244 g/mol, Fig. 6b), and this binding is one of the strongest non-covalent bonds found in nature ($K_D = 10^{-15}$ M) (Green 1975, Green 1990). Biotin is a naturally occurring vitamin found in all living cells.

3.2.1 Biotinylation of proteins and oligonucleotides

Avidin-biotin chemistry was initially used in protein chemistry applications, like labelling and purification, but is currently also used widely in surface applications. Many alternatives for biotinylation of (bio)molecules makes this approach very appealing. Only the bicyclic ring of biotin is involved in the binding interaction with avidin, and the carboxylic acid side-chain of biotin (Fig. 6b) can be extended with different linker molecules and active groups, thus enabling chemical coupling (Bayer and Wilchek 1990). In addition, the biotinylation reaction conditions used for proteins are mostly very mild (physiological pH and salt conditions), retaining the full functionality of the biotinylated molecules prior to the surface attachment (Millner et al. 2009). Biotinylation reaction can be performed also site-specifically with biotinylating enzymes (You et al. 2009). The degree of the biotin labelling is

also easy to measure. There are different kinds of spacer groups of biotinylation reagents available, which offer freedom of movement for the biotin-labelled protein (Millner et al. 2009).

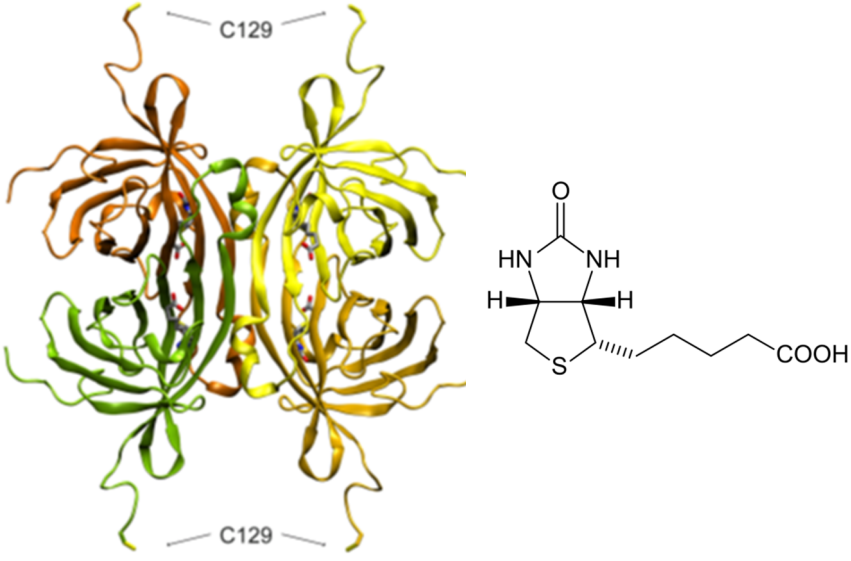

a. **b.**

Figure 6. a) The tetrameric avidin molecule showing the four biotins bound as ball-and-stick models. This avidin is an engineered version of wild-type avidin containing four additional cysteines, marked as C129 (Image adapted from Publication III). b) The molecular structure of biotin.

The NHS ester of biotin is the most commonly used biotinylation reagent to target amine groups (Luo and Walt 1989), whereas biotin hydrazide can be used to target either carbohydrates or carboxyl groups (Bayer and Wilchek 1990). Moreover, site-specific biotinylation of proteins can be performed with biotinylating enzymes, such as *Escherichia coli* biotin ligase BirA (Beckett et al. 1999, You et al. 2009). Biotins are also synthesized with polyethylene glycol (PEG) spacers with different lengths, aiding the protein movement and functionality even though they are attached to surface (Millner et al. 2009).

Genetic engineering of proteins is expensive, but due to the wide applicability of the avidin-biotin chemistry, it is a feasible approach (Laitinen et al. 2007). For example, Neutravidin is an engineered version of avidin not containing any glycans, due to the deleted glycosylation sites.

Biotin-group can be incorporated to DNA-probes within the synthesis of nucleotide-sequence. Thus the biotinylated DNA-probes are easily available.

3.3 DNA probes

A polynucleotide sequence of DNA is composed of four nucleotides (adenine (A), guanine (G), cytosine (C) and thymine (T)), which contain the genetic information of most organisms as coded in their genes. The information contained by DNA is very specific and also an exclusive way of permitting almost absolute identification of its origin: the host-organism, a mutation in a sequence, or a different allelic version of a gene. In nature, DNA is mainly found in a double-stranded form, due to the tendency of these molecules to form stable double strands with the complementary sequence (A always pairs only with T and G pairs with C) according to the Watson-Crick base pairing. In DNA sensors, the goal is to find a complementary pairing strand to the surface-attached DNA-probe sequence that leads to a measurable signal at the detector. DNA-probes are 20–40 base pairs (bp) long single-stranded DNA sequences, which are chosen from distinctive areas from a gene with some other criteria, like tendency to form secondary structures and melting temperature. DNA- biosensors have been used for example in detection of clinically relevant DNA samples, as well as in analysis of food pathogens, in environmental monitoring and for defence applications (Ronkainen et al. 2010). The major obstacles with DNA sensors are in clever probe design and prevention of non-specific binding. Analysis of PCR (polymerase chain reaction) amplicons is definitely more straightforward than analysis of genomic DNA. PCR amplification reduces the complexity of the target DNA by increasing the copy number of the original sample (Lucarelli et al. 2008). The goal with DNA analysis is to find a match from a pool containing 10^5–10^6 possible pairing strands. Detection of DNA down to concentrations of 10^{-18} M has been accomplished (Lucarelli et al. 2008).

4. Immobilisation of biomolecules on surfaces

There are various approaches for attaching biological sensing molecules to sensor surfaces. The main generic attachment types are presented in Fig. 7; they are physical adsorption (physisorption), covalent attachment of molecules onto surfaces and affinity attachment. The first two attachment types lead mostly to non-oriented and heterogeneous, even denatured, surface assemblies of biomolecules. Apart at least partial denaturation of the sensing molecules, a loss or a reduction of the mobility of the molecules is also to be anticipated.

Covalent attachment is also a stable option, ensuring that immobilised molecules will be bound on the surface over the whole binding experiment. The immobilization chemistries are in principle the same, whether the surface bound molecule is a protein, a DNA-probe or even a whole cell.

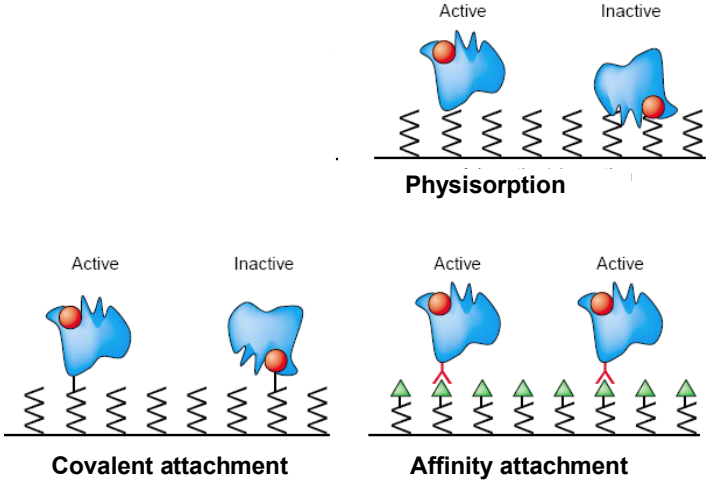

Figure 7. Generic attachment types, such as physisorption or covalent attachment, lead mostly to non-oriented and heterogeneous, even denatured, surface assemblies of proteins. Affinity attachment via protein tags is the method of choice, when the correct orientation of the protein on the surface is a key factor. Image modified from Zhu and Snyder 2003.

4.1 Covalent attachment

Proteins are covalently immobilized to support through accessible functional groups of exposed amino acids. Covalent bonds are mostly formed between side-chain-exposed functional groups of proteins and modified support, resulting in an irreversible binding and producing a high surface coverage. Chemical binding via side chains of amino acids is often random, since it is based on residues typically present on the exterior of the protein. Covalent attachment can, however, also be guided in an orderly manner to attain oriented immobilisation. This attachment (Table 1) is performed via reactive groups within the molecules, like free-thiols, which form covalent bonds with gold (chemisorption).

Chemical linker molecules between the sensor (gold) surface and the biological sensing molecules are commonly used, such as functionalized alkane thiols and alkoxy silanes, that from stable SAMs on gold (Ulman 1996). The linker molecules can also have other functionalities besides amino-groups, like sulphhydryls or disulphides, which can alleviate protein immobilization (Love et al. 2005). The most widely used polymer in biosensors is carboxymethyldextran (CM) (Löfås and Johnsson 1990) (Fig. 8), which is also used in commercial sensors as a base layer (Biacore chips).

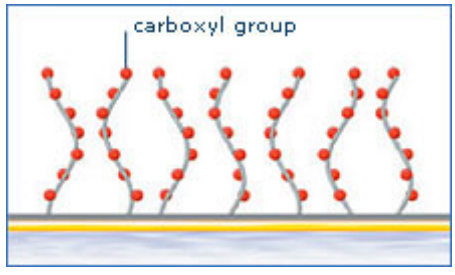

Figure 8. Example of a commercial CM 5 surface for immobilization of amine-, thiol-, aldehyde-, or carboxyl-groups. Image adapted from Biacore 2013.

Covalent attachment of amine groups is commonly performed via EDC (1-ethyl-3-(3-dimethylaminopropyl)-carbodiimide)-NHS (N-hydroxysuccinamidyl) chemistry, where the carboxylic acid groups of the base layer, like CM or hyaluronic acid, are first chemically activated with the NHS group and then linked with an amino group of the ligand forming stable amide-linkages (Fig. 9) (Johnsson et al. 1991). Lysine residues are commonly used, due to their abundance on the protein surface. On the other hand, this abundance can also lead to a multipoint attachment of the protein on the surface, increasing the heterogeneity on the surface as well as restrictions in the conformational flexibility of the proteins (Cooper 2002). Reaction conditions for efficient immobilisation via NHS need to be adjusted carefully with each protein with respect to pH, reaction time and concentration (Rusmini et al. 2007).

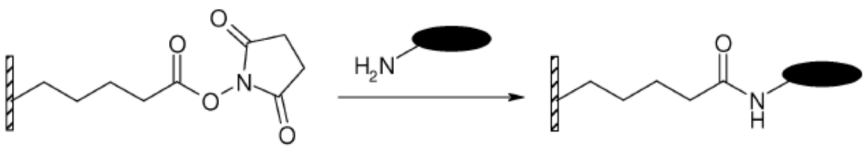

Figure 9. Amine chemistry for covalent attachment of proteins on surfaces: Amino groups of proteins react with NHS esters forming stable amide linkages with the surface. Adapted from Rusmini et al. 2007.

Covalent immobilisation can also be carried out via carboxyl- or thiol-groups (Löfås et al. 1995, Johnsson et al. 1995, Catimel et al. 1997). Carboxyl groups of aspartic and glutamic acid can be activated by carbodiimide (CDI), which leads to covalent coupling with the amine groups of the surface (Fernandez-Lafuente et al. 1993). The amino acid cysteine contains a thiol group, which in proteins normally ensures the stability in the three-dimensional fold by its ability to form disulphide bridges. Since cysteines are not as abundant as lysines, random immobilization is less likely to occur. The main coupling approaches involving thiol side groups of proteins are maleimide-, disulphide- or vinyl sulphone-derivatized surfaces (Rusmini et al. 2007).

However, direct thiol-attachment onto gold surfaces has been successfully employed, especially with antibodies via their hinge-region cysteines. O'Brien et al. (2000) demonstrated first the higher functional epitope density of rabbit Fab'-SH-fragments as compared to the epitope density of gold immobilised whole IgG. After generation of the $F(ab')_2$-fragments (by enzymatic digestion), the inter-chain S-S bridges originating from the hinge-region (Fig. 5) can be reduced by mild partial reduction with dithiothreitol (DTT) (Ishikawa et al. 1983) or cysteamine-HCl (2-MEA) (O'Brien et al. 2000) to obtain the Fab'-fragments with free thiols available for oriented surface binding (Peluso et al. 2003, Bonroy et al. 2006).

Thiol-mediated immobilisation has also been widely used in covalent immobilisation of DNA-probes with free thiol-groups on surfaces. In a pioneering study by Herne and Tarlov (1997), the probe-modified surface was post-treated with a secondary thiol (mercaptohexanol). The secondary thiol displaced the non-specifically absorbed probe molecules, while leaving the remaining ones in an upright position. Immobilisation via chemisorption of thiolated probes is the method of choice for most of the commercially available DNA arrays (Lucarelli et al. 2008). This observation underlines the efficiency, reliability and reproducibility of this chemistry in DNA-probe immobilisation. Thiol-adsorption takes advantage of the strong interaction (chemisorption) which is established between thiolated molecules and a metal surface. With thiols, the reaction is assumed to take place as an oxidative addition to gold with release of hydrogen, whereas in the case of disulphides, a cleavage of the S-S bond occurs. Disulphides, however, adsorb approximately 40% slower than thiols (Jung et al. 1998).

Table 1. Chemically reactive side groups of proteins and the required functionalities of the surface for covalent attachment. Modified from Rusmini et al. 2007.

Side groups in proteins	Amino acids	Required functionalities of the surfaces
-NH_2	Lys, hydroxyl-Lys	Carboxylic acid
		Active ester (NHS)
		Epoxy
		Aldehyde
-SH	Cys	Maleimide
		Pyridyil disulphide
		Vinyl sulphone
-COOH	Asp, Glu	Amine

Besides the techniques presented above, there are also other, not so commonly used, chemistries for covalent attachment of proteins available. For example, epoxy groups have been used, as well as photoactive chemistry, Diels-Alder cycloaddition or peptide ligation (Rusmini et al. 2007, Chen et al. 2011). Proteins can also be immobilised to surfaces via carbohydrates. This interaction is based on formation of cyclic esters with diols (Hoffman and O'Shannessy 1988, Zeng et al. 2012).

Recent progress in the chemoselective protein ligation to surfaces is an oxime ligation (Lempens et al. 2009), which is based on an oxidation of the protein N-terminal site to a ketone with pyridoxal-5´-phosphate. Protein-ketones can then further be immobilised to surfaces via thiol-containing peptide-linkers, which can contain additional features, such as enzymatic digestion sites (Dettin et al. 2011).

4.2 Non-covalent attachment

4.2.1 Physisorption

Physisorption is one approach for immobilization of molecules. The resulting surface is likely heterogeneous and consists of denatured surface assemblies of proteins. Physisorption happens via intermolecular forces, which are mainly ionic bonds and hydrophobic or polar interactions. The primary forces driving protein adsorption to a solid surface are hydrophobic dehydration resulting from the interaction between hydrophobic patches on a protein and a hydrophobic surface and electrostatic interactions between solvent-accessible charged groups on a protein and the surface (Horbett and Brash 1987, Brash and Horbett 1995). However, at high concentration, proteins undergo fewer interactions with the surface, and hence retain their stable conformation and are desorbed more easily. Electrostatic interactions and protein structural properties (softness or rigidity of the structure) also affect to their adsorption on surfaces (Nakanishi et al. 2001), either guiding or

hindering the binding depending on the local surface charges or conformational features.

4.2.2 Affinity attachment

Non-covalent attachment has also been referred as “bioaffinity immobilisation” or “affinity attachment”, describing the gentler action of this immobilisation type, which often also offers a possibility of detaching the proteins from the surface and reusing the surface (Rusmini et al. 2007). Non-covalent attachment takes place via linking groups within the molecules, like biotins, that bind to the surface-attached avidins. Avidin-biotin chemistry is one of the most used non-covalent attachment type for proteins, offering one of the strongest non-covalent bonds and thus enabling use of harsh conditions. The avidin itself can be attached to the surface covalently, as described above, but the interaction of avidin-biotin in the following layer is non-covalent. When avidin is free in solution, there are in total four binding sites for biotin available, but evidently in a surface immobilised form one or more binding sites for biotin are inaccessible. The availability of these sites depends on the size of the biotinylated molecule and the degree of steric hindrance. The freedom of movement, as well as the length of a possible linker between the biotin-tag and the biotinylated molecule may affect to binding to avidin, which is surface immobilised (Millner et al. 2009). Avidins are mostly attached on surfaces by simple physisorption or through a carbodiimide reaction (Tombelli et al. 2002), where amino groups of proteins form an amide bond between carboxyl groups of self-assembled monolayers on the sensor surface. For example, in the commonly used commercially available carboxymethyl dextran chips (CMC), the streptavidins are attached to the SAMs via carbodiimide reaction.

A typical biotin/avidin/biotin multilayer is composed by first immobilising biotin directly on the surface followed by an avidin layer, to which the biotinylated molecules are then attached (Spinke et al. 1993a). Studies with different SAMs showed very low binding of avidin for the close-packed layers, and significantly higher binding for the more loosely packed ones (Spinke et al. 1993b). A good control over the surface density of biotin groups can be obtained by using mixed SAMs composed of two thiol species: one biotinylated and the other non-biotinylated (Spinke et al. 1993a). Table 2 lists the most frequently used non-covalent attachment types of proteins and their advantages and disadvantages.

Proteins engineered with a $(His)_6$ -tag at the C- or N-terminus bind to nickel (Ni^{2+}) or cobalt (Co^{2+}) ions, that are immobilised to surface via nitrilotriacetic acid (NTA) or iminodiacetic acid (IDA) (Sigal et al. 1996, Nieba et al. 1997, Ley et al. 2011). NTA is initially covalently bound to the surface via EDC-NHS on carboxy-dextran surface, or via maleimide chemistry. The covalently linked NTA is then loaded with a divalent metal cation, usually Ni^{2+}. The binding with the $(His)_6$-tag is highly specific and entirely reversible upon addition of a competitive ligand, such as histidine or imidazole, or a chelating agent (such as EDTA), which is able to remove the metal from the complexing agent NTA. His-tags are commercially

available for a large number of functional proteins. The drawbacks are metal-dependent nonspecific protein adsorption to the surface and a low affinity of the $(His)_6$-tag to the Ni^{2+} -NTA complex ($K_D = 10^{-6}$ M). For this reason, anti-$(His)_6$ monoclonal antibodies are also often used to enable more stable, oriented immobilisation of His-tagged receptors (Müller et al. 1998).

Table 2. Most frequently used non-covalent attachment types of proteins on surfaces.

Attachment type	Advantages	Disadvantages
Avidin- biotin pair	– biotinylation kits with different chemistries commercially available – high affinity ($K_D = 10^{-15}$ M)	
His-tag bound to Ni^{2+}-NTA surface	– synthesis kits available for many kinds of proteins	– low affinity to surface ($K_D = 10^{-6}$ M) – metal dependent non-specific protein adsorption
DNA-pairing	– specific and selective pairing – proteins can be washed off by alkaline treatment of the surface	– DNA conjugation to protein can be problematic
Monoclonal antibodies	– commercially available for many different expression tags – highly specific binding	– random immobilisation

Surface attachment of proteins via monoclonal antibodies is a straightforward, specific and very versatile option. Monoclonal antibodies against many protein tags (like his-, flag-, or myc-tags) engineered originally for molecular biology purposes, as well as antibodies against other molecules or domains linked to the proteins (like biotin, Glutathione-S-transferase (GST), Green fluorescent protein (GFP)) are commercially available (Conroy et al. 2009). Antibodies have also been attached via Fc-region carbohydrate moieties (Hoffman and O'Shannessy 1988) to surfaces or through functionalised lipid monolayers (Vikholm et al. 1996).

Protein A (Forsgren and Sjöquist 1966) and protein G (Björck and Kronvall 1984) mediated immobilisation of antibodies has been utilised already for decades. These proteins bind specifically to Fc-parts of the immunoglobulins, ensuring the correct orientation and functionality of the antigen binding arms and have thus been extensively used in immunoassays, surface immobilisations and in many other applications, such as in antibody purification columns (Hober et al. 2007). Recent examples of protein G surfaces are studies by Kausaite-Minkstimiene et al. (2010) and Song et al. (2012). They have compared randomly assembled whole antibody surfaces to the surfaces assembled in oriented manner via protein G or biotin-streptavidin chemistry. In both studies, the antigen (human

growth hormone and prostate-specific antigen, respectively) could not be detected with randomly assembled surfaces, while clinically relevant detection limit (10 pg/ml in the latter) could be obtained with oriented antibody surfaces. Song et al. (2012) also carried out dual polarisation interferometry measurements, verifying the end-on conformation of the antibodies on protein G assembled surfaces.

In a very recent publication by Niu et al. (2012) a surface immobilisation of antibodies via carbon disulphide and protein A is reported. Primary or secondary amine groups (of protein A) react spontaneously with carbon disulphide, forming dithiocarbamates on gold surface (Fig. 10). Thereafter the surface immobilised protein A binds IgG molecules. The protein A binding in this example is covalent and happens randomly on the gold surface. A fraction of the immobilised protein A molecules have a correct orientation for IgG binding.

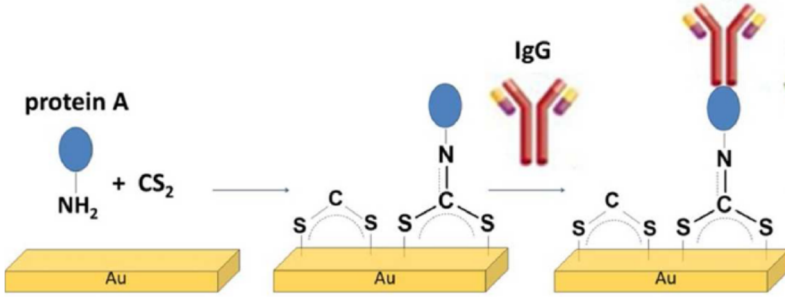

Figure 10. IgG immobilization on the gold surface with a solution of CS_2 and protein A. A gold slide was first immersed into a mixed solution of CS_2 and protein A, and then incubated in IgG solution to form the IgG sensing surface. Image adapted from Niu et al. 2012.

To enhance protein surface attachment, DNA probes have also been attached to proteins in various ways. This has been done directly via disulphide exchange reaction, where a thiopyridyl sulphide of an oligonucleotide binds to the reactive cysteine of a protein (Howorka et al. 2001). Boozer et al. (2004) have used another approach (Fig. 11), where protein conjugates consist of antibodies chemically linked (by sulfosuccinimidyl 4-(*p*-maleimidophenyl) butyrate) to a ssDNA target with a sequence complementary to the surface-bound ssDNA probes and are thus immobilised on the surface via sequence-specific hybridization. DNA directed immobilisation of proteins has also been performed via streptavidin-biotin chemistry by incubating biotinylated antibodies with streptavidin-DNA conjugates and then assembling them on a surface via DNA probes (Niemeyer et al. 1999, Ladd et al. 2004). DNA-directed protein immobilisation is efficient and specific due to the rigid, double-stranded spacer arm between the protein and the surface. DNA can be denatured by alkaline treatment, so the proteins can be removed completely from the surface and replaced.

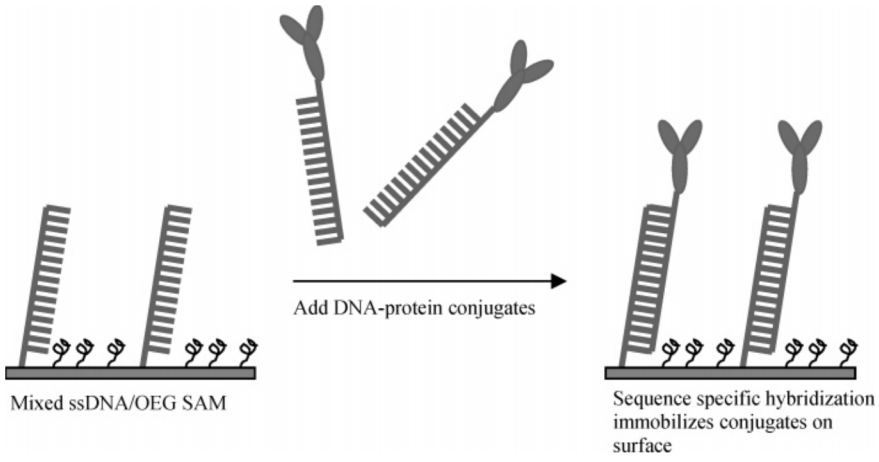

Figure 11. Antibody immobilisation on mixed single-stranded DNA/oligoethyleneglycol (OEG) surfaces via DNA hybridisation. Image adapted from Boozer et al. 2004.

4.3 Orientation of the immobilised molecules

A correct orientation of the molecules (antibodies, receptors, DNA) on sensor surface is vitally important for the optimal functionality of both the molecules and the sensor. The analyte- recognising parts of the molecules have to be facing the analyte and need to have retained their biological functionality. The immobilized molecules need to assemble in uniform layers onto the surface and in an oriented manner. For orienting the molecules on or within the SAM there have to be reactive groups directing the attachment of the molecules, as with affinity attachment (see Fig. 7). Unlike physisorption, the covalent and affinity attachment offer the means for controlling the orientation of the molecules on the surface.

Oriented immobilization is also known as site-specific immobilization. The orienting of the molecules on metal surfaces can be performed, for example, via free thiol groups on the molecules forming a covalent bond with the surface. Hinge-region cysteines of antibodies are an excellent example of this (Fig. 5). In principle, any attachment type is possible, when just the linking chemistry takes place via groups that ensure uniform and site-specific attachment of the proteins. The importance of orientation on surfaces has been demonstrated mainly with antibodies, showing manifold improvement in detection sensitivity when comparing the non-oriented surfaces with the oriented ones, using either thiol- or biotin-avidin chemistry for attaching the Fab'-fragments onto the sensor surface (Ahluwalia et al. 1992, Ahluwalia et al. 1994, O'Brien et al. 2000, Peluso et al. 2003, Vikholm 2005, Vikholm-Lundin 2005, Vikholm-Lundin and Albers 2006, Bonroy et al. 2006).

With DNA-probes, the blocking molecules have been observed to alleviate the correct end-on orientation of the probes on the surface by reorienting them toward a more-upright position upon blocker incorporation (Lee et al. 2006).

Protein engineering is also a powerful technique enabling site-specific orientation of proteins onto surfaces: protein-tags (like $(His)_6$-tags) can be genetically engineered in the protein sequence so that it does not disturb the analyte recognition, and enables more optimal surface attachment.

5. Attachment of cells onto surfaces

Attachment of cells onto surfaces is relevant, for example, in cell-arrays, whole-cell based assays and nowadays especially in tissue engineering experiments. Traditionally, it has been carried out for decades with bacterial biosensors, which as such are beyond the scope of this thesis. However, attachment of cells onto surfaces follows the same principles as attachment of smaller biomolecules: non-covalent attachment via “adhesion sequences” and minimizing non-specific binding are relevant issues. Microfabrication techniques (dry etching, photolithography and microcontact printing) are used to generate patterns of cells on surfaces (Fig. 12) (Otsuka 2010). Grafting of protein resistant PEGs to cell-free areas is also an essential part in patterning technologies for cells (Nath et al. 2004).

Adhesion of cells to a substrate is nevertheless a complex process, involving protein adsorption to a surface and requiring specific peptide sequences called “adhesion sequences”. The density of adsorbed protein and the spatial relationship between adhesion sequences are important factors affecting the cell adhesion to substrates (Raynor et al. 2009). In living organisms, the cells are surrounded by the extracellular matrix, which is a complex network of proteins and polysaccharides (Hubbell 1999). Collagen and fibronectin are the main structural proteins in the extracellular matrix and contain sequences promoting cell adhesion and have thus been mimicked in biomaterials research. Such sequences include Arg-Gly-Asp-Ser (RGDS) found in fibronectins (Ruoslahti and Pierschbacher 1987), Gly-Phe-Hyp-Gly-Glu-Arg (GFOGER), found in collagen (Knight et al. 2000), and Ile-Leu-Val-Ala-Val (IKVAV), found in laminin (Ranieri et al. 1995), and have been utilised in culturing among others human umbilical vein endothelial cells (Jung et al. 2009). When a peptide sequence mimicking the spacing and adhesion characteristics of fibronectin was immobilized on a gold surface assembled with ethyleneglycols (EG_3 and EG_6-COOH), a marked improvement in cell adhesion was observed (Capadona et al. 2003). Besides adhesion sequences also growth factors have been used for cell attachment; for example in a study by Nakaji-Hirabayashi et al. (2007) oriented surfaces of an epidermal growth factor have been used with rat fetal neural stem cells.

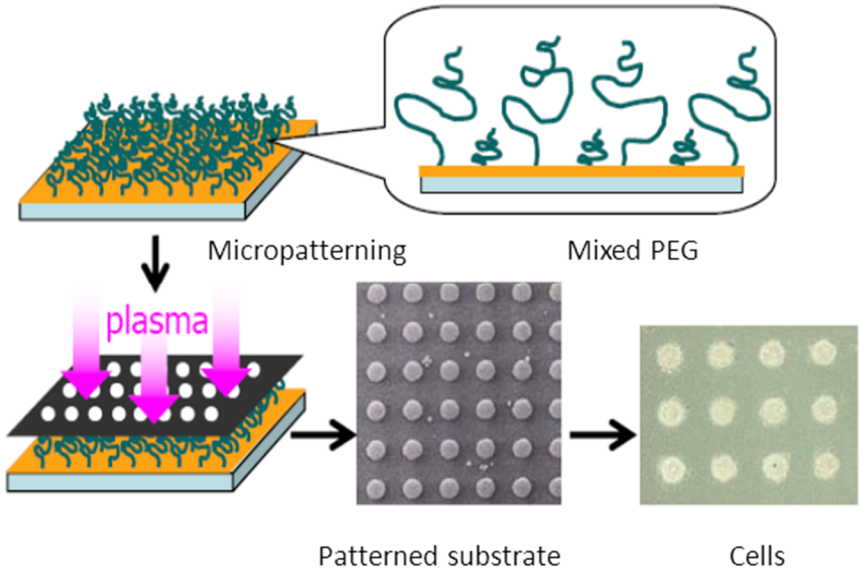

Figure 12. A two-dimensional microarray of endothelial cells. PEG molecules were immobilised on a gold surface and plasma-etched through a metal mask pattern with circular holes. The PEGylated region on the patterned substrate acts to repel proteins and thus inhibits cell adhesion. Image adapted from Otsuka 2010.

Otsuka et al. (2004) have patterned an array of cell-organized spheroids on surfaces mimicking a function of the liver: Bovine aortic endothelial cells (BAECs) were patterned on a α-lactosyl-PEG/polylactide surface and then later rat primary hepatocytes, when BAECs were selectively located in the circular domains. Rat primary hepatocytes formed spheroids only on the circular regions of existing endothelial cells, generating a 2D-arrayed structure of the hepatocyte spheroids. Continuous albumin secretion in hepatocytes co-cultured with BAECs was observed for over 31 days of culture. This is a direct demonstration that the surviving hepatocytes have functions comparable to the ones seen in the liver.

6. Minimising the non-specific binding

Due to the fact that SPR is very sensitive to the mass changes on the sensor surface, it is of the utmost importance that the receptor molecules are correctly folded and oriented on the surface, and that there is minimal non-specific binding, because anything that binds to the sensor surface causes a signal in SPR and can be misinterpreted as specific (potentially leading to false positive diagnosis). Traditionally, the non-specific binding has been reduced in immunoassays by absorbing bovine serum albumin (BSA), casein, fat-free milk, Tween 20 or serum on the detection surface to block free binding sites and to restrict the conformational changes of the immobilised antibodies (Kenna et al. 1985). Several types of molecules have a natural ability to reduce adsorption of proteins at surfaces, e.g. carbohydrates such as agarose and mannitol as well as albumin (Luk et al. 2000, Nelson et al. 2003). However, due to the limited efficiency and stability of these, a number of synthetic materials have been developed (Raynor et al. 2009).

Mixed SAMs are molecular layers combining different organic molecules that are for example either specifically interacting with or repelling biomolecules. SAMs can present a wide range of organic functionalities, including resistance towards protein adsorption. Such “inert” surfaces capable of resisting adsorption of other biomolecules and cells are often composed of hydroxylated polymers such as poly(hydroxyethyl methacrylate), agarose, or oligo- or poly(ethylene glycol) (OEG or PEG) (Bain and Whitesides 1989, Prime and Whitesides 1991, Love et al. 2005). In the most widely used substance, PEG, the monomeric repeating unit is [-CH2-CH2-O]-. Alkanethiols with tri- or hexa(ethylene glycol) groups are commonly used in SAMs and studies of biomolecules (Kingshott and Griesser 1999). Protein resistant surfaces terminated with OEG take either a helical or an amorphous conformation in dehydrated form in air or vacuum, as evidenced by spectroscopic methods (Harder et al. 1998) (Fig. 13).

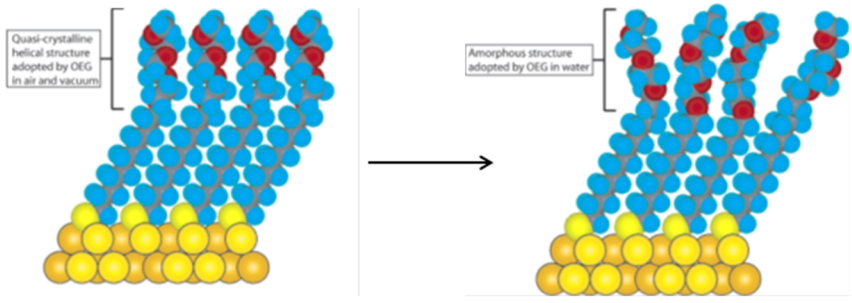

Figure 13. Schematic illustration of the order-disorder transition evidenced by SAMs of alkanethiolates terminated with triethylene glycol. The triethylene glycol group loses conformational ordering upon solvation in water. Image adapted from Love et al. 2005.

Many SAMs with other functional groups have been studied, and different functional groups have been screened by Chapman et al. (2000). They postulate that "A key structural element in protein-resistant surfaces was the elimination of hydrogen bond donor groups: smaller amounts of proteins adsorbed to surfaces that presented compounds with NCH_3 and OCH_3 than to surfaces that presented their more polar analogues with NH and OH groups". Also, oligosarcosines and oligosulfoxides have been found to form reasonably effective protein resistant surfaces (Ostuni et al. 2001). There are many suggested reasons for the protein resistant properties of SAMs: the packing density and hydrophilicity of the chains, the nature of the surrounding environment as well as temperature are among suggested factors enabling the protein resistant properties of OEG and PEG-terminated SAMs (Love et al. 2005). Besides these, also polarity, overall electrostatic neutrality, conformational flexibility and the structure of water present at the surface seem to play key roles (Ostuni et al. 2001). By varying the concentrations of the molecules in a mixed SAM, it is possible to control the surface density and accessibility of the biological ligands on the surface.

Besides reducing non-specific binding, the blocking molecules also have an important role in preserving the hydrophilic environment around the biological sensing molecules, ensuring their functionality, as has been suspected in studies with Fab's assembled with hydrophilic polymers (Vikholm 2005, Vikholm-Lundin 2005, Vikholm-Lundin and Albers 2006). This observation was recently evidenced by Yoshimoto et al. 2010, who could demonstrate the effect of the surface PEGylation on gold immobilised Fab'-fragment conformation by fluorescence spectrometry and AFM studies (Fig. 14).

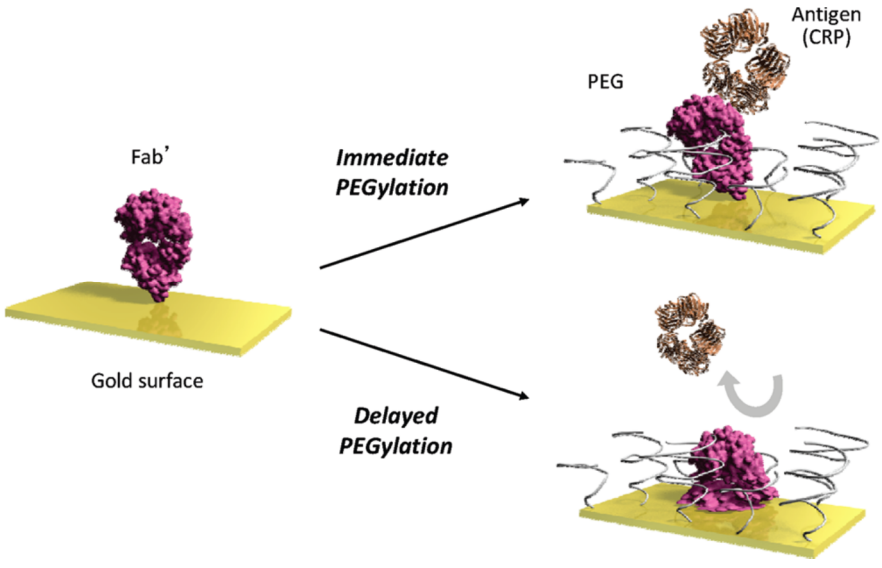

Figure 14. Schematic illustration of time-dependent inactivation of immobilized Fab' surrounded by mixed-PEG layer on gold surface. Immediate PEGylation after Fab' immobilization (above) prevents conformational/orientation changes resulting in antigen (CRP) recognition. At the bottom is shown the situation of delayed PEGylation after Fab' immobilization. Image adapted from Yoshimoto et al. 2010.

When discussing surface immobilisation of molecules, one important issue is the surface density (Rusmini et al. 2007). This relates to the number of molecules on the surface and how tightly they are packed with respect to each other. If the surface density is high, there is less freedom of movement, which means increased steric hindrance. This limitation of movement, particularly of the antibody Fab'-domains, causes reduced antigen binding (Vikholm-Lundin 2005), and frequently higher non-specific binding. However, with smaller (linear) molecules, such as DNA-probes, which do not need as much freedom to move, a higher surface density leads to more bound analyte, i.e. increased detection sensitivity (Steel et al. 1998). The surface density of the molecules also affects the non-specific binding to the surface, and thus also offers a means to control it via concentration and composition of the surface molecules (Unsworth et al. 2005).

An interesting observation was that there seems to be very little correlation between protein resistance and the adhesion of cells. Cell adhesion to surfaces happens via adhesion sequences, which are recognized by cell integrin receptors and promote cell adhesion and migration on surface. Gold surfaces that are modified only with CH_3-terminated SAMs are observed to adsorb proteins, thereby allowing cell adhesion, but SAMs composed of ≥ 50% $(\text{ethylene glycol})_n$, where $n \geq 3$, are resistant to protein adsorption (Raynor et al. 2009).

7. Aims of the present study

The main objectives of this thesis have been the development of sensitive biomolecular surfaces for different sized (biological) analytes. With protein surfaces especially the detection of small-sized drugs that are in general not visible with SPR was one of the aims. For reaching this goal a displacement detection was studied. Also detection of the drugs with SPR in the presence of difficult sample matrix (diluted saliva) was one of the open questions. The good performance of the pTHMMAA-polymer in diminishing non-specific binding on surfaces was already known based on the previous studies on both protein (Vikholm 2005, Vikholm-Lundin 2005, Vikholm-Lundin and Albers 2006) and oligonucleotide surfaces (Vikholm-Lundin and Piskonen 2008). One of the aims in this study was to analyze the diminishing of non-specific binding with Lipa-DEA on oligonucleotide surfaces, instead of pTHMMAA, and whether also oligonucleotides could be analysed sensitively in the presence of diluted serum with SPR. Effect of the differential Fab´-fragment surface immobilization on sensitivity and binding capacity was studied with avidin surfaces. In addition to these, also the suitability of repelling antibody surfaces as a selective growth surface for differentiated stem cells was one of the questions.

The specific aims of this study were:

1. To study the suitability of neuron specific antibody-polymer surface for selective neuronal cell-growth
2. To build sensitive surfaces for small sized drug detection and test the performance of these surfaces also in the presence of diluted saliva
3. To study the effect of differential Fab´-fragment immobilisation on avidin layers to the sensitivity and capacity of the surfaces
4. To test the performance of Lipa-DEA on oligonuleotide surfaces for sensitive DNA detection
5. To analyze DNA samples with SPR in the presence of diluted serum.

8. Materials and methods

A summary of the materials and methodology used is presented below. A detailed description of the materials and methods can be found from the original Publications (I–V).

8.1 Gold surfaces (I–V)

Gold substrates for SPR measurements were manufactured in-house by RF magnetron sputtering (Edwards E306A, BOC Edwards, Crawley, West Sussex, UK) by coating thin glass slides with a 50 nm-thin gold layer with an intermediate layer of indium oxide (Albers 2010). The r.m.s. surface roughness for similar, but 20 nm-thin, gold slides has been assessed with atomic force microscopy to be 1.5 nm and peak-to peak roughness of 11.3 nm and 2.2 and 24 nm for a 150 nm-thick gold layer, respectively (Wang et al. 2010). Just prior to the fuctionalisation, the gold slides were cleaned in a boiling solution of hydrogen peroxide and ammonium hydroxide (28–30% NH_3) in water (1:1:5, vol/vol/vol) for approximately 30 s and rinsed with water. The pre-cleaned slides were mounted in a Biacore-chip cassette and the functionalisation was performed in the Biacore 3000 instrument (GE Healthcare).

8.2 Biomolecules (I–V)

Table 3 lists the biomolecules used in these studies and the corresponding publication, where the details can be found.

Table 3. Biomolecules used in the studies of the surfaces.

Molecule	**1st layer receptor molecules**	**Publication**
anti-NCAM antibodies	Receptor molecules on gold & polystyrene	I
Anti-MDMA Fab'	Receptor molecules on gold	II
Wt-Avd, ChiAvd-Cys	Avidins assembled on gold	III
Molecule	**2nd layer molecules**	**Publication**
BSA-MDMA	Molecules in the 2nd layer: Conjugate	II
Amino-biotin F(ab´)$_2$	Molecules in the 2nd layer	III
SH-biotin Fab'	"	III
Molecule	**Analyte/ antigen molecules**	**Publication**
NCAM	Antigen	I
Anti-MDMA IgG	3rd layer analytes in the MDMA displacement reaction	II
MDMA	Antigen displacing the anti-MDMA antibodies from the surface	II
Human IgG	Antigen	III
Biotin-GFP	"	III
Molecule	**DNA surface probes**	**Publication**
DMT-S-S-PTGS2	Surface probe	IV–V
DMT-S-S-CALCA	"	"
SH-PTGS2	Surface probe with a free thiol-group	IV–V
SH-CALCA	"	"
Molecule	**Analyzed PCR-products**	**Publication**
PTGS2-16, PTGS2-27, PTGS2-123	Complementary strands for PTGS2-probes	IV–V
CALCA-18, CALCA-25, CALCA-92	Complementary strands for CALCA-probes	IV–V
Molecule	**Other used biomolecules**	**Publication**
BSA	Used for determination of NSB	I–V

8.3 Pre-treatment of biomolecules prior the surface functionalisation

8.3.1 Antibody enzymatic digestions and Fab'-fragment generation (II)

In order to obtain Fab'-fragments which can be oriented on the surfaces via free cysteines, the whole antibody molecules need to be fragmented. This was done by bromelain enzyme digestion according to the procedure by Mariani et al. (1991). Antibodies were incubated with bromelain at +37°C for 4–20 hours, and the digested products were purified with the aid of affinity chromatography, which removes the non-digested whole antibodies as well as smaller peptides from the mixture, while the F(ab´)$_2$-fragments were retained in the column (Harlow and Lane 1988).

After purification, the products were verified by SDS-PAGE protein gels (Laemmli 1970), and the protein amount of the purified protein was assessed by measuring the absorption at 280 nm and calculating the concentration by means of Lambert-Beer´s law (A = εcl) and molar absorption coefficient ($\varepsilon^{1\%}$ = 1.56) for (Fab')$_2$s (Carter et al. 1992). The total protein amount was assessed by Bradford's procedure (Bradford 1976) with bovine IgGs as standards, which is based on the Coomassie Brilliant Blue dye binding to primarily basic and aromatic amino acid residues (especially arginine). Protein-bound dye has increased absorbance at 595 nm and is proportional to the amount of Coomassie bound to the protein, and can thus be correlated to the protein concentration.

8.3.2 Reduction of the thiolated molecules (II–V)

Reduction of F(ab´)$_2$s to F(ab´)s was performed with dithiothreitol (DTT) (Ishikawa et al. 1983) or cysteamine-HCl (2-MEA) (O'Brien et al. 2000). DTT reduction was performed by incubating a 50 µg/ml F(ab´)$_2$-fragment solution with 3.7 mM DTT in 50 mM Na_2HPO_4, 150 mM NaCl, 5mM EDTA pH 7.4 buffer for 12–18 hours at +4°C. 2-MEA reduction was performed by incubating a 0.1 mg/ml F(ab´)$_2$-fragment solution by 50 mM 2-MEA in the same buffer as above for 2 hours at +37°C. After the reduction reactions, the reducers were washed away from the mixtures in filter-concentrators by centrifugation prior the surface assembly.

The dimethoxy-trityl -groups (DMT) protecting the reactive thiol-groups in the thiolated DNA-probes were removed according to the supplier´s (Metabion) instructions by DTT reduction, and a subsequent gel-filtration (by ready-to-use Sephadex-columns, GE Healthcare) and stored at -80°C prior to the surface functionalisation. The DNA concentration was verified by measuring the absorption at 260 nm and then calculating the concentration by means of molar absorptivity (ε) by entering the sequence in question to the oligonucleotide calculator program (Kibbe 2007).

8.4 Immobilisation of the biomolecules (I–V)

In general, all the immobilisations were performed in the Biacore instrument by injecting the sensing molecules [antibodies (I), Fab'-fragments (II), avidins (III) or DNA-probes (IV–V)] on the precleaned gold surface. The blocking molecules, pTHMMAA -polymer (poly-N-[tris(hydroxymethyl)methyl]acrylamide) [Mw ~18 000 g/mol (Albers et al. 2010)] with protein surfaces (Fig. 15b) (I–III) or Lipa-DEA (N,N-bis(2-hydroxyethyl)-α-lipoamide, Tappura et al. 2007) with DNA surfaces (Fig. 15a) (IV–V), were added either as a mixture with the reduced biomolecule in the first injection or just the blocker in the following injection.

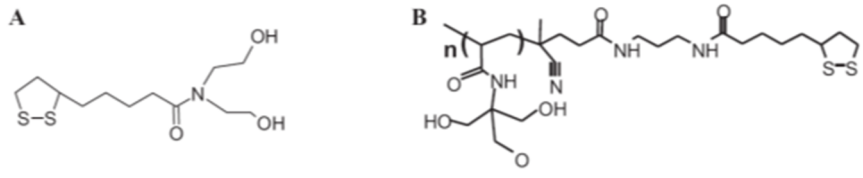

Figure 15. A schematic presentation of a) Lipa-DEA and b) pTHMMAA blocking molecules. Image adapted from Publication II.

The manually dispensed DNA-surfaces (V) were produced in a clean room environment by pipetting the DNA-probes on precleaned gold surfaces and left to assemble for 3–6 days prior the measurement as described in detail in Publication V.

8.5 SPR measurements (I–V)

All the SPR measurements were performed with a Biacore 3000 instrument. Typically, the injection cycle for each compound was 15 minutes, followed by a 10 minute wash-cycle by the running buffer. After injecting the sensing layer, the blocking molecules were run on the surface. Then the amount of the non-specific binding was assessed by injecting BSA (generally 0.5 g/l) (I–III) and non-complementary DNA (0.5 µM solution) (IV–V) on the surface. The amount of the specific binding on the surface was then measured by injecting the molecule of interest in rising concentrations on the surface. The flow in the instrument was in general 20 µl/min, and the temperature was set at 25°C in the measuring chamber.

The SPR response of 1000 RU with Biacore instrument was estimated to correspond to a surface coverage of 100 ng/cm^2 (Stenberg et al. 1991, Di Primo and Lebars 2007). Stenberg et al. (1991) have studied with radiolabeled proteins that protein surface concentrations from 2 to 50 ng/mm^2 correspond linearly to the SPR response, with specific response in the range 0.1 ± 0.01° (ngmm^{-2})$^{-1}$. The surface densities of the hybridized ssPCR-products (single stranded polymerase chain reaction DNA product) as molecules/cm^2 can be obtained by calculating the amount of the molecules via surface mass and Avogadro's number.

8.6 Surfaces on polystyrene for neuronal cell attachment (I)

Anti-NCAM antibodies (Neural Cell Adhesion Molecule) and a blocking polymer of pTHMMAA were physisorbed on the cell-growth plates. Anti-NCAM antibodies were applied to plates in four different concentrations, ranging from 0–100 µg/ml, and after 15 minutes incubation of a 200 µg/ml-solution of pTHMMAA-polymer. The surfaces were left to assemble at +4°C for two days prior to cell seeding. It is observed that the non-fouling properties of surfaces are improved when binary monolayers are left to stand for a few days (Vikholm-Lundin and Albers 2006). The cells were cultured on the antibody-polymer matrix for eight days, during which their growth and morphology was followed.

9. Results and discussion

The biorecognition surfaces studied in this thesis were assembled of whole antibodies, Fab'-fragments, chimeric avidin molecules or DNA-probes. Except for the whole antibodies the sensing molecules were attached to surfaces covalently and in an oriented manner by means of thiol-groups. Also affinity attachment was applied in the following layers formed upon the Fab' or avidin layer.

The sizes of detected analytes varied greatly ranging from huge antibody molecules (~152 000 g/mol) to very small-sized MDMA drugs (193 g/mol) resulting in that the SPR detection formats were also different. Molecules having Mw bigger than ~5000 g/mol can be generally analysed with SPR by a direct measurement (Homola 2008). However, the small-sized MDMA drug was analysed by a displacement reaction based on the affinity difference of the antibody to the non- and protein-conjugated version of the antigen. Both measurements formats resulted in nanomolar detection.

All the analytes were first measured in buffer, but MDMA drugs were analysed from diluted saliva, as well as ssPCR-products from 1% serum thus illustrating the more realistic environment of these applications. The antibody-polymer surfaces were also tested for selective neuronal cell attachment on polystyrene plates, with good results.

Non-specific binding was diminished with antibody and F(ab´)-fragment surfaces (Publications I–III) with a hydrophilic polymer of pTHMMAA (poly-N-[tris (hydroxymethyl)methyl]acrylamide) (Fig. 15b) and with DNA-probes (Publications IV–V) by a shorter lipoamide molecule of Lipa-DEA (Fig. 15a).

9.1 Physisorbed antibody surfaces for neuronal cell attachment (I)

When culturing neurospheres derived from stem cells, the aim is to have them differentiated to neuronal cells. Possibility of culturing only the differentiated neuronal cells was studied with human embryonic stem cell (hESC) -derived neuronal cells and neuronal specific anti-NCAM antibodies physisorbed on cell culture plates.

The concept of the NCAM-antibody and pTHMMAA blocking of the non-specific binding was demonstrated on the gold surfaces with SPR. A 50 µg/ml-solution of anti-NCAM antibody was injected on the gold surface, followed by a 200 µg/ml-solution of pTHMMAA-polymer. The antibody surface gave a surface coverage of 190 ± 20 ng/cm^2 and pTHMMAA-solution 20 ng/cm^2, respectively. In SPR studies on gold surfaces, the non-specific binding of BSA was only 6 ± 4 ng/cm^2, suggesting that the polymer is efficiently shielding the antibodies on the surface. The specific binding of a 10 µg/ml-NCAM antigen solution to the antibody surface gave a surface coverage of 25–35 ng/cm^2 (Fig. 1B in I), which is in accordance to the antigen responses gained for non-oriented antibody surfaces (Bonroy et al. 2006). The specific NCAM antigen detection according to the concentration as well as efficient lowering of non-specific binding could thus be verified with SPR on gold surfaces.

In cell studies, it was found that non-differentiated neurospheres did not attach to the anti-NCAM pTHMMAA-coated well-plates, while the individual neuronal cells did attach. The number of neuronal cells in wells increased according to the anti-NCAM antibody concentration. In the wells, where was just plain polystyrene and pTHMMAA-polymer, was no binding of neuronal cells.

The specific NCAM binding of the antibody could be shown with SPR, even though the antigen responses were quite moderate, which is expected for physisorbed antibody surfaces. Moreover, in the cell experiments the adhering of the neuronal cells was improved in antibody surfaces compared to the controls, suggesting that these surfaces are an effective method for selective cell attachment.

9.2 Oriented Fab'-fragment surfaces for small molecule detection by displacement (II)

Small molecule detection without labels is very challenging. Sensitivity of molecular recognition surfaces can be increased by means of oriented immobilisation of the sensing molecules. For detection of MDMA drug, anti-MDMA Fab'-fragments were attached to a gold surface in an oriented manner by means of free cysteines originating from the hinge-region of the whole antibody-molecule. The different surfaces were studied with respect to the composition and concentration of the molecules and with different blocking molecules. pTHMMAA- polymer was compared to a shorter lipoate blocker Lipa-DEA, and performance of the surfaces and MDMA detection sensitivity was compared in buffer and in diluted saliva.

MDMA has a molecular weight of only 193 g/mol and can thus not be measured directly. Displacement reaction is based on affinity difference of the antibody towards the antigen free in solution or protein-conjugated version of the antigen. As a result of this affinity difference, antibodies attached to the antigen conjugate on the surface are detached from the surface when the free antigen is run over the surface. According to the measuring principle of SPR (SPR detects basically the changes in refractive index on the surface that can be correlated to the mass changes on the surface), the displacement reaction of antibodies causes a very

strong signal even in very dilute analyte solutions, making the assay very sensitive. The principle of the displacement reaction is shown in Fig. 16 D–F (Scheme 1 in Publication II).

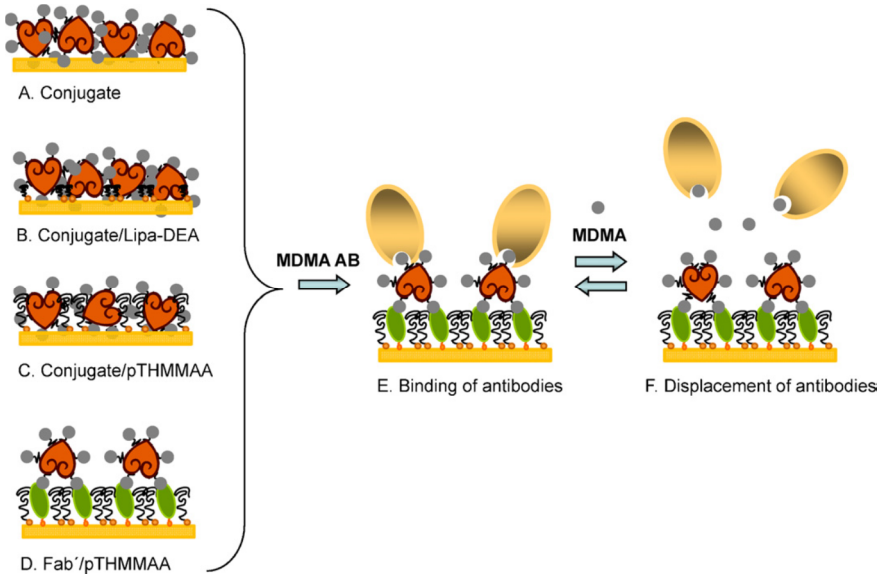

Figure 16. A schematic picture adapted from Publication II illustrating the concept of the displacement: surfaces of MDMA-BSA conjugates with A) no blocking or B-C) with different blocking molecules D) anti-MDMA Fab´-fragment/pTHMMAA-surface binding the MDMA-BSA conjugates E) Binding of the anti-MDMA antibodies (MDMA AB) on the MDMA-BSA conjugate surface F) Displacement of the antibodies from the conjugate surface, when a free MDMA drug is run over the surface.

The concentration of the anti-MDMA Fab´-fragments in the first layer (Fig. 16D) was studied and found to give the highest BSA-conjugate binding (1500 ± 150 RU) at 10 µg/ml (Table 4). The conjugate binding was lower to surfaces made from 25 or 50 µg/ml of Fab´-fragments and only 240 ± 80 RU to a surface, where Fab´-fragment concentration was 100 µg/ml. This is presumably due to a steric hindrance caused by the increased fragment concentration in the surface, as has been observed with binary monolayers of Fab´-fragments and pTHMMAA-polymer (Vikholm 2005). No binding of BSA was observed to the anti-MDMA Fab´/pTHMMAA -surface, nor to a surface composed of just pTHMMAA, which verifies that binding of the MDMA-BSA conjugates took place specifically through the Fab´-fragments to the surface.

Table 4. The SPR responses (as RU) gained when assembling the surfaces in different Fab´-fragment concentrations for MDMA detection.

	Molecules on the surface				
[Fab´] µg/ml	BSA conjugate	Anti-MDMA antibodies	Displacement [MDMA] 1 ng/ml	Displacement [MDMA] 10 ng/ml	Displacement [MDMA] 10 µg/ml
10	1500 ± 150	2400 ± 150	-	-100 ± 50	-1450 ± 100
50	1300 ± 100	2300 ± 150	-490 ± 20 -105 ± 20[a]	-680 ±20 -260 ± 50[a]	-2020 ± 60 -1950 ± 120[a]

[a] displacement responses for MDMA diluted in saliva solution (1:3 PBS-buffer:saliva)

Next, the anti-MDMA antibodies were bound to the anti-MDMA F(ab´)/pTHMMAA-BSA-conjugate -surface (Fig. 16E). A 50 µg/ml solution of anti-MDMA antibodies gave a response of 2300 ± 150 RU (Table 4), when run on the surface. Surfaces made of just BSA-conjugate and BSA-conjugate/Lipa-DEA physisorbed on gold (Fig. 16A and 16B) bound much more of the antibodies (4600 ± 700 RU and 4600 ± 400 RU) due to the much higher amount of conjugates present on the surfaces compared to the surface composed of Fab´-fragments.

Displacement reaction was then analysed on the different surfaces by running increasing concentrations of MDMA over the surface. MDMA was diluted in PBS-buffer or in diluted saliva (PBS-buffer:saliva 3:1). Prior the MDMA injections, the surfaces were washed with 0.01% Tween 20 solution to wash away too loosely bound antibodies from the surface. If no Tween washing was performed, the antibodies were bleeding off the surface even with plain buffer injections.

The displacement from the F(ab´)/pTHMMAA -surface was dependent on the concentration of the Fab´-fragments in the surface being the highest from the surfaces made from a Fab´-fragment concentration of 50 µg/ml. From this surface a MDMA solution of 1 ng/ml displaced 490 ± 20 RU of antibodies (Table 4 and Fig. 17). When MDMA was diluted in saliva solution, the displacement with a 1 ng/ml MDMA was 105 ± 20 RU. Lowering of the signal when measured from saliva was expected, and this actually diminished above MDMA concentrations of 100 ng/ml (Fig. 17). The cut-off value for abused MDMA from saliva is 10 ng/ml, so the sensitivity of these surfaces was found to correspond well to the requirements of the application.

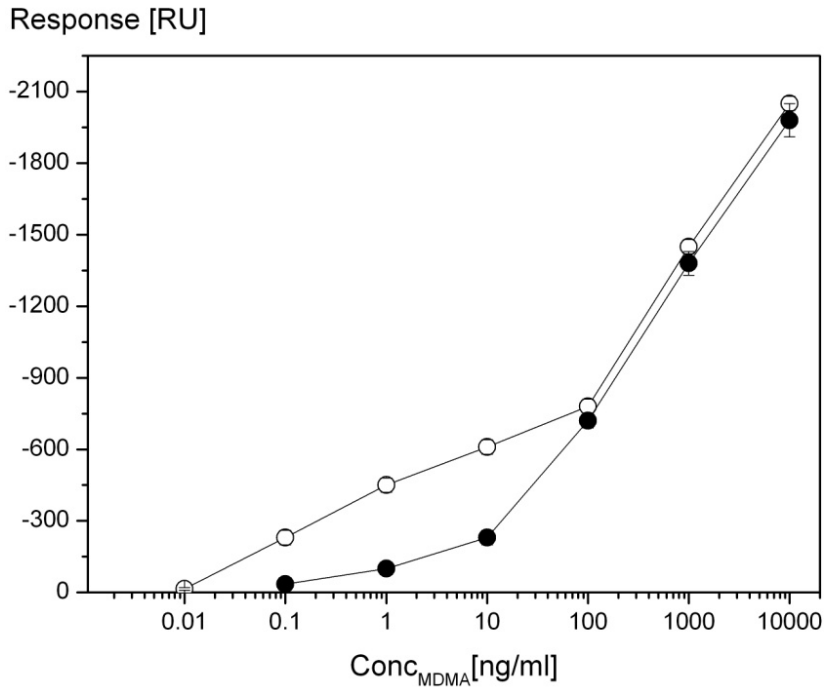

Figure 17. Injection of MDMA spiked in PBS (○) and saliva:PBS 1:3 (●) over anti-MDMA antibodies bound to conjugates through a monolayer of Fab'-fragments/ pTHMMAA (50 / 50 µg/ml). The surfaces were pre-rinsed with Tween-20, and the responses obtained by zero-injections were subtracted. Figure modified from Publication II.

Other compositions for the surfaces were also tested, such as assembling the conjugates straight onto the gold surface and instead of polymer with Lipa-DEA molecules. However, the most sensitive surfaces could be achieved with the Fab´-fragments and the polymer.

A study by Jeong et al. (2013) is a recent example of a very sensitive label-free detection. They demonstrated detection of interferon-gamma and prostate specific antigen at 1 pg/ml (below) with a Fibre-Optic Localized Surface Plasmon Resonance Sensor, which was fabricated with spherical gold nanoparticles.

9.3 Oriented Fab'-fragment surfaces constructed via cys-tagged chimeric avidins (III)

In this study, wild type avidin (hereinafter referred to as wt-Avd) and thermally stabilised genetically engineered chimeric avidin containing C-terminal cysteine groups (hereinafter referred to as ChiAvd-Cys) were immobilised directly on the gold surface. The cysteine-residues (C129) were positioned in the C-terminus of

each polypeptide chain resulting in a tetrameric chimeric avidin containing four additional cysteines (Scheme 1a in III).

First the surface coverages of different avidins on gold were compared. When 25 µg/ml of ChiAvd-Cys was allowed to interact with the Au surface, a surface coverage of 650 ± 50 ng/cm^2 was obtained. 50 µg/ml concentration gave nearly the same response of 700 ± 60 ng/cm^2, suggesting that surface was almost saturated already at the lower concentration. Wt-Avd gave half the surface coverages at the same concentrations: 300 ± 100 and 360 ± 90 ng/cm^2, respectively (Table 5). When ChiAvd-Cys was reduced with TCEP and then run on the surface at 25 µg/ml a surface coverage of 450 ± 20 ng/cm^2 was obtained. This suggests that, when not reduced, ChiAvd-Cys forms network-like or bilayer structures by forming disulphide bridges between individual molecules.

The binding ability of the ChiAvd-Cys surface was determined by coupling various concentrations of a genetically biotinylated (containing a single biotinylation site in the protein sequence) green fluorescent protein (GFP) to the surface. Due to the genetic biotinylation, every biotin-GFP contained only one C-terminal biotin, and there was thus no variation due to differential biotinylation of the analyte. The biotin-GFP binding was independent of the ChiAvd-Cys concentration used for immobilisation when the surface was post-treated with pTHMMAA. A 10 µg/ml-solution of Biotin-GFP gave a surface coverage of 280 ± 20 ng/cm^2 on a 25 µg/ml-surface of ChiAvd-Cys (Table 5). Binding of 100 µg/ml of biotin-GFP was much higher to the ChiAvd-Cys/pTHMMAA -surface (650 ± 50 ng/cm^2) as compared to the reduced ChiAvd-Cys/pTHMMAA -surface (330 ± 30 ng/cm^2). Already biotin-GFP concentrations as low as 10 ng/ml could be detected (7 ± 2 ng/cm^2) with a reduced ChiAvd-Cys/pTHMMAA -surface. Biotin-GFP binding to the wt-Avd surface was very poor. The pTHMMAA –polymer binding varied from 10–30 ng/cm^2, depending on the concentrations of the assembled avidin surface (Table 1 in III). The non-specific BSA binding was in the range of 25–50 ng/cm^2.

Table 5. Surface coverages of the different surfaces (as ng/cm^2) measured by SPR.

	Molecules on the surface			
	Avidin (25 µg/ml)	**Biotin-GFP (10 µg/ml)**	**Biotin$^{a/b}$-F(ab´)$_2$ (40 µg/ml)**	**Antigen, hIgG (100 µg/ml)**
wt-Avd	300 ± 100	<10	70 ± 20^a	15 ± 10
Chi-Avd Cys	650 ± 50	280 ± 20	270 ± 40^a 420 ± 15^b	120 ± 20 200 ± 10^i
SA-chip	n.d.	n.d.	280 ± 5$^{a, ii}$	120 ± 20

^{a} Biotin-NH$_2$-F(ab´)$_2$ ^{b} Biotin-SH-Fab' ^{i} 50 µg/ml ^{ii} 100 µg/ml
n.d. not determined

Amino-biotinylated anti-human IgG F(ab´)$_2$-fragments at a concentration of 40 µg/ml gave a surface coverage of 70 ± 20 ng/cm^2 when injected on a wt-

Avd/pTHMMAA -surface. The optimal antibody concentration on ChiAvd-Cys/pTHMMAA -surface was studied by injecting antibody solutions at concentrations 0–100 µg/ml over the surface. The highest binding of amino-biotinylated F(ab´)$_2$s was found to be on the surface made from an antibody solution of 40 µg/ml. When a 50 µg/ml solution of amino-biotinylated IgG F(ab´)$_2$-fragments was injected on a ChiAvd-Cys/pTHMMAA –surface, a surface coverage of 270 ± 40 ng/cm^2 was obtained, which is four times higher than the amount bound on the wt-Avd surface.

Amino-biotinylation presented above occurs randomly all around the molecule mainly on the surface exposed lysine-groups. Biotinylation can, however, also be done specifically on the free thiol-groups of the Fab'-fragments located moreover opposite on the antigen recognition site. Thiol-biotinylated Fab'-fragments at a concentration of 40 µg/ml bound to the ChiAvd-Cys/pTHMMAA -surface with a surface coverage of 420 ± 15 ng/cm^2, which is 1.5 times the amount of amino-biotinylated F(ab´)$_2$s bound on the same surface (Table 5). The molecular weight of F(ab´)$_2$s (~100 000 Da) is double compared to the Fab's (~50 000 Da), but presumably here the steric hindrance is due to bigger size combined with non-optimal surface orientation results in a clearly lower surface coverage for the F(ab´)$_2$s.

Binding of 100 µg/ml of hIgG (human immunoglobulin G) to the ChiAvd-Cys/ pTHMMAA/biotin-F(ab´)$_2$ -surface gave a surface coverage of 120 ± 20 ng/cm^2, when it was only 15 ± 10 ng/cm^2 to the corresponding surface made of wt-Avd (Table 5, Fig. 18). This higher binding is probably due to improved orientation and stability of the ChiAvd-Cys surface.

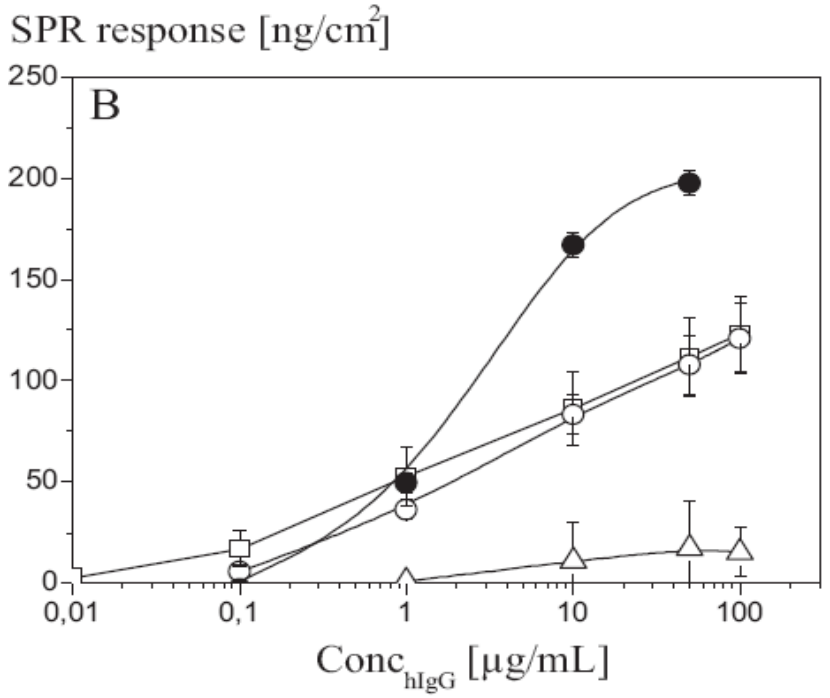

Figure 18. Human IgG-antigen binding onto commercial streptavidin chip coated with amino-biotinylated F(ab´)$_2$s (□), or to ChiAvd-Cys/pTHMMAA/thiol-Fab´-surface (●), or to ChiAvd-Cys/pTHMMAA/biotin-F(ab´)$_2$-surface (○), or to wt-Avd/pTHMMAA/biotin-F(ab´)$_2$-surface (Δ). Figure adapted from Publication III.

When amino-biotinylated F(ab´)$_2$s were bound to the commercial Biacore SA-chip (carboxymethylated dextran coated with streptavidin, Fig. 19), which was used as a reference, a surface coverage of 280 ± 5 ng/cm^2 was gained at a concentration of 100 µg/ml. This is almost the same surface coverage, as gained with ChiAvd-Cys/pTHMMAA –surface and amino-biotinylated F(ab´)$_2$s (270 ± 40 ng/cm^2). Antigen, hIgG, binding to the SA-chip at 100 µg/ml, was 120 ± 20 ng/cm^2, as onto the ChiAvd-Cys/pTHMMAA/biotin-F(ab´)$_2$ –surface, which is almost ten times the amount bound onto the corresponding surface made from the wt-Avd (Table 5, Fig. 18).

Finally, the human IgG binding to the surfaces made of ChiAvd-Cys/pTHMMAA/thiol-F(ab´)s was analysed. As can be seen from Fig. 18, these surfaces had the highest antigen binding: 200 ± 10 ng/cm^2 at hIgG concentration of 50 µg/ml. Binding to this surface made from thiol-biotinylated F(ab´)s was almost twice the amount bound on the amino-biotinylated surface assembled on ChiAvd-Cys/pTHMMAA or to commercial SA-chip.

However, from Fig. 18 it can be seen that the sensitivity below concentrations of 1 µg/ml is higher with the SA-chip. In the CM-matrix, it is possible to immobilize

many receptor molecules due to the multiple attachment sites (carboxyl groups) within the dextran molecules (Fig. 19), especially when compared to the planar layer solutions. Based on the results above, it seems that ChiAvd-Cys surfaces also form network-like structures, especially when the ChiAvd-Cys molecules are not reduced prior to assembly. Possibly, the sensitivity of the ChiAvd-Cys surfaces could still be improved.

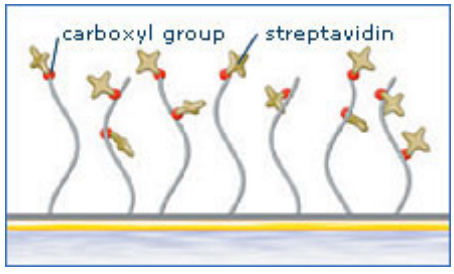

Figure 19. Commercial Biacore SA-chip: carboxymethylated dextran coated with streptavidin. Image adapted from Biacore 2013.

9.4 Long ssDNA detection (IV, V)

With surfaces for MDMA detection a lipoate-based molecule of Lipa-DEA was tested along with pTHMMAA-polymer as discussed in section 9.2. Non-ionic hydrophilic polymer of pTHMMAA is approximately 4 nm long (Vikholm-Lundin 2005, Vikholm-Lundin and Albers 2006), while Lipa-DEA is a shorter molecule and would thus work more efficiently with DNA-probes on surfaces. Polymer assembling with DNA-probes has been studied previously (Vikholm-Lundin et al. 2007, Vikholm-Lundin and Piskonen 2008), but in this study the aim was to test the functionality of Lipa-DEA with DNA-surfaces with respect to the probe, and product length for the hybridisation efficiency and effect of the protective groups (disulphide or thiol-modified probes) for surface assembly. The surface assembly of the probes was performed *in situ,* within 10–15 minutes, when it is normally allowed to take place for 5–16 hours (Boozer et al. 2004, Gong et al. 2006). The assembling process could be followed in real-time with SPR.

With such a real-time measurement it could be seen that adsorption of DMT-S-S-ssDNA and SH-probes on gold was very fast, and saturation coverage of the probes could be obtained within the measuring time of 10–15 minutes (Fig. 1 in IV). The surface coverages for different probes can be seen from Table 6. The blocking of the surface was done with a Lipa-DEA after the probe adsorption. The probe density was highest for the shorter probes of 16 and 18 mers with the DMT-S-S-modification. However, the densities for the complementary DNA were at the same level for the longer probes (25 and 27 mers) with the DMT-S-S- modification. Even SH-PTGS2-27 gave a surface density of $3.0 \pm 0.2 \times 10^{12}$ molecules/cm^2, despite the fact that the probe density was only $1.0 \pm 0.1 \times 10^{13}$ probes/cm^2. The other

probe with thiol-modification (SH-CALCA-25) gave the lowest hybridisation for complementary DNA (2.2 ± 0.2 x 10^{12} molecules/cm^2) with the same probe density as SH-PTGS2-27. Probe density of 1.1 x 10^{13} probes/cm^2 has also been reported by others (Peterson et al. 2002) for thiol-modified oligos. There seems to be a clear difference in surface coverage when comparing the shorter probes to the longer probes. It is likely that longer probes absorb to surfaces via multiple base groups besides the thiol or disulphide modification, and thus also have a lower surface coverage compared to the shorter probes. The SPR-responses of complementary DNA hybridization are, as expected, lower for shorter probes (Table 6).

Table 6. Surface densities of the different probes and of complementary DNA sequences. DMT-S-S refers to a probe with a disulphide (S-S) group and SH- with a free thiol group. Table modified from Publication IV and unpublished results included. The results of dispensed surfaces from Publication V are given in parentheses.

Probe[a]	BSA (RU)	ssDNA (RU)	Probe density[i]	Comp-DNA[b] (RU)	Comp-DNA density[ii]	Long ssDNA[b, c] (RU)
DMT-S-S-CALCA-18	20 ± 5	2200 ± 100	2.6 ± 0.1	270 ± 10	3.0 ± 0.1	n.d.
DMT-S-S-CALCA-25	10 ±5	1920 ± 200	1.5 ± 0.2	430 ± 10 (260 ± 10)	3.0 ± 0.1	950 ± 10[b] (500 ± 10[b])
SH-CALCA-25	70 ± 80	1460 ± 50	1.1 ± 0.05	300 ± 20	2.2 ± 0.2	n.d.
DMT-S-S-PTGS2-16	150 ± 70	1850 ± 100	2.2 ± 0.1	230 ± 20	2.9 ± 0.2	n.d.
DMT-S-S-PTGS2-27	110 ± 20	1430 ± 50	1.0 ± 0.1	360 ± 30 (320 ± 10)	2.7 ± 0.2	780 ± 20[c] (650 ± 10[b])
SH-PTGS2-27	110 ± 30	1400 ± 200	1.0 ± 0.2	410 ± 30	3.0 ± 0.2	1000 ± 20[c]

[a]60 µg/ml (= 4–20 µM) solution [i]10^{13} probes/cm^2 [b] 0.1 µM solution
[ii]10^{12} molecules/cm^2 [c]1.5 µM solution n.d. not determined

Non-specific binding of BSA was very low (Table 6), though markedly higher to PTGS2 surfaces than to CALCA surfaces, suggesting that the nucleotide sequence of PTGS2 is more prone to non-specific protein binding.

Specific hybridisation of the complementary DNA strands to SH-PTGS2-27 and DMT-S-S-PTGS2-27 is shown in Fig. 2a in Publication IV. At 10 nM complementary DNA concentration, the DMT-S-S- modified surface gave a response of 210 ± 10 RU, while the thiol-modified surface gave a response of 320 ± 10 RU. The higher response gained with the thiol-modified probes suggests that these probes have a more end-on orientation on the surface and thus better binding of the complementary oligos. The effect is, however, diminished with increased concentration.

Next, the hybridisation of the double- (ds) and single-stranded (ss) PCR products to the surfaces was studied. Single-stranded PCR products of 92–123 nucleotides

showed high hybridisation on the surfaces (Fig. 2b in IV). But the hybridisation of the corresponding double-stranded PCR products was very low: 33 ± 4 RU to SH-PTGS2-27 surface and 130 ± 25 RU to DMT-S-S-PTGS2-27 surface with a 40 nM solution of double-stranded PTGS2-123. When the same hybridisation was done with corresponding single-stranded PCR products, the responses at 40 nM solution were around 400 and 600 RU (Fig. 2b in IV) for the disulphide- and thiol-modified probe surfaces, respectively. At 1.5 µM concentration of the single-stranded products, the surfaces had yet not reached saturation, but gave very high hybridisation responses of 780 ± 20 RU (DMT-S-S-PTGS2-27) and 1000 ± 20 RU (SH-PTGS2-27). The amount of strands hybridised was 1.2 and 1.6 ± 0.1 x 10^{12} strands/cm^2 for the disulphide-modified and thiol-modified PTGS2 probes, respectively.

Also hybridisation of longer (344–642) single-stranded PCR products was tested, but they showed very little binding (10 ± 5 RU) on the surfaces, presumably due to the extensive secondary structure formation of the sequences hindering the hybridisation in the non-denaturing conditions used.

9.5 Long ssDNA detection in diluted serum (V)

In Publication V, the studies with DNA-surfaces and single-stranded PCR products hybridisation were taken further by studying the hybridisation in a diluted serum. In the previous study, the surfaces were made *in situ*, meaning that they were measured within 10–15 minutes after the initial assembly. In this study (V), the surfaces were dispensed and left to assemble for 3–6 days at 4°C in a humid atmosphere before measurements were taken. Measurements were also performed by FBAR resonators apart from SPR, but resonator measurements were performed elsewhere by other people, and thus only the SPR results are included in this thesis. Serum is the main fouling component in clinical samples, distracting in many measurements. It is especially problematic with systems containing microcapillaries. This is the reason why we wanted to test our DNA-probe surfaces and direct real-time measurements in diluted serum.

First, the amount of the non-specific binding to the probe/Lipa-DEA monolayers was measured in buffer. The NSB for 1.7 µM BSA and 0.5 µM non-complementary DNA solution was in the range 20–140 RU (Table 7) for the PTGS2/Lipa-DEA and CALCA/Lipa-DEA surfaces as measured with SPR. Non-specific binding of both BSA and non-complementary DNA was very low (20–60 RU) due to the Lipa-DEA, efficiently resisting non-specific binding onto the surface. However, the higher NSB for non-complementary DNA onto the CALCA/Lipa-DEA surfaces (140 RU) was also observed in Publication IV and seems to be CALCA-sequence related.

Table 7. SPR responses (RU) for hybridisation of short and long DNA strands with probe/Lipa-DEA dispensed surfaces. Samples were diluted either in buffer or in a 1% serum matrix.

	In buffer						In diluted serum	
Probe	BSA	Non-Comp DNA	Short strand 1nM	Short strand 1000 nM	Long strand 1nM	Long strand 1 000 nM	Long strand 1 nM	Long strand 1 000 nM
PTGS2	20±5	30±5	190±10	330±10	130±5	900±10	80±10	720±10
CALCA	60±20	140±15	130±5*	280±10	160±10	740±10	60±10	380±10

*10 nM
Table modified from Publication V

It was observed that hybridisation of both short and long complementary oligos diluted in buffer was very fast, and saturation was reached within minutes (Fig. 3 in V). As can be seen from the inset in Fig. 20 of PTGS2-27, at concentrations below 1 nM (19 ± 1 ng/cm^2) in buffer the surface densities were clearly lower (6–9 ng/cm^2), suggesting that detection limit lies at 1 nM for the detection of short complimentary oligos with this surface. With CALCA-25/Lipa-DEA surface, the detection limit for measurement of short complimentary oligos in buffer is higher, at 10 nM (Fig. 20 inset), if judged by the hybridisation responses. However, the NSB for CALCA surfaces was 140 ± 20 RU (Table 7), setting the detection limit up to 100 nM for this probe-sequence.

Hybridisation of the surfaces in buffer with 1 µM of complementary PTGS2-27 and CALCA-25 resulted in a response of 330 and 280 ± 10 RU (33 and 28 ± 1 ng/cm^2, respectively) (Table 7 and Fig. 20 inset). These correspond to target densities of 2.4 and 2.2 ± 0.1 x 10^{12} molecules/cm^2 for PTGS2-27 and CALCA-25 and are in accordance with published values in a similar system (Gong et al. 2006). However, when comparing the responses gained *in situ* in the previous section (9.4) to these dispensed surfaces, it can be observed from Table 6 (the values gained from dispensed surfaces are shown in parenthesis), that responses gained from dispensed surfaces are lower compared to the values gained with surfaces made *in situ* and especially with CALCA-sequence. This is most probably due to differences in the arrangement of the surface when the probes and lipoamide are assembled *in situ* or by dispensing, and seems also be related to the sequence.

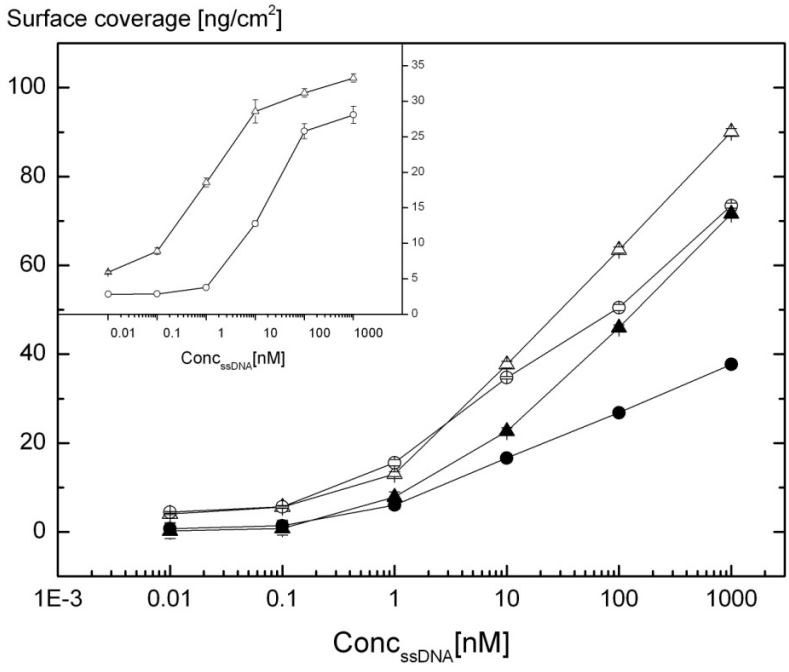

Figure 20. Hybridisation of long ssDNA strands to surfaces of Lipa-DEA and DMT-S-S-PTGS2-27 or DMT-S-S-CALCA-25 as measured with SPR. (Δ) for PTGS2-127 and (○) for CALCA-92. Open symbols refer to measurements performed with samples diluted in buffer and filled symbols with samples diluted in 1% serum. In the inset is shown the hybridisation of the short complementary strands of PTGS2-27 (Δ) and CALCA-25 (○) to the surfaces in buffer.

Serum (1% dilution) injections were performed three times prior to measuring the DNA samples spiked in 1% serum. The serum response gradually decreases with injections, settling down to 200 ± 50 RU after the third injection. Thus, for the zero sample, an NSB was obtained that was higher than that of BSA or non-complementary DNA (Table 7). As this response is already in the range of that obtained for complementary oligos in buffer, sub-nanomolar concentrations of short complementary DNA were not detectable (Fig. 20 inset) in serum. Because the response for hybridisation even at 1 µM concentration for short complementary oligos in buffer was only 105 ± 35 RU higher than the NSB of serum proteins, no marked responses were expected in serum.

Next, the hybridisation of the long ssDNA strands was studied, first in buffer and then in 1% serum. The 0.1 and 1 nM PTGS2-123 ssDNA strands in buffer resulted in a response of 60 and 130 ± 5 RU, respectively (Table 7 and Fig. 20). For CALCA-92 at 1 nM, the response was 160 ± 10 RU. At highest concentration (1 µM), the responses were 900 and 740 ± 10 RU for PTGS2-123 and CALCA-92, respectively, resulting in surface densities of 90 ± 1 ng/cm^2 and 74 ± 1 ng/cm^2.

When the long ssDNA strands were spiked in 1% serum, the responses after the serum baseline (200 ± 50 RU) subtraction were 80 ± 10 RU for PTGS2-127 and 60 ± 10 RU for CALCA-92 at 1 nM concentration. The responses of the lowest concentrations (0.01–0.1 nM) did not differ much from that of the serum. At 1 µM concentration, the response for PTGS2-127 was 720 ± 10 RU, which corresponds to $1.4 \pm 0.01 \times 10^{12}$ targets/cm^2. For CALCA-92 at 1 µM concentration in 1% serum the values were 380 ± 10 RU and $1.5 \pm 0.01 \times 10^{12}$ targets/cm^2, respectively.

By way of conclusion, it can be stated that, when the length of the pairing strand in hybridisation is increased and the non-fouling properties of the surface improved, long ssDNA strands spiked in serum can be detected down to a concentration of 1 nM.

10. Summary and further perspectives

The aim of this research has been to improve the biomolecular surfaces for sensitive detection by means of improved surface orientation of the recognising molecules. This goal has been achieved in all five publications, and demonstrated with antibodies, DNA probes and neuronal cells. The non-specific binding could also be efficiently minimised so that the functionality of the surfaces could also be demonstrated in difficult sample matrices of diluted serum and saliva.

HESC-derived neuronal cells could be attached selectively on polystyrene via NCAM-antibodies embedded in the surface of pTHMMAA-polymer. The number of surface attached neuronal cells was dependent on the amount of antibody on the surface. In the future, the NCAM-antibody polymer surfaces for neuronal cell attachment could be applied in cell-arrays for patterning of the cells in certain areas of the arrays. With different antibodies and concentrations the number of the cells in the array can also be controlled and different cell types applied.

For small molecule detection, a displacement assay with SPR was studied and found to work well even in diluted saliva. The sensitivity of the Fab'-MDMA-conjugate surfaces met the requirements of the application (limit of detection for MDMA in saliva is 10 ng/ml). It would be interesting to test the displacement assay with other small analytes to be detected in serum or even whole blood, but with an applicable measurement system that does not use micro-fluidistics.

ChiAvd-Cys chimeric avidin-molecules are an engineered version of avidin containing four additional C-terminal cysteines. It was demonstrated that one thiol-biotinylated antibody Fab'-fragment was bound to every ChiAvd-Cys molecule on the surface, while amino-biotinylated antibody $F(ab')_2$ fragments could be bound to every 8^{th} conventionally used wild-type avidin molecule. Antigen binding to the thiol-biotinylated Fab'-fragment bound to the ChiAvd-Cys/pTHMMAA -surface was almost two- and four-fold, when compared to that of the amino-biotinylated $F(ab')_2$-fragments assembled either on ChiAvd-Cys/pTHMMAA or on wt-Avd/ pTHMMAA -surface, respectively. These cys-tagged avidin surfaces could be optimized for commercial use in SPR-chips or in immuno well-plates.

The DNA-probes were assembled on surfaces with a lipoate-based molecule, Lipa-DEA. The surface density of these surfaces with shorter probes (16–18 mer) was observed to be twice ($2.4 \pm 0.2 \times 10^{13}$ probes/cm^2) that of the longer probes (25–27 mer) as studied with SPR. Hybridisation of single-stranded PCR products

with a length above 300 base pairs was found to give very low hybridisation responses, while for ssDNA products about 100 nucleotides long the response was high. The surface coverage was comparable to that of complementary ssDNA binding (3.0×10^{12} strands/cm^2). Surfaces made from SH-ssDNA showed a 30% higher hybridisation response than surfaces made from disulphide-modified probes (DMT-S-S-ssDNA). It was also noted that the assembling process of the probes on the gold can be performed within 15 minutes with good results. These observations can be useful in commercial DNA array manufacturing process.

The ~100 nucleotides long ssPCR products could also be detected in 1% serum solution by DNA probes assembled with Lipa-DEA on gold surfaces. A nanomolar detection range could be accomplished for short complimentary strands (25–27 mers) in buffer, while low nanomolar detection range was obtained for long strands both in buffer and in diluted serum. These results are encouraging for DNA analysis in difficult sample matrixes.

The field of SPR-biosensors is evolving very rapidly with the sensing surfaces as well as with the materials and the SPR-devices involved. The spearheads in sensor research aim at fast detection of clinically relevant analytes straight from the source with minimal sample handling, while there is still a need for something envisioned decades ago namely “easy to operate, independent and care-free biosensors” that can be used in solitary locations without the need for trained personnel and yet still saving lives.

References

Adamczyk, M., Gebler, J.C. and Wu, J. (2000) Papain digestion of different mouse IgG subclasses as studied by electrospray mass spectrometry. Journal of Immunological Methods 237: 95–104.

Ahluwalia, A., De Rossi, D., Ristori, C., Schirone, A. and Serra, G. (1992) A comparative study of protein immobilization techniques for optical immunosensors. Biosensors and Bioelectronics 7: 207–214.

Ahluwalia, A., Carra, M., De Rossi, D. and Ristori, C. (1994) Improvement of antibody surface density by orientation of reduced fragments. Thin Solid Films 247: 244–247.

Albers, W.M. (2010) A sensor element and its use. Finnish patent FI120698 B.

Albers, W.M., Munter, T., Laaksonen, P. and Vikholm-Lundin, I. (2010) Journal of Colloid and Interface Science 348: 1–8.

Bain, C.D. and Whitesides, G.M. (1989) Modeling organic surfaces with self-assembled monolayers. Angewandte Chemie-International Edition in English 28: 506–512.

Bayer, E.A. and Wilchek, M. (1990) Protein biotinylation. Methods in Enzymology 184: 138–160.

Beckett, D., Kovaleva, E. and Schatz, P.J. (1999). A minimal peptide substrate in biotin holoenzyme synthetase-catalyzed biotinylation. Protein Science 8: 921–929.

Biacore (2013) http.//www.biacore.com (last accessed 8.4.2013).

Biacore sensor surface handbook (2008) BR-1005-71 Edition AB 05/2008. GE Healthcare Bio-Sciences AB, Uppsala, Sweden.

Biatechnology handbook, version AB (reprinted 1998) Biacore AB, Uppsala, Sweden.

Björck, L. and Kronvall, G. (1984) Purification and some properties of streptococcal Protein G, a novel IgG-binding reagent. The Journal of Immunology 133: 969–974.

Bradford, M.M. (1976) A rapid and sensitive method for the quantitation of microgram quantities of protein utilizing the principle of protein-dye binding. Analytical Biochemistry 72: 248–254

Brash, J.L. and Horbett, T.A. (1995) Proteins at interfaces. Proteins at Interfaces II 5: 1–23.

Bonroy, K., Frederix, F., Reekmans, G., Dewolf, E., De Palma, R., Borghs, G., Declerck, P. and Goddeeris, B. (2006) Comparison of random and oriented immobilisation of antibody fragments on mixed self-assembled monolayers. Journal of Immunological Methods 312: 167–181.

Boozer, C., Ladd, J., Chen, S., Yu, Q., Homola, J. and Jiang, S. (2004) DNA directed protein immobilization on mixed ssDNA/oligo(ethylene glycol) self-assembled monolayers for sensitive biosensors. Analytical Biochemistry 76: 6967–6972.

Borisov, S.M. and Wolfbeis, O.S. (2008) Optical biosensors. Chemical reviews 108: 423–461.

Capadona, J.R., Collard, D.M. and Garcia, A.J. (2003) Fibronectin adsorption and cell adhesion to mixed monolayers of tri(ethylene glycol)- and methyl-terminated alkanethiols. Langmuir 19: 1847–1852.

Carter, P., Kelley, R.F., Rodrigues, M.L., Snedecor, B., Covarrubias, M., Velligan, M.D., Wong, W.L., Rowland, A.M., Kotts, C.E., Carver, M.E., Yang, M., Bourel, J.H., Shepard, H.M. and Henner, D. (1992) High level *Escherichia coli* expression and production of a bivalent humanized antibody fragment. Biotechnology 10: 163–167.

Catimel, B., Nerrie, M., Lee, F.T., Scott, A.M., Ritter, G., Welt, S., Old, L.J., Burgess, A.W. and Nice, E.C. (1997) Kinetic analysis of the interaction between the monoclonal antibody A33 and its colonic epithelial antigen by the use of an optical biosensor; a comparison of immobilization strategies. Journal of Chromatography 776: 15–30.

Chen, Y.-X., Triola, G. and Waldmann, H. (2011) Bioorthogonal chemistry for site-specific labelling and surface immobilization of proteins. Accounts of Chemical Research 44: 762–773.

Chapman, R.G., Ostuni, E., Takayama, S., Homlin, R.E., Yan, L. and Whitesides, G.M. (2000) Surveying for surfaces that resist the adsorption of proteins. Journal of American Chemical Society 122: 8303–8304.

Clark, L.C. Jr and Lyons, C. (1962) Electrode systems for continuous monitoring in cardiovascular surgery. Annals of the New York Academy of Sciences 102: 29–45.

Conroy, P.J., Hearty, S., Leonard, P. and O'Kennedy, R.J. (2009) Antibody production, design and use for biosensor-based applications. Seminars in Cell & Developmental Biology 20: 10–26.

Cooper, M.A. (2002) Optical biosensors in drug discovery. Nature Reviews 1: 515–528.

Dettin, M., Muncan, N., Bugatti, A., Grezzo, F., Danesin, R. and Rusnati, M. (2011) Chemoselective surface immobilization of proteins through a cleavable peptide. Bioconjugate Chemistry 22: 1753–1757.

Di Primo, C. and Lebars, I. (2007) Determination of refractive index increment ratios for protein-nucleic acid complexes by surface plasmon resonance. Analytical Biochemistry 362: 148–155.

Dostalek, J., Ladd, J., Jiang, S. and Homola, J. (2006) SPR biosensors for detection of biological and chemical analytes. Springer Series Chemical Sensing and Biosensing 4: 177–190.

Fan, X., White, I.M., Shopova, S.I., Zhu, H., Suter, J.D. and Sun, Y. (2008). Sensitive optical biosensors for unlabelled targets: A review. Analytica Chimica Acta 620: 8–26.

Fernandez-Lafuente, R., Rosell, C.M., Rodriguez, V., Santana, C., Soler, G., Bastida, A. and Guisan, J.M. (1993) Preparation of activated supports containing low pK amino groups. A new tool for protein immobilization via the carboxyl coupling methods. Enzyme and Microbial Technology 15: 546–550.

Filpula, D. (2007) Antibody engineering and modification technologies. Biomolecular Engineering 24: 201–215.

Forsgren, A. and Sjöquist, J. (1966) "Protein A" from *S. Aureus*. Pseudo-immune reaction with human γ-globulin. The Journal of Immunology 97: 822–827.

Gerdes, M., Meusel, M. and Spener, F. (1997) Development of a displacement immunoassay by exploiting cross-reactivity of a monoclonal antibody. Analytical Biochemistry 252: 198–204.

Gong, P., Lee, C.-Y., Gamble, L.J., Castner, D.G. and Grainger, D.W. (2006) Hybridization behaviour of mixed DNA/alkylthiol monolayers on gold: characterisation by surface plasmon resonance and ^{32}P radiometric assay. Analytical Chemistry 78: 3326–3334.

Green, N.M. (1975) Avidin. Advances in Protein Chemistry 29: 85–133.

Green, N.M. (1990) Avidin and streptavidin. Methods in Enzymology 184: 51–67.

Harder, P., Grunze, M., Dahint, R., Whitesides, G.M. and Laibinis, P.E. (1998) Molecular conformation in oligo(ethylene glycol)-terminated self-assembled monolayers on gold and silver surfaces determines their ability to resist protein adsorption. Journal of Physical Chemistry B 102: 426–436.

Harlow, E. and Lane, D. (1988) Antibodies: a laboratory manual. Cold Spring Harbor Laboratory, Cold Spring Harbor, N.Y.

Herne, T.M. and Tarlov, M.J. (1997) Characterisation of DNA probes immobilized on gold surfaces. Journal of American Chemical Society 119: 8916–8920.

Hober, S., Nord, K. and Linhult, M. (2007) Protein A chromatography for antibody purification. Journal of Chromatography B 848: 40–47.

Hoffman, W.L. and O'Shannessy, D.J. (1988) Site-specific immobilization of antibodies by their oligosaccharide moieties to new hydrazide derivatized solid supports. Journal of Immunological Methods 112: 113–120.

Homola, J. (2003) Present and future of surface plasmon resonance biosensors. Analytical and Bioanalytical Chemistry 377: 528–539.

Homola, J. (2008) Surface plasmon resonance sensors for detetction of chemical and biological species. Chemical Reviews 108: 462–493.

Homola, J., Yee, S.S. and Gauglitz, G. (1999) Surface plasmon resonance sensors: review. Sensors and Actuators B 54: 3–15.

Horbett, T.A. and Brash, J.L. (1987) Proteins at interfaces: Current issues and future prospects. Proteins at Interfaces 13: 1–33.

Howorka, S., Cheley, S. and Bayley, H. (2001) Sequence-specific detection of individual DNA strands using engineered nanopores. Nature Biotechnology 19: 636–639.

Hubbell, J.A. (1999) Bioactive biomaterials. Current Opinion in Biotechnology 10: 123–129.

Inouye, K. and Ohnaka, S. (2001) Pepsin digestion of a mouse monoclonal antibody of IgG1 class formed $F(ab')_2$ fragments in which the light chains as well as the heavy chains were truncated. Journal of Biochemical and Biophysical Methods 48: 23–32.

Ishikawa, E., Imagawa, M., Hashida, S., Yoshitake, S., Hamaguchi, Y. and Ueno, T. (1983) Enzyme-labeling of antibodies and their fragments for enzyme immunoassay and immunohistochemical staining. Journal of Immunoassay 4: 209–327.

Jeong, H.-H., Erdene, N., Park, J.-H., Jeong, D.-H., Lee, H.-Y. and Lee, S.-K. (2013) Real-time label-free immunoassay of interferon-gamma and prostate-specific antigen using a Fiber-Optic Localized Surface Plasmon Resonance sensor. Bionsensors and Bioelectronics 39: 346–351.

Johnsson, B., Löfås, S. and Lindquist, G. (1991) Immobilization of proteins to carboxymethyldextran- modified gold surface for biospecific interaction analysis in surface plasmon resonance sensors. Analytical Biochemistry 198: 268–277.

Johnsson, B., Löfås, S., Lindquist, G., Edström, Å., Müller Hillgren, R.-M. and Hansson, A. (1995) Comparison of methods for immobilization to carboxymethyldextran sensor surfaces by analysis of the specific activity of monoclonal antibodies. Journal of Molecular Recognition 8: 125–131.

Jones, R.G.A and Landon, J. (2003) A protocol for “enhanced pepsin digestion”: a step by step method for obtaining pure antibody fragments in high yield from serum. Journal of Immunological Methods 275: 239–250.

Jung, Ch., Dannenberger, O., Xu, Y., Buck, M. and Grunze, M. (1998) Self-assembled monolayers from organosulfur compounds: A comparison between sulfides, disulfides and thiols. Langmuir 14: 1103–1107.

Jung, J.P., Nagaraj, A.K., Fox, E.K., Rudra, J.S., Devgun, J.M. and Collier, J.H. (2009) Co-assembling peptides as defined matrices for endothelial cells. Biomaterials 30: 2400–2410.

Kamphuis, I.G., Drenth, J. and Baker, E.N. (1985) Thiol proteases. Comparative studies based on the high-resolution structures of papain and actinidin, and amino acid sequence information for cathepsins B and H, and stem bromelain. Journal of Molecular Biology 20: 317–329.

Katardjiev, I. and Yantchev, V. (2012) Recent developments in thin film electro-acoustic technology for biosensor applications. Vacuum 86: 520–531.

Kausaite-Minkstimiene, A., Ramanaviciene, A., Kirlyte, J. and Ramanavicius, A. (2010) Comparative study of random and oriented antibody immobilization

techniques on the binding capacity of immunosensor. Analytical Chemistry 82: 6401–6408.

Kenna, J.G., Major, G.N. and Williams, R.S. (1985) Methods for reducing non-specific antibody binding in enzyme-linked immunosorbent assays. Journal of Immunological Methods 85: 409–419.

Kibbe, W.A. (2007) OligoCalc: an online oligonucleotide properties calculator. Nucleic Acids Research 35: W43–W46.

Kingshott, P. and Griesser, H.J. (1999) Surfaces that resist bioadhesion. Current Opinion in Solid State and Materials Science 4: 403–412.

Klenkar, G. and Liedberg, B. (2008) A microarray chip for label-free detection of narcotics. Analytical and Bioanalytical Chemistry 391: 1679–1688.

Knight, C.G., Morton, L.F., Peachey, A.R., Tuckwell, D.S., Farndale, R.W. and Barnes, M.J. (2000) The collagen-binding A-domains of integrins α1β1 and α2β1 recognize the same specific amino acid sequence, GFOGER, in native (triple-helical) collagens. The Journal of Biological Chemistry 275: 35–40.

Kretschmann, E. and Raether, H. (1971) The determination of optical constants of metal by excitation of surface plasmons. Z. Phys. 241: 313–321.

Ladd, J., Boozer, C., Yu, Q., Chen, S., Homola, J. and Jiang, S. (2004) DNA-directed protein immobilization on mixed self-assembled monolayers via a streptavidin bridge. Langmuir 20: 8090–8095.

Laemmli, U.K. (1970) Cleavage of structural proteins during the assembly of the head of bacteriophage T4. Nature 227: 680–685.

Laitinen, O.H., Nordlund, H.R., Hytönen, V.P. and Kulomaa, M.S. (2007). Brave new (strept)avidins in biotechnology. Trends in Biotechnology 25:269–277.

Larsson, A., Angbrant, J., Ekeroth, J. Månsson, P. and Liedberg, B. (2006) A novel biochip technology for detection of explosives – TNT: Synthesis, characterisation and application. Sensors and Actuators B 113: 730–748.

Lee, C.-Y., Gong, P., Harbers, G.M., Grainger, D.W., Castner, D.G. and Gamble, L.J. (2006) Surface coverage and structure of mixed DNA/alkylthiol monolayers on gold: Characterisation by XPS, NEXAFS, and fluorescence intensity measurements. Analytical Chemistry 78: 3316–3325.

Lee, D. and Ryle, A.P. (1967) Pepsinogen D. A fourth proteolytic zymogen from pig gastric mucosa. Biochemical Journal 104: 735–741.

Lempens, E.H.M., Helms, B.A., Merkx, M. and Meijer, E.W. (2009) Efficient and chemoselective surface immobilization of proteins by using aniline-catalyzed oxime chemistry. Chemical Biological Chemistry 10: 658–662.

Ley, C., Holtmann, D., Mangold, K.-L. and Schrader, J. (2011) Immobilization of histidine-tagged proteins on electrodes. Colloids and Surfaces B: Biointerfaces 88: 539–551.

Liedberg, B., Nylander, C. and Lundström, I. (1983) Surface plasmon resonance for gas detection and biosensing. Sensors and Actuators 4: 299–304.

Liener, I.E. and Friedenson, B. (1970) Ficin. Methods in Enzymology 19:261–273.

Life Technologies (2013) http://www.lifetechnologies.com (last accessed 8.4.2013).

Löfås, S. and Johnsson, B. (1990) A novel hydrogel matrix on gold surfaces in surface plasmon resonance sensors for fast and efficient covalent immobilization of ligands. Journal of Chemical Society: Chemical Communications: 1526–1528.

Löfås, S., Johnsson, B., Edström, Å., Hansson, A., Lindquist, G., Müller Hillgren, R.-M. and Stigh, L. (1995) Methods for site controlled coupling to carboxymethyldextran surfaces in surface plasmon resonance sensors. Biosensors and Bioelectronics 10: 813–822.

Love, J.C., Estroff, L.A., Kriebel, J.K., Nuzzo, R.G. and Whitesides, G.M. (2005) Self-assembled monolayers of thiolates on metals as a form of nanotechnology. Chemical Reviews 105: 1103–1169.

Lucarelli, F., Tombelli, S., Minunni, M., Marrazza, G. and Mascini, M. (2008) Electrochemical and piezoelectronic DNA biosensors for hybridisation detection. Analytica Chimica Acta 609: 139–159.

Luk, Y.-Y., Kato, M. and Mrksich, M. (2000) Self-assembled monolayers of presenting mannitol groups are inert to protein adsorption and cell attachment. Langmuir 16: 9604–9608.

Luo, S. and Walt, D.R. (1989) Avidin-biotin coupling as a general method for preparing enzyme-based fiber-optic sensors. Analytical Chemistry 61: 1069–1072.

Mariani, M., Camagna, M., Tarditi, L. and Seccamani, A. (1991) A new enzymatic method to obtain high-yield $F(ab)_2$ suitable for clinical use from Mouse IgG1. Molecular Immunology 28: 69–77.

Millner, P.A., Hays, H.C.W., Vakurov, A., Pchelintsev, N.A., Billah, M.M. and Rodgers, M.A. (2009) Nanostructured transducer surfaces for electrochemical biosensor construction – Interfacing the sensing component with the electrode. Seminars in Cell & Developmental Biology 20: 34–40.

Müller, K.M., Arndt, K.M., Bauer, K. and Plückthun, A. (1998) Tandem immobilized metal-ion affinity chromatography/immunoaffinity purification of His-tagged proteins – evaluation of two anti-His-tag monoclonal antibodies. Analytical Biochemistry 259: 54–61.

Nakaji-Hirabayashi, T., Kato, K., Arima, Y. and Iwata, H. (2007) Oriented immobilization of epidermal growth factor onto culture substrates for the selective expansion of neural stem cells. Biomaterials 28: 3517–3529.

Nakanishi, K., Sakiyama, T. and Imamura, K. (2001) On the adsorption of proteins on solid surfaces, a common but very complicated phenomenon. Journal of Bioscience and Engineering 91: 233–244.

Nath, N., Hyun, J., Ma, H. and Chilkoti, A. (2004) Surface engineering strategies for control of protein and cell interactions. Surface Science 570: 98–110.

Nelson, C.M., Raghavan, S., Tan, J.L. and Chen, C.S. (2003) Degradation of micropatterned surfaces by cell-dependent and –independent processes. Langmuir 19: 1493–1499.

Nieba, L., Nieba-Axmann, S.E., Persson, A., Hämäläinen, M., Edebratt, F., Hansson, A., Lidholm, J., Magnusson, K., Frostell Karlsson, Å., Plückthun, A. (1997) Biacore analysis of histidine-tagged proteins using a chelating NTA sensor chip. Analytical Biochemistry 252: 217–228.

Niemeyer, C.M., Boldt, L., Ceyhan, B. and Blohm, D. (1999) DNA-directed immobilization: efficient, reversible, and site-selective surface binding of proteins by means of covalent DNA-streptavidin conjugates. Analytical Biochemistry 268: 54–63.

Nisonoff, A., Wissler, F.C., Lipman, L.N. and Woernley, D.L. (1960) Properties of univalent fragments of rabbit antibody isolated by specific adsorption. Archives of Biochemistry and Biophysics 89: 230–244.

Niu, Y., Matos, A.I., Abrantes, L.M., Viana, A.S. and Jin, G. (2012) Antibody oriented immobilization on gold using the reaction between carbon disulfide and amine groups and its application in immunosensing. Langmuir 28: 17718–17725.

O'Brien, J.C., Jones, V.W. and Porter, M.D. (2000) Immunosensing platforms using spontaneously adsorbed antibody fragments on gold. Analytical Chemistry 72: 703–710.

Ostuni, E., Chapman, R.G., Holmlin, R.E., Takayama, S. and Whitesides, G.M. (2001) A survey of structure-property relationships of surfaces that resist the adsorption of protein. Langmuir 17: 5605–5620.

Otsuka, H. (2010) Nanofabrication of nonfouling surfaces for micropatterning of cell and microtissue. Molecules 15: 5525–5546.

Otsuka, H., Hirano, A., Nagasaki, Y., Okano, T., Horiike, Y. and Kataoka, K. (2004) Two-dimensional multiarray formation of hepatocytes spheroids on a microfabricated PEG-brush surface. Chemical Biological Chemistry 5: 850–855.

Otto, A. (1968) Excitation of non-radiative surface plasma waves in silver by the method of frustrated total reflection. Z. Phys. 216: 398–405.

Peluso, P., Wilson, D.S., Do, D., Tran, H., Venkatasubbaiah, M., Quincy, D., Heidecker, B., Poindexter, K., Tolani, N., Phelan, M., Witte, K., Jung, L.S., Wagner, P. and Nock, S. (2003) Optimizing antibody immobilization strategies for the construction of protein microarrays. Analytical Biochemistry 312: 113–124.

Peterson, A.W., Wolf, L.K. and Georgiadis, R.M. (2002) Hybridization of mismatched or partially matched DNA at surfaces. Journal of American Chemical Society 124: 14601–14607.

Prime, K.L. and Whitesides, G.M. (1991) Self-assembled organic monolayers: model systems for studying adsorption of proteins at surfaces. Science 252: 1164–1167.

Ranieri, J.P., Bellamkonda, R. Bekos, E.J. Vargo, T.G., Gardella, J.A. and Aebischer, P. (1995) Neuronal cell attachment to fluorinated ethylene-propylene films with covalently immobilized laminin oligopeptides YIGSR and IKVAV 2. Journal of Biomedical Materials Research 29: 779–785.

Raynor, J.E., Capadona, J.R., Collard, D.M., Petrie, T.A. and Garcia, A.J. (2009) Polymer brushes and self-assembled monolayers: versatile platforms to control cell adhesion to biomaterials (review). Biointerphases 4: FA3–FA16.

Roitt, I., Brostoff, J. and Male, D. (1996) Immunology, 4th edition. Times Mirror International Publishers Limited.

Ronkainen, N.J., Halsall, H.B. and Heineman. W.R. (2010) Electrochemical biosensors. Chemical Society Reviews 39: 1747–1763.

Rowan, A.D., Buttle, D.J. and Barrett, A.J. (1990) The cysteine proteinases of the pineapple plant. Biochemical Journal 266: 869–875.

Ruoslahti, E. and Pierschbacher, M.D. (1987) New perspectives in cell adhesion: RGD and integrins. Science 238: 491–497.

Rusmini, F., Zhong, Z. and Feijen, J. (2007) Protein immobilization strategies for protein biochips. Biomacromolecules 8: 1775–1789.

Sigal, S.B., Bamdad, C., Barberis, A., Strominger, J. and Whitesides, G.M. (1996) A self-assembled monolayer for the binding and study of histidine-tagged proteins by surface plasmon resonance. Analytical Chemistry 68: 490–497.

Song, H.Y., Zhou, X., Hobley, J. and Su, X. (2012) Comparative study of random and oriented antibody immobilization as measured by dual polarization interferometry and surface plasmon resonance spectroscopy. Langmuir 28: 997–1004.

Spinke, J., Liley, M., Schmitt, F.-J., Guder, H.-J., Angermaier, L. and Knoll, W. (1993a) Molecular recognition at self-assembled monolayers: Optimization of surface functionalisation. Journal of Chemical Physics 99: 7012–7018.

Spinke, J., Liley, M., Guder, H.-J., Angermaier, L. and Knoll, W. (1993b) Molecular recognition at self-assembled monolayers: the construction of multicomponent multilayers. Langmuir 9: 1821–1825.

Steel, A.B., Herne, T.M. and Tarlov, M.J. (1998) Electrochemical quantitation of DNA immobilized on gold. Analytical Chemistry 70: 4670–4677.

Stenberg, E., Persson, B., Roos, H. and Urbaniczky, C. (1991) Quantitative determination of surface concentration of protein with surface plasmon resonance using radiolabeled proteins. Journal of Colloid and Interface Science 143: 513–526.

Tappura, K., Vikholm-Lundin, I. and Albers, W.M. (2007) Lipoate-based imprinted self-assembled molecular thin films for biosensor applications. Biosensors and Bioelectronics 22: 912–919.

Tombelli, S., Mascini, M. and Turner, A.P. (2002) Improved procedures for immobilization of oligonucleotides on gold-coated piezoelectric quartz crystals. Biosensors and Bioelectronics 17: 929–936.

Turner, A.P.F., Karube, I. and Wilson, G.S. (1987) Biosensors: Fundamentals and Applications. Oxford University Press, Oxford. 770 p.

Ulman, A. (1996) Formation and structure of self-assembled monolayers. Chemical reviews 96: 1533–1554.

Unsworth, L.D., Sheardown, H. and Brash, J.L. (2005) Protein resistance of surfaces prepared by sorption of end-thiolated poly(ethylene glycol) to gold: effect of surface chain density. Langmuir 21: 1036–1041.

Vashist, S.K. (2012) Effect of antibody modifications on its biomolecular binding as determined by surface plasmon resonance. Analytical Biochemistry 421: 336–338.

Vikholm, I., Györvary, E. and Peltonen, J. (1996) Incorporation of lipid-tagged single-chain antibodies into lipid monolayers and the interaction with antigen. Langmuir 12: 3276–3281.

Vikholm, I. (2005) Self-assembly of antibody fragments and polymers onto gold for immunosensing. Sensors and actuators B: Chemical 106: 311–316.

Vikholm-Lundin, I. (2005) Immunosensing based on site-directed immobilization of antibody fragments and polymers that reduce non-specific binding. Langmuir 21: 6473–6477.

Vikholm-Lundin, I. and Albers, W.M. (2006) Site-directed immobilisation of antibody fragments for detection of C-reactive protein. Biosensors and Bioelectronics 21: 1141–1148.

Vikholm-Lundin, I., Piskonen, R. and Albers, W.M. (2007) Hybridisation of surface-immobilised single-stranded oligonucleotides and polymer monitored by surface plasmon resonance. Biosensors and Bioelectronics 22: 1323–1329.

Vikholm-Lundin, I. and Piskonen, R. (2008) Binary monolayers of single-stranded oligonucleotides and blocking agent for hybridization. Sensors and Actuators B, Chemical 134: 189–192.

Wang, J. (2000) Glucose biosensors: 40 years of advances and challenges. Electroanalysis 13: 983–988.

Wang, F.X., Rodriguez, F.J., Albers, W.M. and Kauranen, M. (2010). Enhancement of bulk-type multipolar second-harmonic generation arising from surface morphology of metals. New Journal of Physics 12: 063009–063020.

Willander, M. and Al-Hilli, S. (2009) Analysis of biomolecules using surface plasmons. Methods in Molecular Biology 544: 201–229.

Wingqvist, G. (2010) AlN-based sputter-deposited shear mode thin film bulk acoustic resonator (FBAR) for biosensor applications – A review. Surface & Coatings Technology 205: 1279–1286.

Wingqvist, G., Anderson, H., Lennartsson, C., Weissbach, T., Yantchev, V. and Lloyd Spetz, A. (2009) On the applicability of high frequency acoustic shear mode biosensing in view of thickness limitations set by the film resonance. Biosensors and Bioelectronics 24: 3387–3390.

Yoshimoto, K., Nishio, M., Sugasawa, H. and Nagasaki, Y. (2010) Direct observation of adsorption-induced inactivation of antibody fragments surrounded by mixed-PEG layer on a gold surface. Journal of American Chemical Society 132: 7982–7989.

You, C., Bhagawati, M., Brecht, A. and Piehler, J. (2009) Affinity capturing for targeting proteins into micro and nanostructures. Analytical and Bioanalytical Chemistry 393: 1563–1570.

Zeng, X., Andrade, C.A.S., Oliviera, M.D.L. and Sun, X.-U. (2012) Carbohydrate-protein interactions and their biosensing applications. Analytical and Bioanalytical Chemistry 402: 3161–3176.

Zhu, H. and Snyder, M. (2003) Protein chip technology. Current Opinion in Chemical Biology 7: 55–63.

Appendix V of this publication is not included in the PDF version.
Please order the printed version to get the complete publication.
(http://www.vtt.fi/publications/index.jsp).

PUBLICATION I

An antibody surface for selective neuronal cell attachment

In: Journal of Neuroscience Methods (2010),
186: 72–76.

Journal of Neuroscience Methods 186 (2010) 72–76

Contents lists available at ScienceDirect

Journal of Neuroscience Methods

journal homepage: www.elsevier.com/locate/jneumeth

Short communication

An antibody surface for selective neuronal cell attachment

Sanna Auer[a,*,1], Riikka S. Lappalainen[b,1], Heli Skottman[b], Riitta Suuronen[b], Susanna Narkilahti[b], Inger Vikholm-Lundin[a]

[a] VTT Technical Research Centre of Finland, P.O. Box 1300, FIN-33101 Tampere, Finland
[b] Regea Institute for Regenerative Medicine, University of Tampere and Tampere University Hospital, Biokatu 12, FM-5, FIN-33520 Tampere, Finland

ARTICLE INFO

Article history:
Received 6 August 2009
Received in revised form 28 October 2009
Accepted 4 November 2009

Keywords:
Antibody
Neural cell adhesion molecule
Neuronal cells
Stem cells
Surface plasmon resonance

ABSTRACT

An optimal surface for culturing human embryonic stem cell (hESC)-derived neuronal cells is of high interest. In this study, a specific antibody to a neural cell adhesion molecule (NCAM) was immobilised on a solid surface of polystyrene and used as a selective matrix for culturing of hESC-derived neuronal cells. Thereafter, hESC-derived neurospheres were seeded on the matrix. The neurospheres did not attach to the NCAM antibody containing matrix whereas individual neuronal cells did. The neuronal cell attachment was depended on the NCAM antibody concentration. The neuronal cells were viable on the NCAM antibody containing matrix during an 8 day follow-up and exhibited typical bipolar morphology of immature neurons. Specific binding of the NCAM antigen to an immunoglobulin-polymer coated surface was verified by surface plasmon resonance (SPR) measurements. This study is to our knowledge the first demonstrating the use of an antibody layer as a selective surface for hESC-derived neuronal cells.

1. Introduction

The growth and maturation of human embryonic stem cell (hESC)-derived neuronal cells requires a supporting matrix to which cells can adhere. The most used matrixes for this purpose are extracellular proteins like laminin, collagen, or fibronectin (Flanagan et al., 2006; Whittemore et al., 1999; Rappa et al., 2004). HESCs are pluripotent cells typically derived from poor quality embryos donated by couples undergoing *in vitro* fertilization treatments. In theory, hESCs can be differentiated into all cell types of the human body including neuronal cells (Skottman et al., 2007). Indeed, hESCs have been differentiated into neural precursor cells and further into different neuronal subtypes and glial cells (Guillaume and Zhang, 2008). Since current differentiation protocols produce not entirely homogenous populations containing both neural and non-neural cells, a selective surface supporting only neural cell attachment, growth and maturation is highly desirable.

Examples of more selective growth matrices for cells can be found: oriented surfaces of an epidermal growth factor have been used with rat fetal neural stem cells (Nakaji-Hirabayashi et al., 2007) and specific terminal peptide sequences of laminin (pentamer IKVAV) or fibronectin (tetramer RGDS) have also been utilized in recent publications in culturing of among others human umbilical vein endothelial cells (Jung et al., 2009). Antibodies for defined cell-surface targets would offer an even more selective attachment and growth surface. The neural cell adhesion molecule (NCAM) is a binding glycoprotein expressed on the surface of neurons, glia, skeletal muscle, and natural killer cells. NCAM has been implicated in having a role in cell–cell adhesion and neurite outgrowth (Ditlevsen et al., 2008). Thus, an NCAM specific antibody might be used as a supportive and selective matrix for binding of neuronal cells.

Our aim in this study has been to clarify if surface immobilised antibodies to a defined target on the cell surface can be used to alleviate cell attachment. We have previously immobilised antibody Fab′-fragments site-directly onto gold through the free thiol groups and included hydrophilic polymers in between the proteins to hinder non-specific binding (Vikholm-Lundin and Albers, 2006; Vikholm-Lundin et al., 2007). The role of the polymer on the surface is to provide a hydrophilic surrounding for the antibodies and to preserve the native-like water-surrounded environment. First, we studied the interaction of NCAM antigen with binary monolayers composed of anti-NCAM antibodies physisorbed on gold and post-treated with a non-ionic hydrophilic polymer *N*-[tris(hydroxymethyl)methyl]-acrylamide (pTHMMAA). Secondly, neuronal cells derived from hESCs were allowed to attach on layers composed of only the polymer, or anti-NCAM antibodies and the polymer on polystyrene, which is the surface normally used for culturing of cells. To our knowledge this is the first study demonstrating the use of a selective antibody surface for attachment of hESC-derived neuronal cells and could be a very useful technique also for other researchers working in this field.

* Corresponding author. Tel.: +358 40 701 9272; fax: +358 20 722 3319.
E-mail address: Sanna.Auer@vtt.fi (S. Auer).
[1] Equal contribution.

0165-0270/$ – see front matter © 2009 Elsevier B.V. All rights reserved.
doi:10.1016/j.jneumeth.2009.11.002

2. Materials and methods

2.1. Materials for surface construction and SPR measurements

The anti-NCAM antibodies developed by P.W. Andrews (Andrews et al., 1990) were purchased from the Developmental Studies Hybridoma Bank (University of Iowa, IA). The NCAM antigen was purchased from Abcam (Cambridge, UK) and was specified as "Recombinant fragment, corresponding to amino acids 20–220 of Human NCAM", which covers the first two extracellular N-terminal Ig-like domains of the protein. Buffers used were 10 mM HEPES-buffer containing 150 mM NaCl, pH 6.8 and phosphate-buffered saline (PBS) composed of 50 mM Na_2HPO_4/NaH_2PO_4, 150 mM NaCl, pH 7.5. HEPES (N-[2-hydroxyethyl] piperazine-N′-[2-ethanesulfonic acid]) (minimum 99.5%) was purchased from Sigma–Aldrich (Steinheim, Germany), Na_2HPO_4 was purchased from Merck, NaH_2PO_4 and NaCl from J.T. Baker. The polymer of *N*-[tris(hydroxymethyl)methyl]-acrylamide (pTHMMAA) (Fig. 1A) was prepared as previously described (Vikholm-Lundin et al., 2007). Polystyrene well plates were purchased from Nunc, Thermo Fisher Scientific, Rochester, NY. Hydrogen-peroxide (30%) was bought from Merck KGaA and ammonium hydroxide (28–30% NH3) and bovine serum albumin (BSA, minimum 98% purity) from Sigma–Aldrich.

2.2. Antibody–polymer layers on gold for SPR measurements

Studies on binary monolayer formation of antibodies and polymer on gold were carried out on gold *in situ* with surface plasmon resonance (SPR) (Biacore 3000, GE Healthcare). Thin glass slides were coated with a 50 nm thin gold layer in-house by RF magnetron sputtering. The gold surfaces were always cleaned in a boiling solution of hydrogen-peroxide–ammonia in water (1:1:5) and rinsed with water prior to surface assembling. Instantly after the cleaning step, the slides were mounted in a plastic chip cassette by double-sided tape and inserted into the Biacore 3000 SPR instrument. First, the antibody was allowed to physisorb on the pre-cleaned gold surface for 15 min, followed typically by 10 min wash with PBS buffer. Next, the pTHMMAA polymer at a concentration of 200 μg/mL was post-adsorbed on the surface. Non-specific binding was measured by running BSA at a concentration of 500 μg/mL on the surface. The NCAM antigen binding was measured in HEPES-buffer by injecting increasing concentrations of antigen (0.0001–10 μg/mL) over the surface and rinsing with HEPES-buffer.

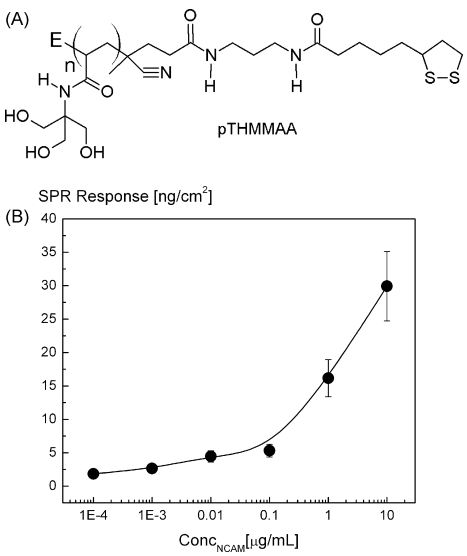

Fig. 1. (A) The structure of the pTHMMAA–polymer. (B) SPR standard curve showing NCAM antigen binding to a layer composed of anti-NCAM antibodies and pTHMMAA–polymer spread from concentration of 50 and 200 μg/mL, respectively.

2.3. Human embryonic stem cells and neural differentiation

The hESC lines used were Regea 06/040 or 08/023, derived and characterized at Regea - Institute for Regenerative Medicine, University of Tampere, Finland (Skottman, in press; European Human Embryonic Stem Cell Registry, www.hescreg.eu). Regea has the approval from the Ethics Committee of the Pirkanmaa Hospital district in Finland to derivate, culture, and differentiate new hESC lines from surplus embryos after obtaining signed informed consent from donating couples undergoing *in vitro* fertilization treatment. Briefly, hESCs were cultured in an undifferentiated stage in Knockout Dulbecco's Modified Eagle Medium (DMEM) supplemented with 20% Knockout serum replacement, 2 mM GlutaMax, 0.1 mM 2-mercaptoethanol (all from Gibco Invitrogen, Carlsbad, CA), 1% non-essential amino acids (Cambrex Bio Science, East Rutherford, NJ), 50 U/mL penicillin/streptomycin (Lonza Group Ltd., Switzerland), and 8 ng/mL basic fibroblast growth factor (bFGF R&D Systems, Minneapolis, MN) on top of a human feeder cell layer (CRL-2429, ATCC, Manassas, CA). The undifferentiated stage of hESCs was assessed daily by morphologic analysis and periodic immunostaining for hESC-markers Nanog, OCT-3/4, SSEA-4, and Tra-1-60. In addition, karyotyping was performed and indicated that the hESC lines maintained normal karyotype. All cultures were tested mycoplasma-free.

The differentiation protocol (Hicks et al., 2009) was further developed from Nat et al. (2007). For neural differentiation the hESC colonies were manually dissected into small clusters containing ~3000 cells which were transferred into 6-well ultra low attachment plates (Nunc), and cultured as floating aggregates, hereafter called neurospheres, for 6 weeks prior to plating on the NCAM antibody matrix. The neural differentiation medium consisted of 1:1 DMEM/F12:Neurobasal media supplemented with 2 mM GlutaMax, 1 × B27, 1 × N2 (all from Gibco Invitrogen), 25 U/mL penicillin and streptomycin (Lonza Group Ltd.) and 20 ng/mL bFGF (R&D Systems). The neurospheres were manually dissected into neural aggregates approximately 300 μm in diameter when they were seeded on the NCAM antibody–pTHMMAA polymer matrix. At the time of seeding and for the follow-up period bFGF was withdrawn from the medium to further induce the neuronal differentiation of neural aggregate cells.

2.4. Construction of antibody–polymer layers onto polystyrene for cell attachment

Anti-NCAM antibodies were allowed to physisorb on polystyrene by applying concentrations of 0, 25, 50, 75, or 100 μg/mL onto the well plates for 15 min. The wells were rinsed with PBS buffer and post-treated with the pTHMMAA polymer (200 μg/mL) for an additional time of 15 min. The wells were thereafter rinsed again with PBS buffer. An improvement of the non-fouling properties of binary monolayers composed of antibodies and polymer have previously been noticed if the layers are allowed to stand for a few days (Vikholm-Lundin and Albers, 2006). Thus, the treated well plates were let to stabilize in the buffer for 2 days at +4 °C before cell seeding. Next, the wells were rinsed once with neural differentiation medium without bFGF after which 800 μL of the same medium was added to each well. The well plate and the medium were pre-warmed at +37 °C

and then the neural aggregates were applied on the surface for attachment. The cells were cultured on the matrix for 8 days and half of the medium without growth factors was changed every second day. At days 3 and 8 the cells were imaged using an Olympus microscope (IX51, Olympus, Finland) to assess the cell types attached and the cell growth. Thereafter, the cells were fixed for immunocytochemical analysis using 4% paraformaldehyde for 20 min at room temperature. Altogether two parallel wells of each NCAM concentration for both hESC line-derived neural cells were prepared.

2.5. Staining of the cells for imaging and analysis

The fixed cells were stained with polyclonal rabbit anti-microtubule associated protein (MAP-2, 1:400, Chemicon, Temecula, CA) for neuronal cells or for mouse anti-human OCT-3/4 (Millipore, Billerica, MA) or monoclonal mouse anti-Tra-1-60 (Chemicon) for undifferentiated hESCs. Briefly, the cells were blocked against non-specific antigen binding with 10% normal donkey serum, 0.1% Triton X-100, and 1% BSA in PBS for 45 min and washed with 1% normal donkey serum, 0.1% Triton X-100, and 1% BSA in PBS. The primary antibody was diluted with the washing solution, added to the cells, and incubated overnight at +4 °C. The next day, the cells were washed with 1% BSA in PBS and incubated for 1 h at RT with the same solution containing Alexa Fluor-488 or -568 (1:400, Invitrogen) conjugated anti-rabbit or anti-mouse secondary antibody. Thereafter, cells were sequentially washed with PBS and phosphate buffer, mounted with Vectashield with 4′,6-diamidino-2-phenylindole (DAPI, Vector Laboratories, Peterborough, UK), and cover-slipped. When primary antibodies were omitted (negative control), no positive labelling was detected. Stained neuronal cells were imaged and counted using an Olympus microscope (Olympus) equipped with a fluorescence unit and camera (DP30BW, Olympus). For statistical analysis, neuronal cell samples derived from two hESC lines were pooled together, thus the number of samples was 4 for each NCAM antibody concentration. A non-parametric Mann–Whitney *U*-test and an SPSS 17.0 statistical software package (SPSS Inc., Chicago, IL) were used for statistical analysis. A *p*-value less than 0.05 was considered significant.

3. Results and discussion

3.1. Binding of NCAM antigen to antibody–polymer layers immobilised on gold

The binding of NCAM antigen to a mixed NCAM antibody and pTHMMAA monolayer was first evaluated with SPR. A fast increase in response was observed when antibodies at a concentration of 50 μg/mL were physisorbed on the gold surface (data not shown). The antibody layer formation showed a response of 1900 ± 200 RU corresponding roughly to 190 ng of antibodies/cm^2 (Vikholm-Lundin and Albers, 2006). Next, the pTHMMAA polymer at a concentration of 200 μg/mL was post-adsorbed on the surface with a response of 200 ± 40 RU. The polymer intercalates on the surface to sites not coated by antibodies and has previously been used in immunoassays for reducing the non-specific binding of interfering molecules (Vikholm-Lundin and Albers, 2006). The non-specific binding was measured by running BSA at a concentration of 500 μg/mL on the surface. Non-specific binding of BSA was 60 ± 40 RU corresponding only to 6 ± 4 ng/cm^2, which suggests that the polymer is intercalated between the antibodies and effectively shielding them. Non-specific binding has otherwise been noticed to take place in the vicinity of the antibodies (Vikholm et al., 1999).

Next, the NCAM antigen binding to the layer was studied (Fig. 1B). The antigen binding to the layer increased with concentration, giving a response of 250–350 RU, when the monolayer was spread from an anti-NCAM concentration of 50 μg/mL. The same surface was also constructed with a lower antibody concentration (25 μg/mL; data not shown) resulting in a 60 units lower response at the highest antigen concentration of 10 μg/mL. These results are in agreement with previous studies when binding antigen to binary layers of antibodies and the pTHMMAA polymer (Vikholm-Lundin and Albers, 2006). Next, the cell-growth studies were carried out encouraged by the good characterization results obtained by SPR.

3.2. Binding of neuronal cells to antibody–polymer layers immobilised on polystyrene

First, the anti-NCAM antibodies at concentrations from 0 to 100 μg/mL were physisorbed on polystyrene and then post-treated with the pTHMMAA polymer (200 μg/mL) to produce a binary monolayer. Neurospheres differentiated for 6 weeks are a heterogeneous cell population containing mostly neural precursor cells. If plated on laminin some non-neural cells can occur (unpublished). In order to verify cell attachment on the antibody/pTHMMAA layer the cells were imaged during culturing and fixed and stained after 8 days on either polystyrene coated with only the polymer or with the polymer (200 μg/mL) and antibodies (25–100 μg/mL). The staining of the cells after fixation verified the phenotypes of attached cells. HESC-derived neuronal cells do not normally adhere on plain polystyrene and this was also observed when only the pTHMMAA polymer was applied on the surface as only MAP-2 negative, non-neuronal cells attached to the wells (Fig. 2C). If NCAM antibodies, on the other hand, were immobilised on the surface, attachment of MAP-2 positive neuronal cells could be observed (Fig. 2D and E). In fact, all the attached cells on NCAM antibody matrices of 25 or 50 μg/mL were MAP-2 positive neurons as 100% co-localization of MAP-2 and nuclear stain DAPI was observed. The cell counts revealed that significantly higher amounts of neuronal cells were attached when the concentration of the NCAM antibody was increased from 25 to 50 μg/mL on the surface ($p < 0.05$, 52 ± 31 cells vs. 206 ± 69 cells, respectively, Fig. 2F). This suggests a specific cellular NCAM protein binding to the immobilised NCAM antibodies on the well plate surface. The polymer seems to hinder quite efficiently non-neural cell attachment.

At an NCAM antibody concentration of 75 or 100 μg/mL, few MAP-2 negative cells were also observed besides neuronal cells (data not shown). Thus, these concentrations were not considered optimal for neuronal cell attachment and not studied further. This suggests that at high NCAM antibody concentrations the binding selectivity starts to diminish due to a steric hindrance with increased non-epitopic binding sites of antibodies available on the surface for non-neuronal cell attachment. Corresponding binding characteristics have been observed for antigen binding to monolayers developed for immunoassays (Vikholm-Lundin and Albers, 2006). The optimum amount of antibodies in the layer is dependent on the size of the antigen. A higher antigen binding and an improved neuronal cell growth could be expected if the antibodies were further site-directly immobilised on polystyrene.

During culturing no significant neuronal cell proliferation or extensive neurite extension was observed (data not shown). Most likely NCAM antibody sites are occupied by attached neuronal cells and thus the pTHMMAA polymer does not support cell proliferation. Also, there was no support for the neurite extension and the cells remained as bipolar immature neuronal cells. Thus, this NCAM antibody–pTHMMAA polymer surface may be used as a selective matrix for immature neuronal cells. It remains to be studied whether adding of different antibodies or patterning of the NCAM antibodies to the matrix would enhance neuronal cell maturation.

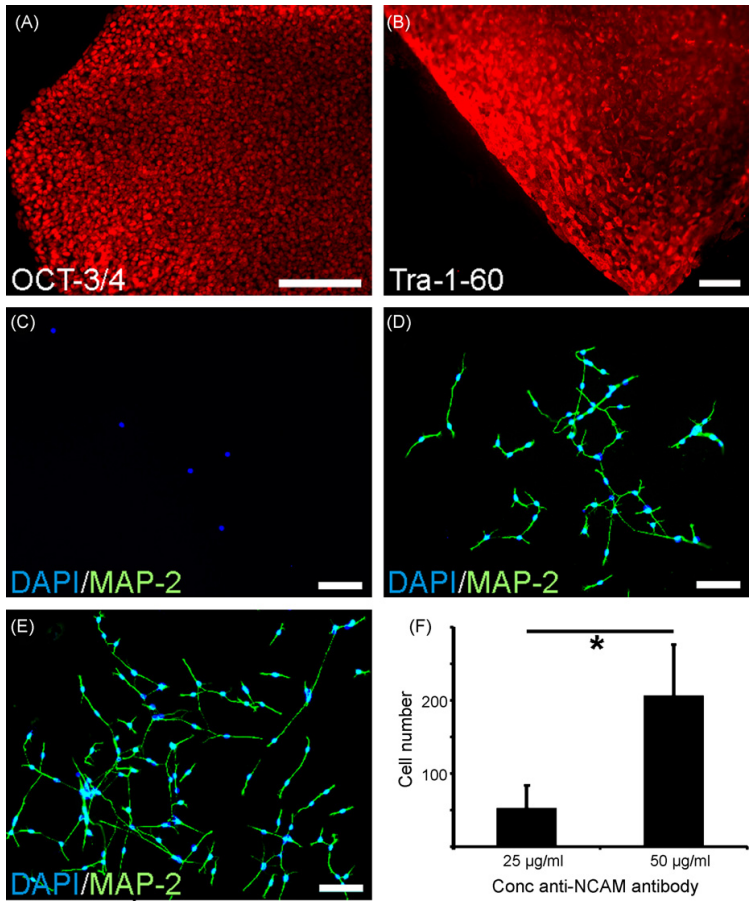

Fig. 2. Human embryonic stem cell (hESC) lines used routinely stained positive for pluripotent markers (A) OCT-3/4 (Regea 06/040) and (B) Tra-1-60 (Regea 08/023). (C) MAP-2 positive hESC-derived neuronal cells did not attach on plain polystyrene surface with pTHMMAA polymer (200 μg/mL) whereas there was concentration dependent attachment on surfaces coated with (D) 25 μg/mL or (E) 50 μg/mL of anti-NCAM antibodies and 200 μg/mL of pTHMMAA. (F) The attachment of MAP-2 positive neuronal cells was significantly higher to surfaces prepared from 50 μg/mL anti-NCAM antibodies compared to surfaces prepared from 25 μg/mL anti-NCAM antibodies ($p < 0.05$). Results represented as mean ± standard error of mean (SEM). Scale bar = 200 μm.

4. Conclusions

In this paper we have shown that hESC-derived neuronal cells can be attached selectively on polystyrene with the aid of NCAM antibodies embedded in a monolayer of hydrophilic pTHMMAA polymer molecules. The amount of neuronal cells on the surface significantly increased in relation to the increased amount of the antibodies in the monolayer. Plain polystyrene with pTHMMAA polymer alone did not present adhering of the neuronal cells. In the future our aim is to increase the amount of the functional antibodies in the layer by using site-directed immobilisation of the antibodies in order to improve the selective neuronal cell attachment and maturation.

Acknowledgements

The research was supported by the Academy of Finland and Biosensing Competence Centre, Tampere, Finland. Tony Munter is gratefully acknowledged for synthesis of pTHMMAA polymer. Technical assistance of Petri Heljo and Jarno Mäkelä is also acknowledged. We want to thank the personnel of Regea for support in stem cell research.

References

Andrews PW, Nudelman E, Hakomori S-I, Fenderson BA. Different patterns of glycolipid antigens are expressed following differentiation of TERA-2 human embryonal carcinoma cells induced by retinoic acid, hexamethylene bisacetamide (HMBA) or bromodeoxy uridine (BudR). Differentiation 1990;43:131–8.

Ditlevsen DK, Povlsen GK, Berezin V, Bock E. NCAM-induced intracellular signaling revisited. J Neurosci Res 2008;86:727–43.

Flanagan LA, Rebaza LM, Derzic S, Schwartz PH, Monuki ES. Regulation of human neural precursor cells by laminin and integrins. J Neurosci Res 2006;83:845–56.

Guillaume DJ, Zhang S-C. Human embryonic stem cells: a potential source of transplantable neural progenitor cells. Neurosurg Focus 2008;24:E3.

Hicks AU, Lappalainen RS, Narkilahti S, Suuronen R, Corbett D, Sivenius J, et al. Transplantation of human embryonic stem cell-derived neural precursor cells and enriched environment after cortical stroke in rats: cell survival and functional recovery. Eur J Neurosci 2009;29(3):562–74.

Jung JP, Nagaraj AK, Fox EK, Rudra JS, Devgun JM, Collier JH. Co-assembling peptides as defined matrices for endothelial cells. Biomaterials 2009;30:2400–10.

Nakaji-Hirabayashi T, Kato K, Arima Y, Iwata H. Oriented immobilization of epidermal growth factor onto culture substrates for the selective expansion of neural stem cells. Biomaterials 2007;28:3517–29.

Nat R, Nilbratt M, Narkilahti S, Winblad B, Hovatta O, Nordberg A. Neurogenic neuroepithelial and radial glial cells generated from six human embryonic stem cell lines in serum-free suspension and adherent cultures. Glia 2007;55: 385–99.

Rappa G, Kunke D, Holter J, Diep DB, Meyer J, Baum C, et al. Efficient expansion and gene transduction of mouse neural stem/progenitor cells on recombinant fibronectin. Neuroscience 2004;124:823–30.

Skottman H. Derivation and characterization of three new human embryonic stem cell lines in Finland. In Vitro Cell Dev Biol Anim; in press.

Skottman H, Narkilahti S, Hovatta O. Challenges and approaches to the culture of pluripotent human embryonic stem cells. Regen Med 2007;2: 265–73.

Vikholm I, Viitala T, Albers WM, Peltonen J. Highly efficient immobilisation of antibody fragments to functionalised lipid monolayers. Biochim Biophys Acta 1999;1421:39–52.

Vikholm-Lundin I, Albers WM. Site-directed immobilisation of antibody fragments for detection of C-reactive protein. Biosens Bioelectron 2006;21:1141–8.

Vikholm-Lundin I, Piskonen R, Albers WM. Hybridisation of surface-immobilized oligonucleotides and polymer monitored by surface plasmon resonance. Biosens Bioelectron 2007;22:1323–9.

Whittemore SR, Morassutti DJ, Walters WM, Liu R-H, Magnuson DSK. Mitogen and substrate differentially affect the lineage restriction of adult rat subventricular zone neural precursor cell populations. Exp Cell Res 1999;252:75–95.

PUBLICATION II

Detection of 3,4-methylene-dioxymethamphetamine (MDMA, ecstasy) by displacement of antibodies

In: Sensors and Actuators B: Chemical,
156: 28–34.

Sensors and Actuators B 156 (2011) 28–34

Contents lists available at ScienceDirect

Sensors and Actuators B: Chemical

journal homepage: www.elsevier.com/locate/snb

Detection of 3,4-methylenedioxymethamphetamine (MDMA, ecstasy) by displacement of antibodies

Inger Vikholm-Lundin[a,*], Sanna Auer[a], Ann-Charlotte Hellgren[b]

[a] VTT Technical Research Centre of Finland, P.O. Box 1300, FIN-33101 Tampere, Finland
[b] Biosensors Applications AB, SE-17154 Solna, Sweden

ARTICLE INFO

Article history:
Received 18 February 2011
Received in revised form 29 March 2011
Accepted 30 March 2011
Available online 7 April 2011

Keywords:
Immobilisation
Antibody displacement
Surface plasmon resonance
Drugs of abuse
MDMA
Ecstasy

ABSTRACT

A molecular layer with low non-specific binding enabling determination of low concentrations of 3,4-methylenedioxymethamphetamine (MDMA) by the displacement of antibodies has been developed. Antibody Fab′-fragments at various concentrations have been site-directly immobilised on gold and intercalated with a hydrophilic non-ionic polymer that reduces non-specific binding. Bovine serum albumin conjugated with MDMA and various concentrations of anti-MDMA antibodies were bound to the layer. The amount of conjugates and antibodies bound was dependent on the amount of Fab′-fragments in the layer. Antibodies were also bound to the conjugates physisorbed directly onto the gold surface and in mixtures with the polymer or with a lipoamide. A high displacement of antibodies was observed by surface plasmon resonance (SPR) on interaction of MDMA with the different layers in buffer solution. No displacement could, however, be observed in saliva with the pure conjugate layer because of a high non-specific binding of proteins. When the conjugates were coupled to the surface through the antibody Fab-fragment/polymer layer, MDMA concentrations as low as 0.02 ng mL^{-1} (0.14 nM) could easily be detected in buffer. In diluted saliva the lowest limit of detection was 0.4 ng mL^{-1} enabling determination of drugs from saliva with a cut-off concentration of 2 ng mL^{-1}. The molecular layer of antibody Fab′-fragments and polymer thus shows great potential for binding conjugates and antibodies that can be displaced on the interaction with very low concentrations of small-sized molecules. A low non-specific binding is guaranteed by the presence of the hydrophilic polymer.

1. Introduction

Driving under the influence of drugs has become a major problem worldwide as the use of drugs in combination with driving increases the accident risk [1]. Testing for alcohol intoxication can be done today at the roadside, but there is currently no rapid method for detecting drugs of abuse that meet all the standards set by police authorities. To test for drugs, blood- and urine samples have to be taken and analysed in a certified laboratory.

The laboratory methods currently being used for the detection and analysis of drugs of abuse such as cocaine, morphine, heroin, etc., are either instrument-based procedures and include chromatographic (TLC, GC, HPLC) and spectroscopic (IR, MS, and NMR) techniques or immunoassay-based like radioimmunoassay, solid phase enzyme immunoassay and fluoro-immunoassay [2]. Quantification of the antibody–antigen complex relies on a marker molecule, such as a radioisotope, an enzyme or a fluorescent probe. Several incubations, washing and separation steps have to be carried out. Analysis can take several days, which is impossible for on-site testing at the road-side. Current on-site screening methods mostly rely on lateral chromatographic immunoassays, which are, although sensitive, quite unreliable due to the great amount of false-positive results. This precludes their use in mass-screening e.g. traffic controls. The need for fast, sensitive, reliable, more easy-to-use non-invasive tests for drug abuse has increased considerably in the last years and saliva has become the matrix of choice in most applications. For saliva screening of drugs of abuse, a cut-off value of not more than 10 ng of drug per mL saliva is desirable. A fast and specific method could also be used for clinical diagnosis of various target molecules and for screening of drugs by the pharmacological industry. High requirements are imposed on both the detection method and on the sensing surface layer to be used. In immunoassays, antibodies are normally bound to the surface by methods that give a random immobilisation and only few of the antibodies are available for binding of the target molecules. If low concentrations of target molecules are to be detected the antibodies have to be site-directly immobilised on the surface and the non-specific binding has to be low [3,4]. If

* Corresponding author. Tel.: +358 40 538 9484; fax: +358 20 722 3319.
E-mail addresses: Inger.Vikholm-Lundin@vtt.fi, inger.vikholm@vtt.fi (I. Vikholm-Lundin).

0925-4005/$ – see front matter © 2011 Elsevier B.V. All rights reserved.
doi:10.1016/j.snb.2011.03.069

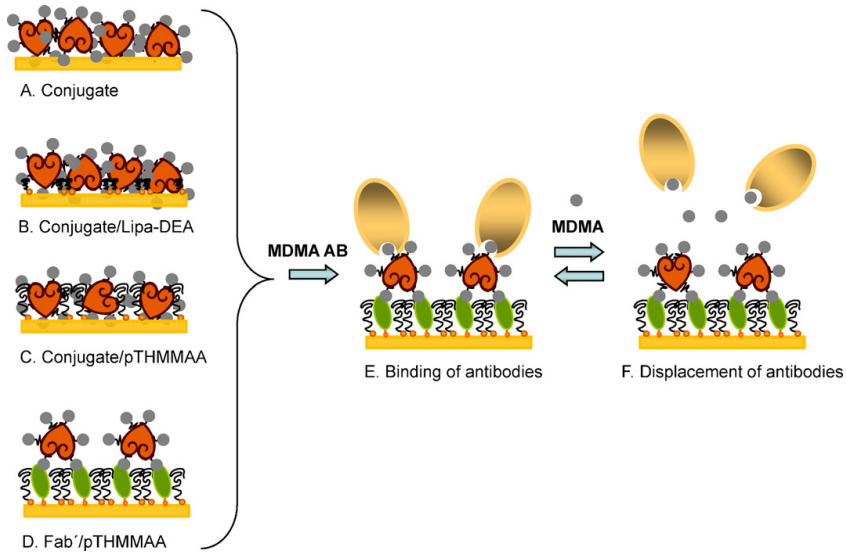

Scheme 1. Cartoon showing BSA-conjugates physisorbed on gold (A) alone and in a mixture with (B) Lipa-DEA, (C) pTHMMAA and attached through (D) an antibody Fab′-fragment/pTHMMAA layer. (E) Binding and (F) displacement of anti-MDMA antibodies on injection of MDMA.

these conditions are fulfilled it may still, however, be difficult to detect low concentrations of small-sized molecules.

Surface plasmon resonance, SPR, and thickness shear mode resonators are very sensitive and binding reactions can be followed in real-time without labelling [5–8]. Generally direct detection by SPR is, however, limited to molecules larger than approximately 10 kDa or to substances with a high refractive index [9]. Inhibition assay is used for detecting low molecular weight analytes that cannot be satisfactorily measured directly [10]. Morphine detection in the ppb range based on inhibition has been demonstrated by SPR [11]. Displacement assay formats where antibodies are displaced from the detecting surface upon addition of the analyte are widely used by fluorescence methods, but are rarely applied with SPR [12–15]. Most SPR devices are not adequate for on-site testing at the roadside. This paper will, however, not solve the problems related to the detection method, but focus on the surface layer.

We have previously developed a method for obtaining an oriented immobilisation of antibodies by attaching antibody Fab′-fragments directly on the gold surface and reduced the non-specific binding by intercalating a disulfide bearing non-ionic hydrophilic polymer of *N*-[tris-(hydroxymethyl)methyl]acrylamide, pTHMMAA between the antibody fragments [16–19]. We have now used this layer to bind bovine serum albumin, BSA, conjugated with 3,4-methylenedioxymethamphetamine, MDMA to the surface. MDMA, also called ecstasy, is a small molecule (molecular weight of 193 g mol^{-1}) that has become a major drug of abuse worldwide [20]. The surface was tested along with three other surface layers where the BSA-conjugate was physisorbed directly on the gold surface either alone or from binary solutions with either the pTHMMAA-polymer or with a lipoamide, Lipa-DEA previously used as a blocking agent for oligonucleotide surfaces [8,21]. Antibodies of high affinity to MDMA were then attached to the conjugates immobilised on the surfaces (Scheme 1). SPR was used to determine the amount of conjugates and antibodies bound to the different surface layers and, in the case of the Fab′/pTHMMAA-surfaces, also how the sensitivity depended on the amount of antibody fragments in the layer. When MDMA was injected over the surfaces, antibodies were displaced due to a higher affinity of the antibody to MDMA than to the BSA-conjugate and MDMA of different concentrations could be detected.

2. Materials and methods

2.1. Chemicals

The *N,N*-bis(2-hydroxyethyl)-α-lipoamide, Lipa-DEA (Scheme 2A) was obtained by conjugation of lipoic acid (thioctic acid) and diethanolamine as previously described [22]. The polymer pTHMMAA (Scheme 2B) was prepared by thermal polymerisation of *N*-[tris-(hydroxymethyl)methyl]acrylamide in the presence of 2 mol% of a lipoic acid functionalised radical initiator according to the literature [23,24].

Polyethylene glycol sorbitan monolaurate, Tween 20, ammonium hydroxide (28–30% NH_3) and bovine serum albumin (BSA, minimum 98% purity) were obtained from Sigma (Mannheim, Germany). Hydrogen peroxide (30%) and Na_2HPO_4 were purchased from Merck KGaA, sodium chloride (NaCl) from J.T. Baker and sodium hydroxide (NaOH) from Akzo Nobel (Sweden). The chemicals were all of analytical grade. 3,4-Methylenedioxymethamphetamine, MDMA was obtained from Cerilliant Corporation. Anti-MDMA antibodies and BSA conjugated MDMA were obtained from Biosensors Applications AB. Saliva was collected and centrifuged at 8000 × *g* for 15 min at +4° to get rid of solid particles. The supernatant was further diluted to a 25% solution (v/v) in PBS-buffer and filtrated through a 0.45 μm syringe filter (PALL Corporation) prior to use.

2.2. Antibody digestion, F(ab′)$_2$ and Fab′-fragments generation

Anti-MDMA antibodies were cleaved to F(ab′)$_2$-fragments with bromelain according to Mariani et al. [25]. The enzymatic digestion with bromelain was allowed to proceed for 5–6 h at +37 °C. The F(ab′)$_2$-fragments were purified from the other digestion products by affinity purification with the aid of a Protein G Column (GE Healthcare).

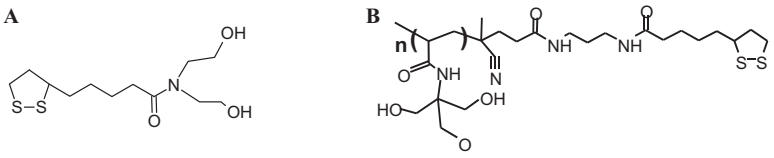

Scheme 2. Schematic view of (A) the lipoamide, Lipa-DEA and (B) the poly-N-[tris(hydroxymethyl)methyl]acrylamide, pTHMMAA polymer.

$F(ab')_2$ –fragments were further reduced to Fab′-fragments to have the free thiol-groups from the antibody hinge-region available for covalent and site-directed immobilisation on the gold surface. The reduction reactions were performed with dithiotreitol (DTT, Merck) in a phosphate buffer solution of 50 mM Na_2HPO_4, 150 mM NaCl and 5 mM EDTA pH 7.4. $F(ab')_2$-fragments were reduced at a concentration of 50 μg mL^{-1} with 3.7 mM DTT in PBS/EDTA buffer at 4 °C for 12–18 h [24].

2.3. Functionalisation of gold slides

All of the studies were carried out in a Biacore 3000 instrument (Biacore AB, Uppsala, Sweden) with at least four replicas. Glass slides coated with a thin film of gold were cleaned in a boiling solution of hydrogen peroxide/ammonium hydroxide (28–30% NH_3)/water (1/1/5, v/v/v) for about 30 s and rinsed with water. The slide was mounted in a plastic chip cassette and inserted into the Biacore SPR instrument. The slide was rinsed with 50 mM NaH_2PO_4/Na_2HPO_4, 150 mM NaCl pH 7.4 PBS buffer at a constant flow rate of 20 μL min^{-1} for 1 min. The BSA-conjugate, 50 μg mL^{-1}, binary solutions of the BSA-conjugate, 50 μg mL^{-1} and pTHMMAA, 50 μg mL^{-1} or Lipa-DEA, 200 μg mL^{-1} were allowed to interact with the pre-cleaned gold surface typically for 10 min, followed by rinsing of the surface with PBS buffer for 10 min. The Fab′-fragment/pTHMMAA layers were produced by manually dispensing about 50 μL of the immobilisation solutions directly on pre-cleaned gold slides. The Fab′-fragment layer was post-treated twice by applying the pTHMMAA polymer at a concentration of 100 and 350 μg mL^{-1} and rinsing in between with water. The layers were rinsed with water and stored in a closed dish on a moist paper at 4 °C.

Non-specific binding of BSA was tested before injecting the BSA-conjugate on the Fab′/pTHMMAA layers. Anti-MDMA antibodies at concentrations ranging from 10 to 120 μg mL^{-1} were allowed to bind to the different BSA-conjugate surfaces for 10 min. The surfaces were rinsed with buffer or Tween 20. MDMA dissolved in PBS buffer or PBS: saliva 3:1 at concentrations ranging from 0.01 ng mL^{-1} to 10 μg mL^{-1} was injected sequentially from the lowest to the highest concentration and the layers were rinsed with buffer in between. Due to the refractive index of proteins a SPR response of 1000 RU was estimated to correspond to a surface coverage of 100 ng cm^{-2} [26].

3. Results and discussion

3.1. BSA-conjugate layer formation

3.1.1. Physisorption on gold

BSA-conjugates, alone or in solutions with pTHMMAA or Lipa-DEA respectively, were allowed to assemble on gold simply by physisorption (Scheme 1A–C). The polymer and Lipa-DEA are expected to bind covalently onto the gold surface through the disulfide groups and be intercalated between the BSA-conjugate molecules physisorbed on the surface. The BSA-conjugates should thus not be as tightly packed when they are mixed with the blocking molecules as when standing alone on the surface. Denaturation of conjugates upon binding might also be avoided due to less available surface area when mixed with the blocking molecules. Lipa-DEA is a small molecule hindering non-specific binding of molecules onto the gold surface [21], whereas the polymer with a length of approximately 4 nm is able to "surround" the conjugates and might thus keep them in a liquid environment in a similar way as with the antibody Fab′-fragments/pTHMMAA layer [17,19].

Physisorption of BSA-conjugates at a concentration of 50 μg mL^{-1} alone or in a mixture with Lipa-DEA and pTHMMAA onto pre-cleaned gold surfaces was very fast and dissociation was very low (Fig. 1). The response corresponded to 3700 ± 600, 4600 ± 100 and 2700 ± 500 RU for the conjugate alone or in a mixture with the lipoamide and polymer, respectively (Table 1).

The surface coverage of the BSA-conjugates was about four-fold compared to the surface coverage by the same concentration of pure BSA physisorbed on gold (1000 ± 50 RU). BSA does not form a fully saturated monolayer at a concentration of 50 μg mL^{-1}. At a concentration of 1 mg mL^{-1} the surface is saturated with a response of 1700 ± 200 RU (170 ± 20 ng cm^{-2}), which agrees with the theoretical estimation of a closely packed BSA monolayer. ^{1}H NMR studies and X-ray crystallographic data indicate that bovine albumin has a heart-shaped structure with dimensions of 8 × 8.7 × 6 nm (Mw = 65 kD) and not an ellipsoid shape as generally believed [27–29]. A closely packed monolayer of BSA would take up a surface coverage of 226 or 129 ng cm^{-2} depending on the adsorption model used [30]. The conjugation of BSA with MDMA may have altered the structure and hydrodynamic volume of BSA and might be the reason for the much higher surface coverage of the BSA-conjugate layer.

The amount of BSA-conjugates physisorbed on the surface from the binary solutions are not known, but the concentrations of pTHMMAA and Lipa-DEA used give responses of 1500 and 1650 ± 100 RU, respectively when adsorbed alone on gold [31]. Lower amounts will probably be adsorbed from the binary solutions with the con-

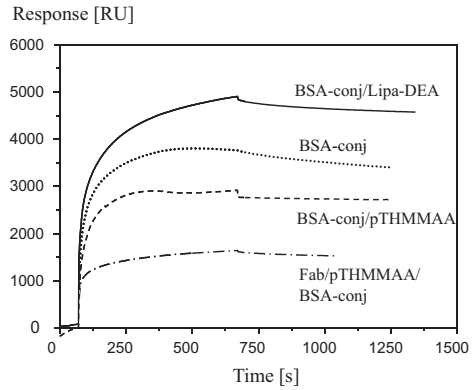

Fig. 1. Binding of BSA-conjugates alone or in a mixture with Lipa-DEA and pTHMMAA and binding of BSA-conjugates to a binary monolayer of Fab′-fragments and pTHMMAA polymer immobilised on gold.

Table 1
Responses for binding of conjugate with or without the blocking molecules Lipa-DEA and pTHMMAA on gold or to Fab′-fragment/pTHMMAA layers. Subsequent binding of anti-MDMA antibodies and washing of the layers with 0.01% Tween.

Layer	(RU)		
	Response conjugate/(blocker)	Response anti-MDMA antibodies	Response 0.01% Tween
Conjugate	3700 ± 600	4600 ± 700	−800 ± 200
Conjugate/Lipa-DEA	4600 ± 100	4600 ± 400	−1100 ± 150
Conjugate/pTHMMAA	2700 ± 500	1400 ± 500	−50 ± 25
Fab′/pTHMMAA[a]	1500 ± 150	2400 ± 150	−100 ± 50
Fab′/pTHMMAA[b]	1300 ± 100	2300 ± 150	−200 ± 50

[a] Layers made from 10 μg mL^{-1} Fab′-fragments.
[b] Layers made from 25–50 μg mL^{-1} Fab′-fragments.

jugate and thus a large amount of the total response from the mixtures must be due to a physisorption of conjugates on the surface. A considerably lower amount of conjugates seems to be adsorbed from the binary solution of pTHMMAA. The variation in surface coverage was quite large (60 ng cm^{-2}) for the pure conjugate and for the mixture with the pTHMMAA polymer, whereas the layer formation was much more reproducible for the conjugate and Lipa-DEA mixture. Physisorption of proteins onto a surface is likely to produce layers with a variation in surface coverage due to an unfolding of proteins. The lipoamide might hinder conjugates from unfolding on the gold surface giving more reproducible layers. The surface coverage was also more reproducible when the conjugates were bound to the surface through the Fab′-fragments as will be discussed in the next section.

3.1.2. Binding to monolayers of Fab′-fragments/pTHMMAA

Next, the binding of BSA-conjugates to a monolayer of Fab′-fragments and pTHMMAA polymer was studied (Scheme 1D). A Fab′-fragment concentration of 50 μg mL^{-1} has been used before to obtain an optimum packing density of Fab′s in the layer with a maximal binding of antigen [17,19]. This concentration was therefore initially used for studying binding of BSA-conjugates to the surface. Considerably lower amounts of BSA-conjugates were attached to a monolayer made from 50 μg mL^{-1} Fab′-fragments and pTHMMAA polymer (1300 ± 100 RU) compared to the physisorbed layers (Fig. 1). This agrees with the value for a pure 50 μg mL^{-1} solution of BSA physisorbed on a gold surface.

The amount of BSA-conjugates bound was, however, dependent on the amount of Fab′-fragments in the monolayer (Fig. 2). The highest binding response corresponding to 1500 ± 150 RU was obtained when the layer was made from 10 μg mL^{-1} Fab′-fragments (Table 1). This amount was less than half of the amount of conjugates physisorbed directly on gold. A similar response has been obtained when binding BSA-conjugates to a carboxymethyl dextran surface (1600 RU at 100 μg mL^{-1}) [32] and when BSA was physisorbed directly on gold, as discussed above. The binding was somewhat lower to layers made from 25 to 50 μg mL^{-1} Fab′-fragments and the response decreased with increasing amount of Fab′-fragments in the layers to only 240 ± 80 RU when the layer was made from Fab′-fragments at a concentration of 100 μg mL^{-1}. At higher concentrations there might be a steric hindrance for binding of the conjugates, similar to that observed for binding of antigen to binary monolayers of the antibody Fab′-fragments and the pTHMMAA polymer [16]. No binding of BSA-conjugates could be observed to a layer composed of only the pTHMMAA polymer, which indicates that the conjugates were bound to the antibody fragments, nor was there any binding of BSA to a Fab′/pTHMMAA surface, which further verifies that there was a specific binding of the conjugates through MDMA.

3.2. Binding of anti-MDMA antibodies to the BSA-conjugate layers

In the next step, anti-MDMA antibodies were bound to the different conjugate layers (Scheme 1E). Binding of anti-MDMA antibodies at a concentration of 50 μg mL^{-1} was very fast to all of the layers and saturation was reached within 5 min (Fig. 3).

The highest amount of anti-MDMA antibodies were bound to the BSA-conjugate and BSA-conjugate/Lipa-DEA layer (4600 ± 700 and 4600 ± 400 RU, Table 1). The reproducibility of the binding to the pure conjugate layer was quite poor. The binding was only half

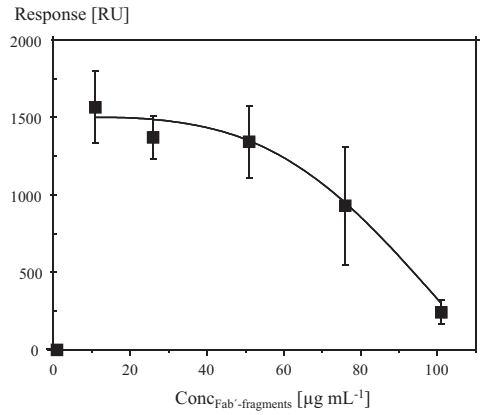

Fig. 2. Total response for binding of BSA-conjugates to binary monolayers of Fab′-fragments and pTHMMAA polymer.

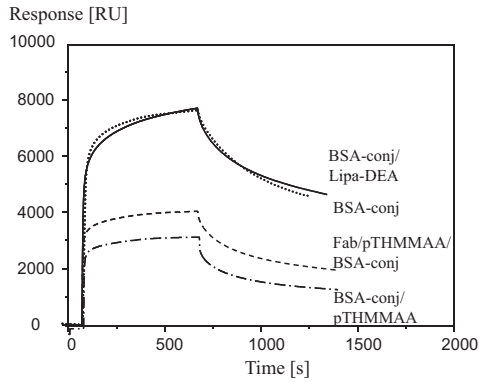

Fig. 3. Binding of 50 μg mL^{-1} anti-MDMA antibodies to layers of BSA-conjugates, BSA-conjugates/Lipa-DEA, BSA-conjugate/pTHMMAA and to BSA-conjugates bound to a binary monolayer of Fab′-fragment/pTHMMAA.

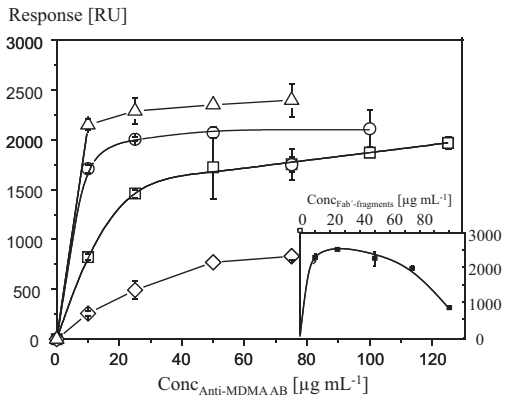

Fig. 4. Binding of anti-MDMA antibodies to BSA-conjugates bound to Fab′-fragments/pTHMMAA made from Fab′-fragment concentration of 10–25 (△), 50 (○), 75 (□) and 100 μg mL^{-1} (◊). The inset shows the anti-MDMA antibody binding at saturation to the monolayers.

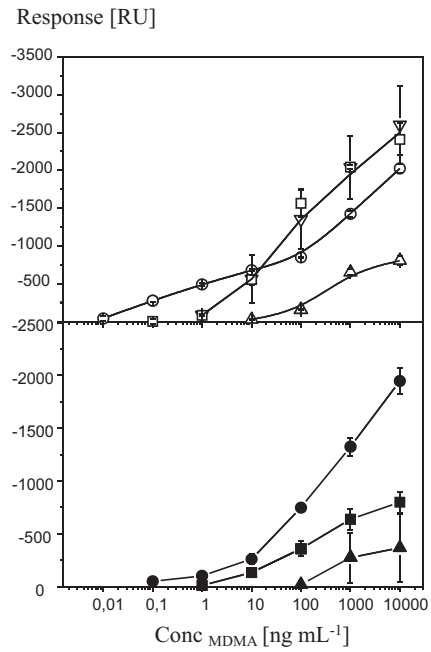

Fig. 5. Response on injection of MDMA diluted in a) PBS (open symbols) and b) PBS: saliva 3:1 (filled symbols) over antibodies bound to layers of BSA-conjugates (▽), BSA-conjugates/Lipa-DEA (□, ■), BSA-conjugates/pTHMMAA (△, ▲) and Fab′-fragments/pTHMMAA/BSA-conjugates (○, ●) made from a Fab′-fragment concentration of 50 μg mL^{-1}. The surfaces were pre-rinsed with Tween-20 and the responses obtained by zero-injections were withdrawn.

to the Fab′/pTHMMAA/BSA-conjugate layer (2300 ± 150 RU) and it was even lower to the BSA-conjugate/pTHMMAA layer (1400 ± 500 RU). This could be expected because much higher amounts of conjugates were physisorbed directly on gold than attached to the Fab′/pTHMMAA layers. However, when taking the molecular weight of the conjugate and the antibody into account (67 and 150 kDa, respectively) it seems like 55% of the conjugates physisorbed on the surface bind antibodies. When the conjugates are bound to the Fab′/ pTHMMAA – conjugate layer, even 70 - 80% of the conjugates bind antibodies depending on the amount of Fab′-fragment in the layer (10 versus 50 μg mL^{-1}). This is not surprising because a large part of the conjugates physisorbed on the surface are unfolded, whereas the conjugates were covalently linked to the Fab′/pTHMMAA layer and a higher amount would be expected to have a preserved activity.

The amount of anti-MDMA antibodies bound to conjugates in the Fab′-fragment /pTHMMAA-layer was dependent on the amount of Fab′-fragments in the layer, but also on the antibody concentration applied (Fig. 4). There was a very high binding to layers made from a concentration of 10 and 25 μg mL^{-1} Fab′-fragments already at low anti-MDMA antibody concentrations. The amount of antibodies bound was somewhat lower to a layer prepared from 50 μg mL^{-1} Fab′-fragments and as the Fab′-fragment concentration increased further the amount of anti-MDMA antibodies bound to the layer decreased (Fig. 4, inset). This is in accordance with the binding of BSA-conjugates to the layers.

3.3. Displacement of anti-MDMA antibodies on injection of MDMA onto the BSA-conjugate layers

MDMA was injected sequentially from the lowest to the highest concentration over surfaces covered by anti-MDMA antibodies and BSA-conjugates physisorbed on gold with or without Lipa-DEA or the pTHMMAA polymer and to the Fab′-fragment/pTHMMAA/BSA-conjugate/antibody layer. Before injection of MDMA the surfaces were pre-washed with Tween 0.01% to remove too loosely bound antibodies. PBS buffer, or PBS: saliva 3:1 was injected and the zero responses obtained were subtracted to obtain the standard displacement curve. High amounts of antibodies were bleeding off when injecting the zero samples, if no pre-rinsing was performed. The highest amount of antibodies was washed off from the pure conjugate and BSA-conjugate/Lipa-DEA layer (Table 1). After the washing the dissociation of antibodies caused by injecting only PBS decreased considerably and corresponded to 10% of the total response at 10 ng mL^{-1} and to only 2% at 10 μg mL^{-1} MDMA for the BSA-conjugate/Lipa-DEA layer. Dissociation caused by buffer was much less from the Fab′/pTHMMAA layer (4% of the total response at 10 ng mL^{-1} and only 1% at 10 μg mL^{-1} MDMA).

Displacement of anti-MDMA antibodies in buffer was highest from the layers of BSA-conjugates and BSA-conjugates/Lipa-DEA for MDMA concentrations above 100 ng mL^{-1} (Fig. 5a). The displacement from the conjugate and conjugate/lipa-DEA layer, however, corresponded to only −80 ± 50 RU at an MDMA concentration of 1 ng mL^{-1} (Table 2). At the same MDMA concentration the displacement from the Fab′-fragment/pTHMMAA was considerably larger (−490 ± 20 RU). The displacement from the Fab′/pTHMMAA layer depended on the amount of Fab′-fragments in the layer. Layers made from a Fab′-fragment concentration of 10–25 μg mL^{-1} showed a much lower displacement than those made from a Fab′-fragment concentration of 50 μg mL^{-1} (Table 2). No displacement could be observed for an MDMA concentration of 1 ng mL^{-1} from the Fab′/pTHMMAA layer made from 10 to 25 μg mL^{-1}, whereas a high displacement was observed from the layer made from 50 μg mL^{-1}. The packing density of anti-MDMA antibodies bound to conjugates in a layer made from 50 μg mL^{-1} antibody Fab′-fragments seems to favour displacement of antibodies and this Fab′/pTHMMAA layer was used for the further measurements. The highest antigen binding has also previously been obtained to an antibody Fab′-fragment/pTHMMAA layer made from a Fab′-fragment concentration of 50 μg mL^{-1} [19].

At the concentration of interest for detection of MDMA from saliva (10 ng mL^{-1}) the displacement from the Fab′/pTHMMAA/BSA-conjugate layer was higher than that of

Table 2
Displacement on injecting various concentrations of MDMA diluted in PBS or PBS:saliva 3:1 over anti-MDMA antibody surface layers bound to BSA-conjugates physisorbed on gold with or without the blocking molecules, Lipa-DEA and pTHMMAA or conjugates bound to monolayers of Fab′/pTHMMAA.

Layer in PBS	(RU)			LOD (ng mL^{-1})
	Displacement 1 ng mL^{-1}	Displacement 10 ng mL^{-1}	Displacement 10 μg mL^{-1}	
Conjugate	−80 ± 50	−560 ± 100	−2600 ± 500	2
Conjugate/Lipa-DEA	−80 ± 50	−550 ± 70	−2400 ± 250	2
Conjugate/pTHMMAA		−25 ± 10	−800 ± 60	20
Fab′/pTHMMAA/conjugate[a]	–	−100 ± 50	−1450 ± 100	15
Fab′/pTHMMAA/conjugate[b]	−490 ± 20	−680 ± 20	−2020 ± 60	0.02
In PBS:saliva 3:1				
Conjugate	–	–	–	–
Conjugate/Lipa-DEA	−10 ± 20	−130 ± 50	−800 ± 100	20
Conjugate/pTHMMAA	–	–	−400 ± 300	–
Fab′/pTHMMAA/conjugate[b]	−105 ± 20	−260 ± 50	−1950 ± 120	0.4

[a] Layers made from 10 to 25 μg mL^{-1} Fab′-fragments.
[b] Layers made from 50 μg mL^{-1} Fab′-fragments.

either the BSA-conjugate/pTHMMAA or BSA-conjugate/Lipa-DEA layer. Below 10 ng mL^{-1} there was a very low displacement from the BSA-conjugate and BSA-conjugate/Lipa-DEA layers, whereas the displacement from the Fab'/pTHMMAA/BSA-conjugate layer was linear on a logarithmic scale in a concentration range of 0.01–100 ng mL^{-1} (Fig. 5a). Concentrations as low as 0.1 ng mL^{-1} MDMA showed a response corresponding to −275 ± 50 RU, which indicates that very low concentrations can be measured by displacement from Fab′/pTHMMAA/BSA-conjugate layers. In fact, the lowest limit of detection, LOD, calculated as the concentration providing a response three times larger than the standard deviation of the response from a blank sample was as low as 0.02 ng mL^{-1}. Thus a 100-fold lower LOD value compared to that of the conjugates physisorbed directly on gold could be obtained (Table 2). And the LOD was only 20 ng mL^{-1} for the BSA-conjugate/pTHMMAA layer. This was expected, because considerably lower amounts of anti-MDMA antibodies were bound to this layer. The antibody Fab′-fragment/pTHMMAA layer could thus be used to bind conjugates and anti-MDMA antibodies that are displaced from the surface when interacting with very low concentrations of MDMA.

High non-specific binding of proteins from saliva corresponding to 1200 ± 600 RU could be observed to the BSA-conjugate surface when MDMA was spiked in a solution of PBS:saliva 3:1. Proteins and other interfering molecules from the saliva solution adsorbed on the surface and no displacement could be observed. The layer can thus not be used for detecting MDMA in saliva. The non-specific binding was much lower to the BSA-conjugate surfaces mixed with Lipa-DEA or pTHMMAA polymer. The blocking molecules Lipa-DEA and pTHMMAA seemed to reduce non-specific binding of proteins to the conjugate surface and enable a detection of molecules displaced from the surface. When MDMA was diluted in saliva and injected over the binary layers of BSA-conjugate and Lipa-DEA or pTHMMAA, the displacement in diluted saliva was, however, much lower compared to that in buffer (Fig. 5b). Due to the high non-specific binding of proteins from saliva the LOD for the BSA-conjugate/Lipa-DEA layer was 20 ng mL^{-1} (Table 2).

The Fab′-fragment/pTHMMAA layer has been used for detecting low concentrations of C-reactive protein from diluted patient serum samples with a low non-specific binding of serum proteins [19]. The non-specific binding of proteins from diluted saliva was also very low to the Fab′/pTHMMAA/conjugate layer. The displacement of MDMA was somewhat reduced at lower concentrations when MDMA was spiked in a solution of PBS:saliva 3:1 and injected over the surface compared to that in PBS buffer (Fig. 5b). But at MDMA concentrations above 100 ng mL^{-1} the response was only slightly lower than that of MDMA diluted in buffer. At 10 ng mL^{-1} a response of −260 ± 50 RU could be obtained in saliva. The LOD in the diluted saliva was 0.4 ng mL^{-1} enabling determination of drug concentrations in saliva as low as 2 ng mL^{-1}. The measuring time used in these studies was 10 min, but could probably be considerably reduced by taking only the slope of the curve during the first minute(s) in account.

4. Conclusions

Low concentrations of molecules of small size, here exemplified by the drug of abuse MDMA, can easily be detected by displacing antibodies from conjugates bound to the surface through an oriented antibody-fragment/polymer layer. High displacement can also be obtained, if the conjugate was physisorbed on gold or intercalated with a blocking molecule like a lipoamide. However, the high non-specific binding of proteins from saliva hinder the use of the pure conjugate layer in real applications. When the conjugates are bound to the surface through a monolayer of antibody Fab′-fragments and pTHMMAA the amount of MDMA antibodies displaced from the layer was dependent on the amount of Fab′-fragments immobilised on the surface, but also on the amount of MDMA antibodies bound to the conjugates. An optimum displacement was obtained with a Fab′-fragment layer made from a concentration of 50 μg mL^{-1} and with anti-MDMA antibodies bound to the conjugate layer from a solution with the same concentration. MDMA diluted in buffer or buffer:saliva 3:1 to a concentration 10 ng mL^{-1} can displace a large amount of antibodies as detected by SPR. Diluted saliva can thus be used as a sample matrix with a high sensitivity of detection. Next we will study these surfaces for detection of drugs by surface sensitive fluorescence [33].

Acknowledgements

This research has been funded by the Nordic Innovation Centre, "Intoxsign" (07135). Dr. Tony Munter is greatly acknowledged for the synthesis of Lipa-DEA and pTHMMAA.

References

[1] E. Raes, T. Van den Neste, A.G. Verstraete, Drug use, impaired driving and traffic accidents, in: D. Lopez, B. Hughes, P. Griffiths (Eds.), EMCDDA Insights, European Monitoring Centre for Drugs and Drug Addiction, Lisbon, 2008, pp. 37–45.
[2] J.C. Eichhorst, M.L. Etter, N. Rousseaux, C. Denis, D.C. Lehotay, Drugs of abuse testing by tandem mass spectrometry: a rapid, simple method to replace immunoassays, Clin. Biochem. 42 (2009) 1531–1542.
[3] A. Ahluwalia, D. de Rossi, A. Schirone, C. Serra, A comparative study of protein immobilization techniques for optical immunosensors, Biosens. Bioelectron. 7 (1991) 207–214.
[4] I. Vikholm, T. Viitala, W.M. Albers, J. Peltonen, Highly efficient immobilisation of antibody fragments to functionalised lipid monolayers, Biochim. Biophys. Acta 1421 (1999) 39–52.

[5] J. Homola, Surface plasmon resonance sensors for detection of chemical and biological species, Chem. Rev. 108 (2008) 462–493.
[6] C. Di Natale, G. Pennazza, A. Macagnano, E. Martinelli, R. Paolesse, A. D'Amico, Thickness shear mode resonator sensors for the detection of androstenone in pork fat, Sens. Actuators B 91 (2003) 169–174.
[7] R. Patel, R. Zhou, K. Zinszer, F. Josse, Real-time detection of organic compounds in liquid environments using polymer-coated thickness shear mode quartz resonator, Anal. Chem. 72 (2000) 4888–4898.
[8] S. Auer, M. Nirschl, M. Schreiter, I. Vikholm-Lundin, Detection of DNA hybridisation in a diluted serum matrix by surface plasmon resonance and film bulk acoustic resonators, Anal. Bioanal. Chem. (2011), doi:10.1007/s00216-011-4871-0.
[9] W. Haasnoot, P. Stouten, P. Cazemier, A. Lommen, J.F. Nouws, H.J. Keukens, Immunochemical detection of aminoglycosides in milk and kidney, Analyst 124 (1999) 301–305.
[10] A.J. Tudos, L. van den Bos, E. Stigter, E, Rapid surface plasmon resonance-based inhibition assay of deoxynivalenol, J. Agric. Food Chem. 51 (2003) 5843–5848.
[11] N. Miura, K. Ogata, G. Sakai, T. Uda, N. Yamazoe, Detection of morphine in ppb range by using SPR (Surface Plasmon Resonance) immunosensor, Chem. Lett. 26 (1997) 713–714.
[12] M. Gerdes, M. Meusel, F. Spener, Influence of antibody valency in a displacement immunoassay for the quantitation of 2,4-dichlorophenoxyacetic acid, J. Immunol. Methods 223 (1999) 217–226.
[13] A. Larsson, J. Angbrant, J. Ekeroth, P. Månsson, B. Liedberg, A novel biochip technology for detection of explosives – TNT: synthesis, characterisation and application, Sens. Actuators B: Chem. 113 (2006) 730–748.
[14] D.R.S. Hankaran, K.V. Gobi, N. Miura, Recent advancements in surface plasmon resonance immunosensors for detection of small molecules of biomedical, food and environmental interest, Sens. Actuators B: Chem. 121 (2007) 158–177.
[15] G. Klenkar, B. Liedberg, A microarray chip for label-free detection of narcotics, Anal. Bioanal. Chem. 391 (2008) 1679–1688.
[16] I. Vikholm, Self-assembly of antibody fragments and polymers onto gold for immunosensing, Sens. Actuators B 106 (2005) 311–316.
[17] I. Vikholm-Lundin, Immunosensing based on site-directed immobilization of antibody fragments and polymers that reduce nonspecific binding, Langmuir 21 (2005) 6473–6477.
[18] I. Vikholm, J. Sadowski, Method Biosens. Anal., US 7,332,327; 2008-02-19.
[19] I. Vikholm-Lundin, W.M. Albers, Site-directed immobilisation of antibody fragments for detection of C-reactive protein, Biosens. Bioelectron. 21 (2006) 1141–1148.
[20] S.B. Karch, B.G. Stephens, C.H. Ho, Methamphetamine-related deaths in San Francisco: demographic, pathologic, and toxicologic profiles, J. Forensic Sci. 44 (1999) 359–368.
[21] I. Vikholm-Lundin, S. Auer, T. Munter, H. Fiegl, S. Apostolidou, Assembling of single-stranded oligonucleotides and short blocking agent, Surf. Sci. 603 (2009) 620–624.
[22] K. Tappura, I. Vikholm-Lundin, W.A. Albers, Lipoate-based building blocks for construction of imprinted, self-assembled molecular thin film, Biosens. Bioelectron. 22 (2007) 912–919.
[23] A. Laschewsky, E.-D. Rekai, E. Wischerhoff, Tailoring of stimuli-responsive water soluble acrylamide and methacrylamide polymers, Macromol. Chem. Phys. 202 (2001) 276–286.
[24] W.M. Albers, S.S. Auer, H. Helle, T. Munter, I. Vikholm-Lundin, Functional characterisation of Fab'-fragments self-assembled onto hydrophilic gold surfaces, Colloids Surf. B: Biointerfaces 68 (2009) 193–199.
[25] M. Mariant, M. Camagna, L. Tarditi, E. Seccamani, A new enzymatic method to obtain high-yield $F(ab)_2$ suitable for clinical use from mouse IgGl, Mol. Immunol. 28 (1991) 69–77.
[26] E. Stenberg, B. Persson, H. Roos, C. Urbaniczky, Quantitative determination of surface concentration of protein with surface plasmon resonance by using radiolabeled proteins, J. Colloid Interface Sci. 143 (1991) 513–526.
[27] O.J.M. Bos Labro, F.A. Jan, M.J.E. Fischer, J. Wilting, L.H.M. Janssen, The molecular mechanism of the neutral-to-base transition of human serum albumin. Acid/base titration and proton nuclear magnetic resonance studies on a large peptic and a large tryptic fragment of albumin, J. Biol. Chem. 264 (1989) 953–959.
[28] D.C. Carter, X.M. He, S.H. Munson, P.D. Tw, K.M. Gernert, M.B. Broom, T.Y. Miller, Three-dimensional structure of human serum albumin, Science 244 (1989) 1195–1198.
[29] S. Curry, H. Mandelkow, P. Brick, N. Franks, Crystal structure of human serum albumin complexed with fatty acid reveals an asymmetric distribution of binding sites, Nat. Struct. Biol. 5 (1998) 827.
[30] F. Höök, J. Vörös, M. Rodahl, R. Kurrat, P. Böni, J.J. Ramsden, M. Textor, N.D. Spencer, P. Tengvall, J. Gold, B. Kasemo, A comparative study of protein adsorption on titanium oxide surfaces using in situ ellipsometry, optical waveguide lightmode spectroscopy, and the quartz crystal microbalance/dissipation, Colloids Surf. B: Biointerfaces 24 (2002) 155–170.
[31] I. Vikholm-Lundin, R. Piskonen, Binary monolayers of single-stranded oligonucleotides and blocking agent for hybridisation, Sens. Actuators B 134 (2008) 189–192.
[32] G. Strachan, S.D. Grant, D. Learmonth, M. Longstaff, A.J. Porter, W.J. Harris, Binding characteristics of anti-atrazine monoclonal antibodies and their fragments synthesised in bacteria and plants, Biosens. Bioelectron. 13 (1998) 665–673.
[33] H. Välimäki, K. Tappura, A novel platform for highly surface-sensitive fluorescent measurements applying simultaneous total internal reflection excitation and super critical angle detection, Chem. Phys. Lett. 473 (2009) 358–362.

Biographies

Inger Vikholm-Lundin made her Ph.D. in 1996 at Åbo Akademi University at the department of Physical Chemistry. She is a Chief Research Scientist at VTT Technical Research Centre of Finland. Her research has focused on surfaces for DNA hybridisation and on oriented immobilisation of antibodies for immunoassays using blocking molecules to reduce non-specific binding.

Sanna Auer is a Ph.D. student and a Research Scientist at VTT Technical Research Centre of Finland.

Ann-Charlotte Hellgren obtained her Ph.D. in Organic chemistry at Uppsala University in 1985. She has over 15 years of experience as research and project leader in the field of applied surface chemistry at the Institute for Surface Chemistry (YKI) in Stockholm. Ann-Charlotte Hellgren is Manager of the Chemistry Department at Biosensor Applications since August 2000.

PUBLICATION III

Cysteine-tagged chimeric avidin forms high binding capacity layers directly on gold

In: Sensors and Actuators B: Chemical,
171–172: 440–448.

Sensors and Actuators B 171–172 (2012) 440–448

Contents lists available at SciVerse ScienceDirect

Sensors and Actuators B: Chemical

journal homepage: www.elsevier.com/locate/snb

Cysteine-tagged chimeric avidin forms high binding capacity layers directly on gold

Inger Vikholm-Lundin[a,*], Sanna Auer[a], Maija Paakkunainen[a,b], Juha A.E. Määttä[b], Tony Munter[a], Jenni Leppiniemi[b], Vesa P. Hytönen[b,c], Kirsi Tappura[a]

[a] VTT Technical Research Centre of Finland, Sinitaival 6, FI-33100 Tampere, Finland
[b] IBT Institute of Biomedical Technology, University of Tampere, BioMediTech and Tampere University Hospital, FI-33014 University of Tampere, Finland
[c] Center for Laboratory Medicine, Tampere University Hospital, Tampere, Finland

ARTICLE INFO

Article history:
Received 1 February 2012
Received in revised form 2 May 2012
Accepted 2 May 2012
Available online 12 May 2012

Keywords:
Self-assembled monolayer
Cysteine tagged
Avidin
Biotin
Non-specific binding

ABSTRACT

Cysteine-tagged, genetically engineered avidin named ChiAvd-Cys and wild-type avidin form monolayers or bilayer structures when immobilised directly on gold. Non-specific binding can be reduced by a post-treatment of the avidin layers with a *N*-[tris(hydroxymethyl)methyl]-acrylamide (pTHMMAA) polymer. ChiAvd-Cys showed excellent activity when immobilised on gold. About 70% of the ChiAvd-Cys molecules were able to bind two biotinylated green fluorescent proteins (per avidin tetramer). Amino-biotinylated antibody F(ab′)$_2$ fragments could be bound to every 4th and 8th ChiAvd-Cys and wild-type avidin molecule, respectively, whereas on average one thiol-biotinylated antibody Fab′-fragment was bound to every ChiAvd-Cys. Antigen binding to the thiol-biotinylated Fab′-fragment bound to the ChiAvd-Cys/pTHMMAA layer was almost twice compared to that of the amino-biotinylated F(ab′)$_2$-fragments. The high antigen binding was due to a site-directed orientation of the thiol-biotinylated fragments. The ChiAvd-Cys/pTHMMAA layers offer high capacity that may be used to couple biotinylated compounds on biosensor surfaces.

1. Introduction

A fast detection of low concentrations of clinically relevant compounds is of increasing interest. A convenient alternative approach to traditional analytical methods is provided by biosensors. When building a biosensor the sensing or recognition molecules need to be attached on the sensor surface. Molecules can be physisorbed on the surface or attached via chemical linkers through, for example, amino- or cysteine groups available on the protein surface. However, antibodies immobilised on the surface by physical adsorption or chemical coupling have a random orientation and only 10% of the antibodies are available for the binding of analytes [1,2]. The correct orientation and preserved folding of the sensing molecule are vitally important for an optimal function of the molecule and thereby prerequisite for the detection of low amounts of small sized molecules.

Avidin is a tetrameric glycoprotein with four specific binding sites for a biotin molecule. The (strept)avidin–biotin pair is often used in affinity based assays because of the very high affinity of avidin and streptavidin to the biotin molecule (K_a 10^{15} M^{-1} and K_a 10^{13} M^{-1} in solution, respectively) [3–5]. The biotin-binding capacity of a surface is, however, not necessarily directly related to the amount of avidin immobilised. Once bound to the surface the binding potential of avidin is generally decreased. Molecular simulations have suggested that two of the four biotin-binding sites of each immobilised streptavidin molecule are very unlikely to be available for binding to biotin due to their close proximity to the solid surface [6,7]. Often only about 10% of the biotin-binding sites of immobilised avidins are available for ligand binding [8].

Avidins are usually attached on the surface by simple physisorption or through carbodiimide chemistry, where amino groups of the proteins form an amide bond with carboxyl groups of a self-assembled monolayer [9]. In addition, avidin has been bound to biotinylated lipid layers [10–13], including phospholipid layers made by fusion of biotin-containing vesicles [14–16], as well as to commercial carboxymethyl dextran and biotinylated polymers [17,18]. There are many options available for chemical and metabolic biotinylation of biomolecules with different kinds of spacer groups that offer freedom of movement for the biotin-labelled immobilised protein [19].

In the present study wild type avidin and a thermally stabilised genetically engineered chimeric avidin containing C-terminal cysteine groups were immobilised directly on the gold surface [20,21]. The cysteine-residues (C129) were positioned in the C-terminus of each polypeptide chain resulting in a tetrameric

* Corresponding author. Tel.: +358 40 538 9484; fax: +358 20 722 3319.
E-mail addresses: Inger.Vikholm-Lundin@vtt.fi, inger.vikholm@vtt.fi (I. Vikholm-Lundin).

0925-4005/$ – see front matter © 2012 Elsevier B.V. All rights reserved.
http://dx.doi.org/10.1016/j.snb.2012.05.008

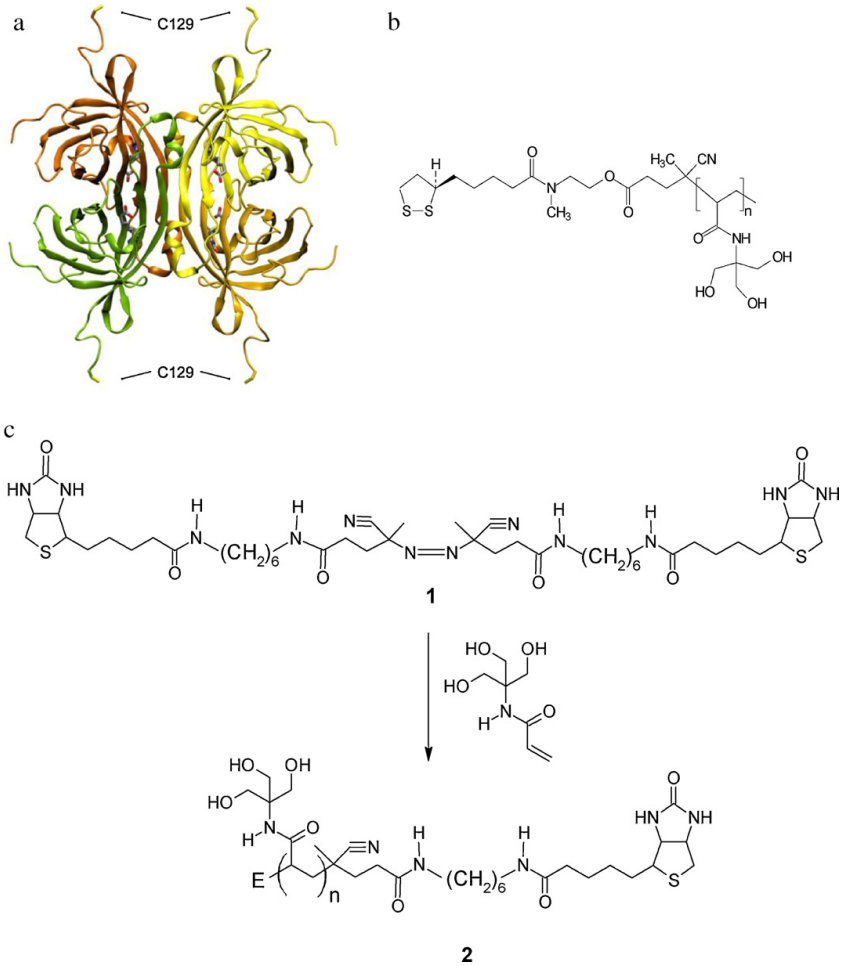

Scheme 1. (a) C-terminally cysteine-tagged chimeric avidin, ChiAvd-Cys, with biotin-binding groups (grey) and side-chains of the C-terminal cysteines (yellow). Schematic view of (b) *N*-[tris(hydroxy-methyl)methyl]acrylamide, pTHMMAA and (c) reaction scheme showing the azo-initiator (**1**) required for the synthesis of the biotinyl-pTHMMAA (**2**). (For interpretation of the references to colour in this figure legend, the reader is referred to the web version of the article.)

chimeric avidin containing four additional cysteines, hereafter referred to as ChiAvd-Cys (Scheme 1a) [22]. A non-ionic hydrophilic *N*-[tris(hydroxymethyl)methyl]-acrylamide (pTHMMAA) polymer (Scheme 1b) was used to reduce non-specific binding. The polymer has previously been intercalated between antibody Fab′-fragments directly immobilised on gold [23–25]. Binding of a genetically biotinylated green fluorescent protein (biotin-GFP), chemically biotinylated antibody F(ab′)$_2$ and Fab′-fragments specific to human IgG as well as the antigen binding were measured by surface plasmon resonance (SPR), one of the major techniques for non-labelled real-time measurement of substances on surfaces [26].

2. Materials and methods

2.1. Chemicals and reagents

The ChiAvd-Cys was a genetically engineered chicken avidin, a chimeric avidin (ChiAvd (I117Y, 129C)) further modified to contain C-terminal cysteine residues [21,22]. *N*-(6-Aminohexyl)biotinamide and 4,4′-azobis(4-cyanopentanoic acid)-*N*,*N*-disuccinimidyl ester were prepared according to procedures by Basak et al. [27] and Kitano et al. [28]. Both ChiAvd-Cys and wild-type chicken avidin, hereafter called wt-Avd, was prepared by overexpression in *Escherichia coli* [29]. All the used reagents were of analytical grade.

Human IgG, polyclonal goat anti-human IgG F(ab′)$_2$ and biotinylated anti-human F(ab′)$_2$ fragments (Fc-specific) were obtained from Jackson ImmunoResearch. *N*-[Tris(hydroxymethyl)methyl]acrylamide, pTHMMAA was synthesised as previously described (Scheme 1b) [25].

2.2. Preparation of azo-initiator

Eight milliliters of a solution of 4,4′-azobis(4-cyanopentanoic acid)-*N*,*N*-disuccinimidyl ester (83 mg, 0.175 mmol) in dimethylformamide, DMF was added to a solution of *N*-(6-aminohexyl)biotinamide (120 mg, 0.35 mmol) in DMF (14 mL) and the reaction mixture was stirred for 5 h. The product was

precipitated by pouring the mixture into ice-cold diethyl ether (100 mL) and collecting the precipitate by filtration. The white solid was dried under vacuum to give the azo-initiator as a white solid (115 mg, 71%). ^{1}H NMR (300 MHz, DMSO-d_6): δ 7.92 (t, 2H, J = 5.8 Hz), 7.72 (t, 2H, J = 5.5 Hz), 6.41 (s, 2H), 6.35 (s, 2H), 4.28 (m, 2H), 4.09 (m, 2H), 3.05 (m, 2H), 2.97 (m, 8H), 2.79 (dd, 2H, J = 12.4, 5,1 Hz), 2.55 (d, 2H, J = 12.2 Hz), 2.38–2.12 (m, 8H), 2.02 (t, 4H, J = 7.2 Hz), 1.66 (s, 6H), 1.63–1.12 (m, 28H). ESI-MS: m/z 929.7 (100, MH^+), 951.4 (6, MNa^+). The azo-initiator is shown in Scheme 1c (compound **1**).

2.3. Preparation of biotinyl-pTHMMAA polymer

The polymer was prepared according to an earlier published method using 2 mol% of the azo-initiator **1** in the reaction to give **2** as a white fine solid (178 mg) [25]. ^{1}H NMR (300 MHz, DMSO-d_6): δ 7.37 (br m, 1H, N*H*), 4.97 (br m, 3H, 3× CH_2OH), 3.54 (br, 6H, 3× CH_2OH), 2.3–1.8 (br, 1H, C*H*), 1.8–0.9 (br, 2H, CH_2). The biotinyl-pTHMMAA is shown in Scheme 1c (compound **2**).

2.4. Preparation of the biotin-GFP

Biotin-GFP (green fluorescent protein) was constructed as an EGFP-1.3S fusion protein (~39 kDa) containing a single biotinylation site. The biotin was attached post-translationally by biotin holo-carboxylate synthetase (BHS) to a ε-amino group of the Lys89 of the biotin carboxyl carrier 1.3S subunit of transcarboxylase (TC) from *Propionibacterium shermanii* [30].

In brief, the EGFP (Clontech) insert was cloned into pHIS plasmid using standard protocols to produce an EGFP equipped with a C-terminal His-tag [31]. The DNA encoding for 1.3S was amplified from a PinPoint Xa vector (Promega) by PCR with primers containing BamHI restriction sites. The BamHI digested PCR product was extracted from an agarose gel and ligated into the BamHI-treated pHIS-EGFP plasmid by T4 DNA ligase. The DNA sequenced construct was used to express the protein in *E. coli* BL21-Star™ (DE3) cells (Invitrogen) and the protein was purified by Ni–NTA metal affinity chromatography according to the manufacturers' instructions (Qiagen). A homogeneous protein of correct molecular weight was detected with SDS-PAGE analysis gel stained with Coomassie Brilliant Blue (results not shown). The protein was dialysed against 50 mM Na-phosphate buffer (pH 7.0) containing 100 mM NaCl.

2.5. Biotinylation of the Fab′-fragments and reduction of ChiAvd-Cys

Biotinylation of the SH-groups of the Fab′-fragments (originating from the hinge-region of the whole IgG molecules) were performed by firstly reducing 0.1 mg/mL of anti-human IgG F(ab′)$_2$-fragments (Jackson Immuno Research; 109-003-098) to Fab′-fragments by 0.5 mM cysteamine–HCl (Sigma–Aldrich) in 50 mM Na_2HPO_4, 150 mM NaCl, 5 mM EDTA, pH 7.1, buffer for 2 h at +37 °C. Excess cysteamine–HCl was washed off after the reduction reaction by a Nanosep (PALL Corporation) centrifuge (cut-off 10 000 MWCO). Biotinylation of the free —SH groups were performed by Pierce's EZ-link Maleimide PEG_2-Biotin reagent (Thermo Scientific) in PBS-buffer (15 mM Na_2HPO_4/NaH_2PO_4, 150 mM NaCl, pH 7.4). Excess reagent was removed by Nanosep. Biotinylation of the Fab′-fragments was verified by a standard western blotting procedure by NuPAGE protein gels (Invitrogen) [32], a PVDF-membrane (Invitrogen), an avidin-alkaline phosphatase reaction (Roche) and a NBT-BCIP (Bio-Rad) colouring reaction. The protein concentrations were assessed by UV-absorption according to Carter et al. [33]. ChiAvd-Cys reduced by Tris(2-carboxyethyl)phosphine hydrochloride (TCEP) (Sigma–Aldrich).

2.6. Immobilisation of avidin and biotinylated antibodies

All of the studies were carried out in a Biacore 3000 instrument (GE Healthcare, Uppsala, Sweden) with at least four replicas (n). Gold substrates for SPR with an intermediate layer of ITO were prepared by RF magnetron sputtering using an Edwards E306A two-target sputter coater [34]. Glass slides coated with a 50 nm film of gold (Edwards E306A sputter coater) were cleaned in a hot solution of hydrogen peroxide/ammonium hydroxide (28–30% NH_3)/water (1/1/5, vol/vol/vol) for about 30 s and rinsed with water. The pre-cleaned slides were mounted in a plastic chip cassette and inserted into the Biacore instrument. Streptavidin-coated sensor chips (SA) – used as a reference – were obtained from GE Healthcare. ChiAvd-Cys or wt-Avd was injected over the surface at 20 μL/min typically for 10 min and then rinsed with 50 mM NaH_2PO_4/Na_2HPO_4, 150 mM NaCl, pH 7.4, buffer (PBS). The surface was post-treated by injecting the disulphide bearing pTHMMAA polymer at a concentration of 0.2 g/L. After rinsing with buffer, biotinylated antibody fragments were coupled to the avidin layers for 15 min. Alternatively, avidin and pTHMMAA were co-adsorbed on the surface. The non-specific binding of 0.5 g/L of bovine serum albumin (BSA) was measured and then the interaction with antigen was determined by sequentially injecting 10 ng/mL–50 μg/mL of human IgG from the lowest to the highest concentration. All the sample dilutions were made in the PBS, which was used as a running buffer. All the measurements were performed at 25 °C. An SPR response of 1000 RU was estimated to correspond to a surface coverage of 100 ng/cm^2 [35].

3. Results and discussion

3.1. Binding of wild type avidin to gold

When wt-Avd at concentrations of 25 and 50 μg/mL was allowed to physisorb on a pre-cleaned gold surface a coverage corresponding to 300 and 360 ± 25 ng/cm^2 (n = 8) was obtained (Scheme 2a, Table 1a). This surface coverage agrees quite well with that of Lee et al. [18], and Yang et al. [17], who reported a streptavidin surface coverage of 260 and 360 ± 30 ng/cm^2 on an ethylene-glycol–biotin layer and a 10% biotinylated self-assembled layer, respectively. Avidin produced in *E. coli* with a molecular weight of about 59 kDa and a molecular size of 4.0 nm × 5.5 nm × 6.0 nm would have a monolayer surface coverage of 300–445 ng/cm^2 depending on the orientation of the molecule [36,21]. The response for wt-Avd indicates that the molecules form a monolayer with the molecules mainly standing on their 5.5 nm × 6.0 nm faces when physisorbed from this concentration. At even higher concentrations (500 μg/mL) the avidin packing became higher (500 ± 50 ng/cm^2) suggesting that the molecules may stand end-on.

Post-treatment of the wt-Avd layer with the pTHMMAA polymer gave an additional increase of 100 ± 25 ng/cm^2 in surface coverage (Scheme 2b, Table 1). The polymer possesses a low non-specific binding, and can be covalently attached onto the gold surface by disulphide anchors [23,24,37]. The polymer is supposed to become intercalated between the wt-Avd molecules in a similar way to that of antibody Fab′-fragments immobilised directly on gold [24]. The wt-Avd/pTHMMAA layer would therefore have a total surface coverage of about 400–460 ± 25 ng/cm^2.

3.2. Binding of ChiAvd-Cys to gold

The binding of ChiAvd-Cys to gold was studied and compared to that of wt-Avd. When 25 μg/mL of ChiAvd-Cys was allowed to interact with the Au surface a surface coverage of 650 ± 50 ng/cm^2 was obtained (Table 1a). The surface was almost saturated as

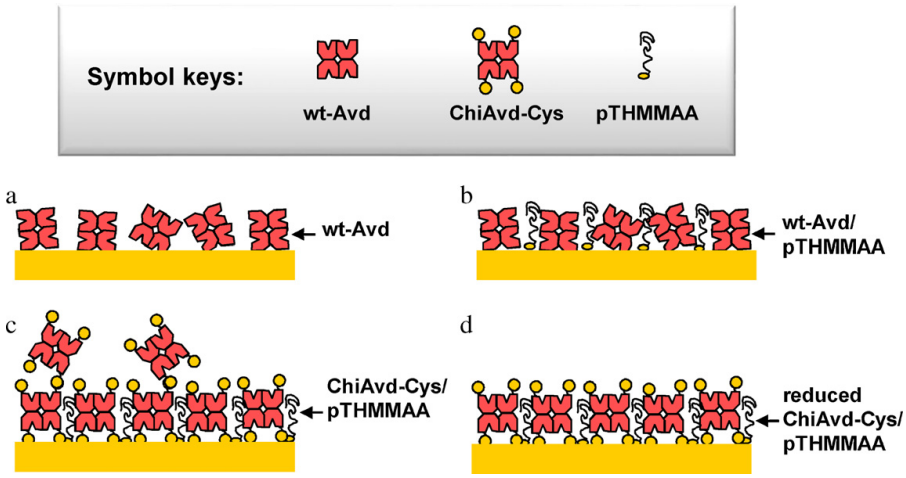

Scheme 2. Schematic illustrations of the studied assemblies. (a) Wild-type avidin physisorbed on the gold surface, (b) wt-Avd post-treated with pTHMMAA polymer and (c) non-reduced ChiAvd-Cys and (d) reduced ChiAvd-Cys attached to the surface through cysteine and post-treated with pTHMMAA.

the interaction with a two-fold higher concentration of ChiAvd-Cys showed nearly the same response (700 ± 60 ng/cm^2). This response is more than two times as high as that for the physisorbed wt-Avd, somewhat higher than that for avidin and streptavidin bound to a carboxylated dextran layer (400–600 ng/cm^2) [18,38], and agree with that of streptavidin on poly(oligo(ethylene glycol) methacrylate)–biotin layers (650 ng/cm^2 [17]. Higher binding has been obtained for coupling of 5 mM neutravidin (corresponding to a considerably higher concentration of 300 mg/mL) to a mixed biotinylated self-assembled layer (900 ng/cm^2) [39]. At a ten-fold higher ChiAvd-Cys concentration (500 μg/mL) binding to gold was in the range of 800 ± 50 ng/cm^2.

ChiAvd-Cys standing end-on at their 4.0 nm × 5.5 nm faces would have a surface coverage of about 445 ng/cm^2. It thus seems likely that on average, a layer corresponding to 1.5-fold the thickness of a monolayer of ChiAvd-Cys have been formed. Free thiol groups of the ChiAvd-Cys molecules on the surface may induce a further coupling with ChiAvd-Cys. ChiAvd-Cys might stack to each other forming disulphide bridges in between the individual molecules, which might lead to network-like structures (Scheme 2c). Another possibility is that ChiAvd-Cys forms dimers in solution and that these form bilayer structures when adsorbed on the surface. Post-treatment with pTHMMAA also gave a much higher coverage than that of the wt-Avd surface (300 ± 20 ng/cm^2). The polymer might, apart from being bound to the Au surface, interact with cysteine groups in the avidin layer. This would, however, prevent binding of biotinylated molecules to the surface because the polymer is highly hydrophilic. The total surface coverage of the ChiAvd-Cys/pTHMMAA layer was as high as 1000 ± 50 ng/cm^2. Considerably lower amounts of ChiAvd-Cys reduced with TCEP prior to injection adsorbed on the gold surface (450 ± 20 ng/cm^2) indicating coverage of one monolayer (Scheme 2d). When applied on the surface in the reduced form, cysteine groups do not seem to enable attachment of additional ChiAvd-Cys molecules. It therefore seems likely that non-reduced ChiAvd-Cys oligomerised in solution and formed partial bilayers on gold.

Binary monolayers of antibody Fab′-fragments and pTHMMAA can be obtained by post-treating antibody Fab′-fragments immobilised on gold with the pTHMMAA polymer or by co-adsorption of the Fab′-fragments and the pTHMMAA polymer [23,37]. Our

Table 1
Surface densities for immobilisation of (a) avidin on gold and post-treatment of the avidin surface with 200 μg/mL pTHMMAA. Immobilisation of (b) binary solutions of avidin and 200 μg/mL pTHMMAA on gold. Non-specific binding of BSA and binding of biotin-GFP as measured by SPR.

Protein	$Conc_{Avd}$ [μg/mL]	Avidin [ng/cm^2]	pTHMMAA [ng/cm^2]	BSA [ng/cm^2]	Biotin-GFP (10 μg/mL) [ng/cm^2]	Biotin-GFP (100 μg/mL]) [ng/cm^2]	Capacity[a] [%]
(a)							
wt-Avd	25	300 ± 100	100 ± 25				
wt-Avd	50	360 ± 90	–				
wt-Avd	500	500 ± 100	–				
ChiAvd-Cys	25	650 ± 50	300 ± 20	30 ± 5	280 ± 20	650 ± 50	36 ± 5
ChiAvd-Cys[b]	25	450 ± 20	130 ± 20	25 ± 5	130 ± 10	330 ± 30	26 ± 5
ChiAvd-Cys	50	700 ± 60	280 ± 20	50 ± 5	280 ± 20	650 ± 50	33 ± 5
ChiAvd-Cys	500	800 ± 60	290 ± 20	50 ± 5	280 ± 20	650 ± 50	29 ± 5

$Conc_{ChiAvd-Cys}$ [μg/mL]	Cys-Avd/pTHMMAA [ng/cm^2]	BSA [ng/cm^2]	Biotin-GFP (10 μg/mL) [ng/cm^2]
(b)			
25	500 ± 50	40 ± 5	180 ± 20
25[b]	440 ± 50	10 ± 5	170 ± 20
50	580 ± 50	40 ± 5	200 ± 20

[a] Assuming four biotin binding sites per avidin; number of replicas at least 8.
[b] ChiAvd-Cys reduced by TCEP treatment.

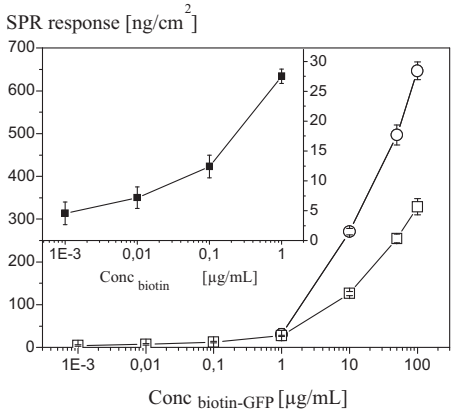

Fig. 1. Standard curves for binding of biotin-GFP to binary layers of non-reduced (○) and reduced (□, ■) ChiAvd-Cys and pTHMMAA.

hypothesis is that ChiAvd-Cys might be oriented on the gold surface a bit similar to that previously shown for antibody Fab′-fragments. Wild type avidin is physisorbed and thus randomly oriented on the surface due to the lack of cysteine groups, but wt-Avd might also be unfolded to a higher degree than the ChiAvd-Cys, which is known to be also thermally more stable [20]. The gold surface is highly energetic and it is generally recognised that proteins easily unfold on the gold surface.

ChiAvd-Cys/pTHMMAA layers were also formed by co-immobilisation of ChiAvd-Cys and the polymer. The surface coverage was lower than that of ChiAvd-Cys immobilised alone on gold indicating that a high amount of pTHMMAA was adsorbed on the surface (Table 1b). The polymer pTHMMAA takes a surface coverage of 340 ± 20 ng/cm^2 when adsorbed alone on the surface at this concentration. The amount of polymer in the solution is of high importance when co-adsorbing the substances [23]. The pTHMMAA concentration might have been too high in relation to the ChiAvd-Cys concentration. Thiols and disulphides form stable self-assembled monolayers on gold via a polar covalent bond. With thiols the reaction is assumed to take place as an oxidative addition to gold with release of hydrogen whereas in the case of disulphides, a cleavage of the S—S bond occurs. Disulphides, however, adsorb approximately 40% slower than thiols [40].

The lowest surface coverage, as well as the lowest non-specific binding of all the layers, was obtained when co-adsorbing pTHMMAA and the reduced ChiAvd-Cys. The approach of co-adsorption was not further studied, but might be an option for future studies provided that optimised ChiAvd-Cys and pTHMMAA concentrations are used.

3.3. Binding of biotin-GFP to the Avd/pTHMMAA layers

The biotin binding ability of the ChiAvd-Cys layer was determined by coupling various concentrations of a biotinylated-GFP to the layer. Biotin was genetically fused to GFP so that each molecule contains one biotin at the C-terminal side of the molecule. All of the biotinylated GFPs were thus identical causing no variation due to a differing number of biotins per molecule. The biotin-GFP binding was independent on the ChiAvd-Cys concentration used for immobilisation when the surface was post-treated with pTHMMAA (Table 1b). Biotin-GFP binding to binary layers composed of pTHMMAA and ChiAvd-Cys is as shown in Fig. 1. Binding of biotin-GFP was much higher to the ChiAvd-Cys/pTHMMAA layer as compared to the reduced ChiAvd-Cys/pTHMMAA layer. The binding of 100 μg/mL of biotin-GFP to the reduced ChiAvd-Cys/pTHMMAA layer was about 330 ± 30 ng/cm^2, whereas it was as high as 650 ± 50 ng/cm^2 to the ChiAvd-Cys/pTHMMAA layer (Table 1a). Already concentrations as low as 10 ng/mL could be detected with a response corresponding to 7 ± 2 ng/cm^2 (Fig. 1, insert). A closely packed monolayer of BSA with a molecular weight of 65 kDa and with dimensions of 8 nm × 8.7 nm × 6 nm would take up a surface coverage of 129 or 226 ng/cm^2 depending on the adsorption model used [41,42]. Biotin-GFP is a ~39 kDa protein with GFP domain having the shape of a cylinder with a diameter of ~3 nm and a height of 4 nm and a 1.3S-biotinylation domain of 2.5 nm × 2.5 nm × 2 nm, excluding the 45 residues missing from the N-terminus of the X-ray structure [43]. GFP standing side-on or end-on would have a monolayer surface coverage of 540 or 916 ng/cm^2, not taking the biotinylation domain into account. Thus biotin-GFP with a side-on orientation would take about 60% of a monolayer on the reduced ChiAvd-Cys, whereas 70% of a monolayer with biotin-GFP standing end-on seems to have formed when bound to the ChiAvd-Cys/pTHMMAA layer. In fact, steric hindrance would prevent a higher amount of binding to the ChiAvd-Cys layer.

About 33–36% of the four biotin-binding sites of avidin in the ChiAvd-Cys/pTHMMAA layer bound biotin-GFP if all biotin binding sites per avidin molecules were assumed to be available for binding (Table 1a). The binding to the reduced ChiAvd-Cys layer was somewhat lower (26%). The binding activity of the ChiAvd-Cys layer was therefore much higher than that reported by Reznik et al. for a cys-tagged streptavidin (12% of the biotin binding sites) [8]. Most probably the ChiAvd-Cys molecules were oriented so that not all the four biotin-ligand binding sites from each avidin tetramer were available for ligand binding. Some of the binding sites are probably oriented towards the Au surface and therefore unavailable for biotin. When assuming an orientation with two of the biotin-binding sites unavailable for biotin-GFP binding, binding capacities of 66–72% and 52% were obtained for the pTHMMAA layers with ChiAvd-Cys and reduced ChiAvd-Cys, respectively. A schematic cartoon of the binding is presented in Scheme 3a and b. High amounts of biotinylated molecules could thus be coupled to the ChiAvd-Cys/pTHMMAA surface.

The biotin binding specificity of the avidin layer was verified by saturating the ChiAvd-Cys molecules with biotin prior to injection over the surface. The amount of bound biotin-GFP on a biotin saturated ChiAvd-Cys/pTHMMAA layer corresponded to 50 ± 20 ng/cm^2, which was less than 10% of the binding of biotin-GFP to a non-saturated ChiAvd-Cys/pTHMMAA layer.

Biotin-GFP binding to the wt-Avd/pTHMMAA layer was very poor (data not shown). When wt-Avd was physisorbed on the metal surface, it is likely that most of the available biotin-binding sites were wasted due to an un-proper orientation on the surface. Some of the wt-Avd molecules might also denaturated when physisorbed on the gold surface.

3.4. Binding of amino-biotinylated F(ab′)$_2$-fragments to wt-Avd/pTHMMAA layers

Although the binding of biotin-GFP to the wt-Avd/pTHMMAA layer was poor, amino-biotinylated anti-human IgG F(ab′)$_2$-fragments at a concentration of 40 μg/mL were injected over the wt-Avd/pTHMMAA layer. A response corresponding to a surface coverage of 70 ± 20 ng/cm^2 was obtained. It seems that about 12% of the wt-Avd molecules were able to bind biotinylated antibodies assuming only one binding site per avidin molecule (Table 2; 3% of all the binding sites). More than one F(ab′)$_2$-fragment per avidin molecule would not be sterically possible. A low binding is not surprising because conventionally used wild type (strept)avidins have no residues that would specifically orient the avidins correctly on the surface although this is often claimed.

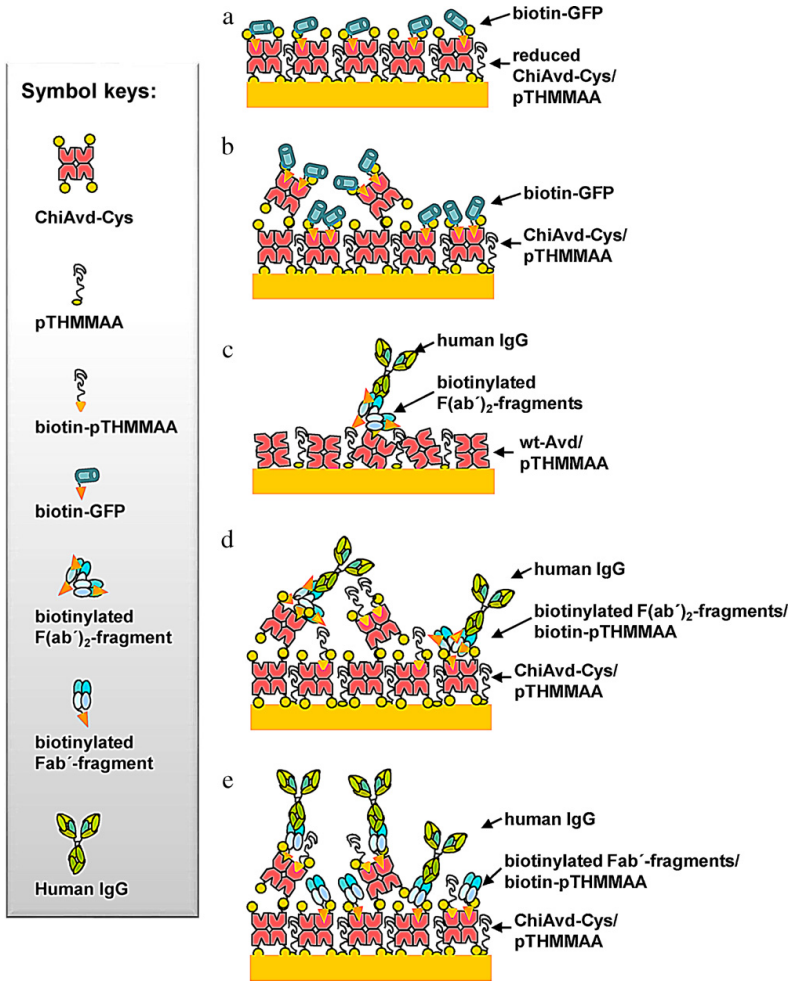

Scheme 3. A schematic view of biotinylated-GFP bound to (a) reduced and (b) non-reduced ChiAvd-Cys intercalated with pTHMMAA. Binding of amino-biotinylated F(ab′)$_2$-fragments and human IgG to layers of (c) wt-Avd/pTHMMAA and (d) non-reduced ChiAvd-Cys/pTHMMAA. (e) Site-directed binding of SH-biotinylated Fab′-fragments to non-reduced ChiAvd-Cys/pTHMMAA layers and binding of hIgG.

Table 2
Surface densities for immobilisation of 50 μg/mL avidin on gold, post-treatment with pTHMMAA, binding of 40 μg/mL (a) amino- and (b) SH-biotinylated human IgG Fc specific antibody fragments. Non-specific binding of BSA and the antigen hIgG at (a) 100 μg/mL and (b) 50 μg/mL.

Protein	Biotin-NH_2-F(ab′)$_2$ [ng/cm^2]	Capacity[a] [%]	Biotin-pTHMMAA [ng/cm^2]	BSA [ng/cm^2]	hIgG (100 μg/mL) [ng/cm^2]	Capacity [%]
(a)						
wt-Avd	70 ± 20	12 ± 1	−20 ± 10	9 ± 1	15 ± 10	7 ± 5
ChiAvd-Cys	270 ± 40	24 ± 1	20 ± 4	<0	120 ± 20	14 ± 5
Streptavidin	280 ± 20			0.5 ± 0.1	120 ± 20	13 ± 5
Avidin	Biotin-SH-Fab′ [ng/cm^2]	Capacity [%]	Biotin-pTHMMAA [ng/cm^2]	BSA [ng/cm^2]	hIgG (50 μg/mL) [ng/cm^2]	Capacity [%]
(b)						
ChiAvd-Cys	420 ± 15	76 ± 1	−7 ± 0.5	<0	200 ± 10	15 ± 5

[a] Assuming one binding site per avidin; number of replicas at least 8.

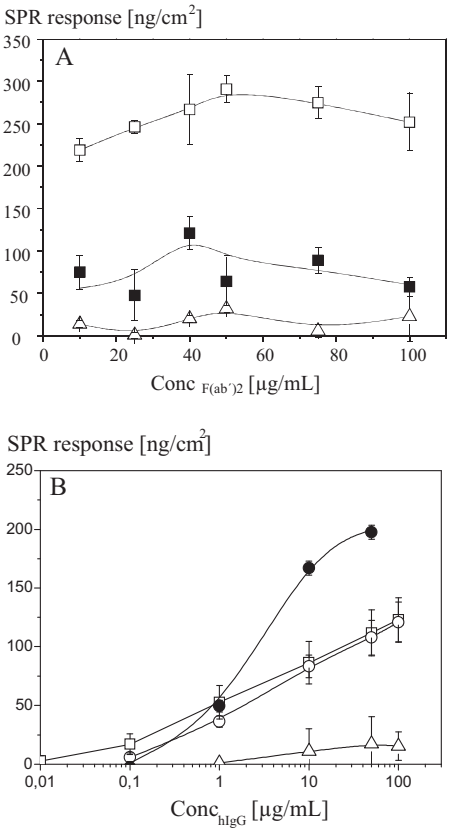

Fig. 2. (a) Binding of biotinylated hIgG Fc specific antibody F(ab′)$_2$-fragments (□) and subsequent binding of biotin–pTHMMAA (△) to a binary layer of ChiAvd-Cys and pTHMMAA. Binding of human IgG at 100 μg/mL (■) to the biotin-F(ab′)$_2$-fragments/biotin–pTHMMAA layer. Number of replicas, *n* was 4–12. (b) Standard curve for binding of human IgG to antibodies (40 μg/mL) bound to binary layers of avidin and pTHMMAA. wt-Avd/amino-biotinylated F(ab′)$_2$-fragments (△), ChiAvd-Cys/amino-biotinylated F(ab′)$_2$-fragments (○), ChiAvd-Cys/sulphhydryl-biotinylated F(ab′)-fragments (●). A commercial SA-chip coated with amino-biotinylated F(ab′)$_2$-fragments (□) was used as a reference.

In order to reduce the non-specific binding to the surface the free biotin-binding sites were blocked with biotin–pTHMMAA (Scheme 1c, compound **2**). Further blocking of the layer with a biotin–pTHMMAA seemed to remove molecules from the surface as a decrease in response was observed. Two subsequent interactions with BSA showed a non-specific binding of only 9 ± 1 and 10 ± 5 ng/cm^2 to the surface.

3.5. Binding of amino-biotinylated F(ab′)$_2$-fragments to ChiAvd-Cys/pTHMMAA layers

The concentration of the antibody immobilisation solution has a remarkable effect on both the specificity and the sensitivity of the antigen binding [23]. A sufficiently high antibody surface density ensures a high antigen binding, but a too high binding might inhibit antigen binding due to steric hindrance. To determine the optimal antibody concentration solutions of 0 to 100 μg/mL of amino-biotinylated F(ab′)$_2$-fragments were injected over the ChiAvd-Cys/pTHMMAA layer (Fig. 2a). The amount of biotinylated antibody fragments bound to the avidin layer increased with antibody concentration and showed the highest binding corresponding to 290 ± 20 ng/cm^2 at a concentration of about 50 μg/mL. This response was comparable with that of biotinylated anti-cardiac troponin antibodies bound to streptavidin coupled to a carboxy-methylated dextran surface (200 ± 20 ng/cm^2) [44]. Antigen binding was, however, highest at an antibody concentration of 40 μg/mL and this concentration of biotinylated anti-human IgG F(ab′)$_2$-fragments was used for the following studies.

A tightly packed monolayer of Fab′-fragments would have a surface coverage of 400–700 ng/cm^2 when standing side-on 8.0 nm × 7.0 nm or end-on 10.0 nm × 7.0 nm [45]. Based on the size of the fragments it is expected that avidin is not able to bind more than one antibody per molecule. Thus, the results suggest that 24% of the ChiAvd-Cys molecules (6% of all the biotin binding sites) in the layer bind one amino-biotinylated (Fab′)$_2$-fragment. This binding capacity is twice as high as that measured for cysteine-tagged streptavidin immobilised through maleimide on microtitre wells [8]. The biotinylated antibody fragments are randomly oriented when bound to the surface, because the fragments were biotinylated through the amino-group. A considerably higher amount of specific binding could be expected if the biotin-tag was attached on the antibody opposite to the antigen binding domain.

3.6. Binding of SH-biotinylated Fab′-fragments to ChiAvd-Cys/pTHMMAA layers

The free thiol groups generated when reducing the disulphide bridge of F(ab′)$_2$-fragments can be used to provide an oriented immobilisation of the antibody. Biotinylation to the amino-groups is random to groups anywhere on the molecule, while biotinylation to the thiol-groups takes place in the hinge-region of the Fab′-fragment that is ideally situated opposite to the antigen-recognition site. Fab′-fragment binding to the ChiAvd-Cys/pTHMMAA layer at a concentration of 40 μg/mL corresponded to 420 ± 15 ng/cm^2. Thus it seems that about 76% of the ChiAvd-Cys molecules bind two SH-biotinylated Fab′-fragments (Table 2), which is a considerable higher binding capacity compared to the binding of F(ab′)$_2$-fragments to wt-Avd and ChiAvd-Cys where only 12 and 24% of the avidins bind one antibody fragment, respectively.

3.7. Antigen binding to biotin-(Fab′)$_2$-fragments bound to avidin/pTHMMAA

The antibody fragments used were Fc specific and a binding of hIgG corresponding to 40 ± 5 and 120 ± 20 ng/cm^2 for 1 and 100 μg/mL, respectively, could be observed to the ChiAvd-Cys/pTHMMAA/biotin-F(ab′)$_2$ layer (Fig. 2b). In contrast, a response of only 15 ± 10 ng/cm^2 was obtained at a concentration of 100 μg/mL for the wt-Avd/pTHMMAA. Injection of human IgG caused slight removal of material from the surface and a negative response was observed at concentrations below 1 μg/mL. The binding efficiency of the antibody fragments was in the range of 7 and 14%, for the fragments on the wt-Avd and ChiAvd-Cys/pTHMMAA surface, respectively (Table 2). The much higher amount of antigen binding to antibody fragments in the ChiAvd-Cys/pTHMMAA layer compared to the wt-Avd/pTHMMAA layer was probably due to a higher orientation and stability of the ChiAvd-Cys. Wild-type avidin was physisorbed on the surface and thus only randomly oriented and denaturated to a higher extent (Scheme 3c and d).

A commercial Biacore streptavidin-coated carboxymethylated dextran layer (SA-chip) was used as a reference surface. The amino-biotinylated F(ab′)$_2$ binding corresponded to 280 ± 5 ng/cm^2. This is four-fold to that for the wt-Avd/pTHMMAA layer (70 ± 15 ng/cm^2) and close to that of the ChiAvd-Cys/pTHMMAA layer (270 ± 40 ng/cm^2). Antigen binding to the surface corresponded to 120 ± 20 ng/cm^2, which is almost ten-fold that of the

wt-Avd/pTHMMAA and equals to that measured for the ChiAvd-Cys/pTHMMAA layer. The binding capacity of the layer was 13%. It is expected that less than 10% of antibodies remain active when immobilised in a random orientation [1].

3.8. Antigen binding to SH-biotinylated-Fab′-fragments bound to ChiAvd-Cys/pTHMMAA

Human IgG binding to the SH-biotinylated Fab′-fragments was very high (200 ± 10 ng/cm^2 at 50 μg/mL), with a binding efficiency of 15%. This antigen to antibody ratio was the same as that of Fab′-fragments and pTHMMAA immobilised directly on gold (hIgG binding of 275 ± 8 ng/cm^2 at 100 μg/mL). The surfaces were not completely saturated at this concentration and a higher binding efficiency could be expected at a higher concentration. A human IgG binding response of 50 ± 8 ng/cm^2 was obtained at concentrations as low as 1 μg/mL. The binding was almost twice as high as that of the commercial SA-chip and ChiAvd-Cys/pTHMMAA layer with amino-biotinylated F(ab′)$_2$-fragments. The higher binding response of the Fab′-fragment layer compared to that of the F(ab′)$_2$-fragment layers verify the importance of an orientation of the antibodies.

4. Conclusions

Cys-tagged chimeric avidin can be immobilised directly on gold and intercalated with a non-ionic hydrophilic pTHMMAA polymer. Monolayers can be formed by a reduction of ChiAvd-Cys prior to immobilisation on the surface otherwise ChiAvd-Cys formed partial bilayer structures, probably due to a dimerisation of ChiAvd-Cys molecules in solution. The ChiAvd-Cys/pTHMMAA showed a high binding capacity of a small biotinylated green fluorescent protein (GFP) molecule. If ChiAvd-Cys are oriented in the layer with only two of the biotin-binding sites available for binding on the average 66–72% of the ChiAvd-Cys molecules bind two biotin-GFPs. The capacity was somewhat lower for the layer made from the reduced ChiAvd-Cys (52%). Only 12% of the avidin in the wt-Avd/pTHMMAA layer were able to bind one amino-biotinylated antibody F(ab′)$_2$-fragment. The binding capacity of the ChiAvd-Cys/pTHMMAA layer was twice as high and one biotinylated Fab′-fragment were bound to 76% of the ChiAvd-Cys molecules on average.

Cysteine modified avidins can be used for anchoring high amounts of biotinylated molecules to the surface. Antigen binding to the ChiAvd-Cys/pTHMMAA/antibody layers was much higher than that of the wt-Avd/pTHMMAA/antibody layer. Improved orientation of the antibodies in the ChiAvd-Cys/pTHMMAA layer further increased the antigen binding. The layer could be further improved by pre-washing to remove molecules not firmly attached to the surface. Overall, the ChiAvd-Cys/pTHMMAA layer is easy to produce and could be used as a general binding scaffold for biotinylated antibodies and be an alternative to the dextran-based streptavidin layers.

Acknowledgements

The authors gratefully acknowledge the financial support from the Biosensing Competence Centre and VTT Technical Research Centre of Finland. We also thank Biocenter Finland for support in the research infrastructure and Academy of Finland for funding.

References

[1] K.L. Brogan, K.N. Wolfe, P.A. Jones, M.H. Schoenfisch, Direct oriented immobilization of F(ab′) fragments on gold, Analytica Chimica Acta 496 (2003) 73–80.
[2] B. Lu, M.R. Smyth, O'Kennedy, Oriented immobilization of antibodies and its application in immunoassays and immunosensors, Analyst 121 (1996) 29R–32R.
[3] N.M. Green, Avidin, Advances in Protein Chemistry 295 (1975) 85–133.
[4] N.M. Green, Avidin and streptavidin, Methods in Enzymology 184 (1990) 51–67.
[5] O.L. Laitinen, H.R. Nordlund, V.P. Hytönen, M.S. Kulomaa, Brave new (strept)avidins in biotechnology, Trends in Biotechnology 25 (2007) 269–277.
[6] P.C. Weber, D.H. Ohlendorf, J.J. Wendoloski, F.R. Salemme, Structural origins of high-affinity biotin binding to streptavidin, Science 243 (1989) 85–88.
[7] W.A. Hendrickson, A. Pahler, J.L. Smith, Y. Satow, E.A. Merritt, R.P. Phizackerley, Crystal structure of core streptavidin determined from multiwavelength anomalous diffraction of synchrotron radiation, Proceedings of the National Academy of Sciences of the United States of America 86 (1989) 2190–2194.
[8] G.O. Reznik, S. Vajda, C.R. Cantor, T. Sano, A streptavidin mutant useful for directed immobilization on solid surfaces, Bioconjugate Chemistry 12 (2001) 1000–1004.
[9] S. Tombelli, M. Mascini, A.P. Turner, Improved procedures for immobilisation of oligonucleotides on gold-coated piezoelectric quartz crystals, Biosensors and Bioelectronics 17 (2002) 929–936.
[10] J. Spinke, M. Liley, F.-J. Schmitt, Molecular recognition at self-assembled monolayers: optimization of surface functionalization, The Journal of Chemical Physics 99 (1993) 7012–7019.
[11] A. Schmidt, J. Spinke, T. Bayer, E. Sackmann, W. Knoll, Streptavidin binding to biotinylated lipid layers on solid support, Biophysical Journal 63 (1992) 1185–1192.
[12] P. Ihalainen, J. Peltonen, Immobilization of streptavidin onto biotin-functionalized Langmuir–Schaefer binary monolayers chemisorbed on gold, Sensors and Actuators B 102 (2004) 207–221.
[13] S. Hleli, C. Martelet, A. Abdelghani, N. Burais, N. Jaffrezic-Renault, Atrazine analysis using an impedimetric immunosensor based on mixed biotinylated self-assembled monolayer, Sensors and Actuators B 113 (2006) 711–717.
[14] Y. Ishizuka-Katsura, T. Wazawa, T. Ban, K. Morigaki, S. Aoyama, Biotin-containing phospholipid vesicle layer formed on self-assembled monolayer of a saccharide-terminated alkyl disulfide for surface plasmon resonance biosensing, Journal of Bioscience and Engineering 105 (2008) 527–535.
[15] A.L. Plant, M. Brigham-Burke, E.C. Petrella, D.J. O'Shannessy, Phospholipid/alkanethiol bilayers for cell-surface receptor studies by surface plasmon resonance, Analytical Biochemistry 226 (1995) 342–348.
[16] S. Mun, S.-J. Choi, Optimization of the hybrid bilayer membrane method for immobilization of avidin on quartz crystal microbalance, Biosensors and Bioelectronics 24 (2009) 2522–2527.
[17] N. Yang, X. Su, V. Tjong, W. Knoll, Evaluation of 2-D and 3-D streptavidin chips for study DNA–DNA and protein–DNA interactions, Biosensors and Bioelectronics 22 (2007) 2700–2706.
[18] B.S. Lee, Y.S. Chi, K.-B. Lee, Y.-G. Kim, I.S. Choi, Functionalization of poly(oligo(ethylene glycol)methacrylate) films on gold and Si/SiO_2 for immobilization of proteins and cells: SPR and QCM studies, Biomacromolecules 8 (2007) 3922–3929.
[19] P.A. Millner, H.C.W. Hays, A. Vakurov, N.A. Pchelintsev, M.M. Billah, M.A. Rodgers, Nanostructured transducer surfaces for electrochemical biosensor construction – interfacing the sensing component with the electrode, Seminars in Cell & Developmental Biology 20 (2009) 34–40.
[20] V.P. Hytönen, J.A. Määttä, T.K. Nyholm, O. Livnah, Y. Eisenberg-Domovich, D. Hyre, H.R. Nordlund, J. Hörhä, E.A. Niskanen, T. Paldanius, T. Kulomaa, E.J. Porkka, P.S. Stayton, O.H. Laitinen, M.S. Kulomaa, Design and construction of highly stable, protease-resistant chimeric avidins, Journal of Biological Chemistry 280 (2005) 10228–10233.
[21] J.A. Määttä, Y. Eisenberg-Domovich, H.R. Nordlund, R. Hayouka, M.S. Kulomaa, O. Livnah, V. Hytönen, Chimeric avidin shows stability against harsh chemical conditions – biochemical analysis and 3D structure, Biotechnology and Bioengineering 108 (2011) 481–490.
[22] J.J. Heikkinen, L. Kivimaki, J.A.E. Määttä, I. Mäkela, L. Hakalahti, K. Takkinen, M.S. Kulomaa, V.P. Hytönen, O.E.O. Hormi, Versatile bio-ink for covalent immobilization of chimeric avidin on sol–gel substrates, Colloids and Surfaces B: Biointerfaces 87 (2011) 409–414.
[23] I. Vikholm-Lundin, Immunosensing based on site-directed immobilization of antibody fragments and polymers that reduce nonspecific binding, Langmuir 21 (2005) 6473–6477.
[24] I. Vikholm-Lundin, W.M. Albers, Site-directed immobilisation of antibody fragments for detection of C-reactive protein, Biosensors and Bioelectronics 21 (2006) 1141–1148.
[25] M.A. Albers, T. Munter, P. Laaksonen, I. Vikholm-Lundin, Functional characterisation of Fab′-fragments self-assembled onto hydrophilic gold surfaces, Journal of Colloid and Interface Science 348 (2009) 1–8.
[26] J. Homola, Surface plasmon resonance sensors for detection of chemical and biological species, Chemical Reviews 108 (2008) 462–493.
[27] A. Basak, F. Jean, H. Dugas, C. Lazure, Biotinylation of an enkephalin-containing heptapeptide via various spacer arms. Synthesis, comparative binding studies toward avidin, and application as substrates in enzymic reactions, Bioconjugate Chemistry 5 (1994) 301–305.
[28] H. Kitano, Y. Akatsuka, N. Ise, pH-responsive liposomes which contain amphiphiles prepared by using lipophilic radical initiator, Macromolecules 24 (1991) 42–46.
[29] V.P. Hytönen, O.H. Laitinen, T.T. Airenne, H. Kidron, N.J. Meltola, E.J. Porkka, J. Hörhä, T. Paldanius, J.A. Määttä, H.R. Nordlund, M.S. Johnson, T.A. Salminen,

K.J. Airenne, S. Ylä-Herttuala, M.S. Kulomaa, Efficient production of active chicken avidin using a bacterial signal peptide in *Escherichia coli*, Biochemical Journal 384 (2004) 385–390.
[30] D.V. Reddy, B.C. Shenoy, P.R. Carey, F.D. Sonnichsen, Biotin carboxyl carrier domain of transcarboxylase, Biochemistry 39 (2000) 2509–2516.
[31] J. Farres, M.P. Rechsteiner, S. Herold, A.D. Frey, P.T. Kallio, Ligand binding properties of bacterial hemoglobins and flavohemoglobins, Biochemistry 44 (2005) 4125–4134.
[32] U.K. Laemmli, Cleavage of structural proteins during the assembly of the head of bacteriophage T4, Nature 227 (1970) 680–685.
[33] P. Carter, R.F. Kelley, M.L. Rodrigues, B. Snedecor, M. Covarrubias, M.D. Velligan, W.L. Wong, A.M. Rowland, C.E. Kotts, M.E. Carver, M. Yang, J.H. Bourel, H.M. Shepard, D. Henner, High level *Escherichia coli* expression and production of a bivalent humanized antibody fragment, Biotechnology 10 (1992) 163–167.
[34] W.M. Albers, Sensor element and its use, Pat. FI-120698 (B1) (2007).
[35] E. Stenberg, B. Persson, H. Roos, C. Urbaniczky, Quantitative determination of surface concentration of protein with surface plasmon resonance using radiolabeled proteins, Journal of Colloid and Interface Science 143 (1991) 513–526.
[36] O. Livnah, E.A. Bayer, M. Wilchek, J.L. Sussman, Three-dimensional structures of avidin and the avidin–biotin complex, Proceedings of the National Academy of Sciences of the United States of America 90 (1993) 5076–5080.
[37] I. Vikholm, J. Sadowski, US20070254382 (2007-11-01).
[38] D.J. O'Shannessy, M. Brigham-Burke, K. Peck, Immobilization chemistries suitable for use in the BIAcore surface plasmon resonance detector, Analytical Chemistry 205 (1992) 132–136.
[39] H.C.W. Hays, P.A. Millner, M.I. Prodromidis, Development of capacitance based immunosensors on mixed self-assembled monolayers, Sensors and Actuators B 114 (2006) 1064–1070.
[40] Ch. Jung, O. Dannenberger, Y. Xu, M. Buck, M. Grunze, Self-assembled monolayers from organosulfur compounds: a comparison between sulfides, disulfides, and thiols, Langmuir 14 (1998) 1103–1107.
[41] D.C. Carter, X.M. He, S.H. Munson, P.D. Tw, K.M. Gernert, M.B. Broom, T.Y. Miller, Three-dimensional structure of human serum albumin, Science 244 (1989) 1195–1198.
[42] F. Höök, J. Vörös, M. Rodahl, R. Kurrat, P. Böni, J.J. Ramsden, M. Textor, N.D. Spencer, P. Tengvall, J. Gold, B. Kasemo, A comparative study of protein adsorption on titanium oxide surfaces using in situ ellipsometry, optical waveguide lightmode spectroscopy, and quartz crystal microbalance/dissipation, Colloids and Surfaces B: Biointerfaces 24 (2002) 155–170.
[43] F. Yang, L.G. Moss Jr., G.N. Phillips, The molecular structure of green fluorescent protein, Nature: Biotechnology 14 (1996) 1246–1251.
[44] R.F. Dutra, L.T. Kubota, An SPR immunosensor for human cardiac troponin T using specific binding avidin to biotin at carboxymethyldextran-modified gold chip, Clinica Chimica Acta 376 (2007) 114–120.
[45] I. Vikholm, E. Györvary, J. Peltonen, Incorporation of lipid-tagged single-chain antibodies into lipid monolayers and the interaction with antigen, Langmuir 12 (1996) 3276–3281.

Biographies

Inger Vikholm-Lundin is Senior Principal Scientist at VTT Technical Research Centre of Finland. She received her Ph.D. from Åbo Akademi University in 1996. She has been engaged in biosensor research over 25 years and she has mainly focused on the oriented immobilisation of antibodies and oligonucleotides with the aim of obtaining high specific binding and reduction of the non-specific binding of interfering molecules.

Sanna Auer is a PhD student and Research Scientist at VTT Technical Research Centre of Finland.

Maija Paakkunainen is a M.Sc. student at the Institute of Biomedical Technology, University of Tampere, Finland.

Juha A.E. Määttä received his Ph.D. from University of Tampere in 2010 after studies on physicochemical properties of new avidin proteins with Professor Markku Kulomaa. Since then he has worked as post-doc researcher and coordinator in Biocenter Finland core facility project in the University of Tampere. His present research interests cover interaction studies and novel protein production and purification for clients and collaborators.

Tony Munter received his Ph.D. degree in organic chemistry in 2000 from Åbo Akademi University, Turku, Finland. From 2001 to 2003 he has been a postdoctoral researcher at the Department of Chemistry, University of Newcastle upon Tyne, UK and from 2003 to 2005 at the Syngenta Central Toxicology Laboratory, Macclesfield, UK. Since 2005 he has been working as a research scientist at VTT Technical Research Centre of Finland. His main research interests are organic synthesis and surface chemistry.

Jenni Leppiniemi is a Ph.D. student at the Institute of Biomedical Technology, University of Tampere, Finland. Her research aims to develop functional materials by combining synthetic or natural materials and biomolecular building blocks, including engineered proteins. She graduated as M.Sc. in Engineering in 2005 at the Institute of Biomaterials, Department of Materials Science, Tampere University of Technology, Finland.

Vesa P. Hytönen received his Ph.D. from University of Jyväskylä, Finland in 2005 focusing on engineered avidin forms with Professor Markku Kulomaa. He then joined the laboratory of Professor Viola Vogel at ETH Zurich, Switzerland and got involved in mechanobiology research. He lately established own research group in the Institute of Biomedical Technology at University of Tampere, Finland. His current research focuses on mechanical tension as a regulator of protein-protein interactions.

Kirsi Tappura received her M.Sc. and D.Sc. (Tech) degrees in technical physics from the Tampere University of Technology (TUT), Finland, in 1990 and 1993, respectively, and conducted research on semiconductors, optoelectronic materials and devices at TUT until she joined Nokia Research Center to work on novel electronic displays. Currently she is acting as a principal scientist and a team leader at VTT with her research interests in the various areas of materials and sensor physics, plasmonics, as well as molecular and device modelling. She is also adjunct professor at TUT.

PUBLICATION IV

Hybridization of binary monolayers of single stranded oligonucleotides and short blocking molecules

In: Surface Science, 603: 620–624.

Surface Science 603 (2009) 620–624

Contents lists available at ScienceDirect

Surface Science

journal homepage: www.elsevier.com/locate/susc

Hybridization of binary monolayers of single stranded oligonucleotides and short blocking molecules

Inger Vikholm-Lundin [a,*], Sanna Auer [a], Tony Munter [a], Heidi Fiegl [b], Sophia Apostolidou [b]

[a] VTT Technical Research Centre of Finland, P.O. Box 1300, FI-33101 Tampere, Finland
[b] University College London, London W1T 4JF, United Kingdom

ARTICLE INFO

Article history:
Received 8 October 2008
Accepted for publication 19 December 2008
Available online 27 December 2008

Keywords:
Oligonucleotides
Immobilization
Self-assembly
Hybridization
Surface plasmon resonance

ABSTRACT

We have studied the immobilization of single stranded (ss) DNA oligonucleotides of 16–27 base pairs on gold. The oligonucleotides were thiol-modified (SH-ssDNA) or disulfide-modified via a dimethoxytrityl-group (DMT-S-S-ssDNA). Immobilization was performed by adsorption of the probes on the gold surface for 10–15 min, a time within which saturation coverage was obtained for both thiol- and disulfide-modified probes. Hereafter the layer was post-treated with hydroxyalkyl substituted lipoamides also for a time of 10–15 min. The surface density of layers with shorter probes (16–18 mer) was twice ($2.4 \pm 0.2 \times 10^{13}$ probes/cm^2) that of the longer probes (25–27 mer) as studied with surface plasmon resonance. Hybridization of single stranded polymerase chain reaction (PCR) amplified products with a length above 300 base pairs gave a very low hybridization response. For amplicons with about 100 base pairs the response was high. The surface coverage was comparable to that of complementary ssDNA binding (3.0×10^{12} strands/cm^2). Surfaces made from SH-ssDNA showed a 30% higher hybridization response than surfaces made from DMT-S-S-ssDNA. The PCR amplified products used are of relevance in breast cancer diagnosis. The results clearly demonstrate that the single stranded PCR products might be used in label-free cancer diagnostics.

1. Introduction

Detection of single stranded oligonucleotides (ssDNA) is currently of increasing interest because of potential application for example in diagnosis of genetic diseases [1], gene transfection [2], mutation [3] and species identification [4]. An efficient method for immobilization of DNA-probes is essential when developing a sensitive surface for DNA detection. Probes have been attached onto various surfaces by adsorption [5], copolymerization [6], complexation [7] and by covalent linkage [8–13]. Methods for covalent attachment include use of silane and self-assembly of thiol-modified oligos. Thiols are known to form self-assembled monolayers on gold, and the thiol-modified oligos are expected to immobilize on gold in a similar manner. Surface hybridization depends strongly on probe-length and density, surface orientation and target sequence of the oligos [8,11,14]. Thiol-modified ssDNA assembled on gold have often been post-treated with 6-mercapto-1-hexanol in order to reduce non-specific binding (NSB) of interfering proteins from the sample solution and to improve the attachment of the probes to the surface [8,11,15]. The affinity of adenine base pairs for gold has also recently been utilized for ssDNA monolayer formation [16].

The immobilization is normally allowed to take place for 12–16 h. If array type sensors are to be produced this assembling time is too long. A fast and easy to perform immobilization procedure is required. Our approach has been to use an immobilization time of 10–15 min and to follow the assembling procedure *in situ* by surface plasmon resonance, SPR. We have previously co-adsorbed SH-ssDNA and a hydroxyalkyl substituted lipoamide or a non-ionic hydrophilic polymer directly onto gold or post-treated the probe surface with the blocking agents [17,18]. The lipoamide and the polymer possess low NSB and can be covalently attached onto the gold surface by disulfide anchors [19–22]. In this paper the hybridization response of monolayers made from SH-ssDNA and DMT-S-S-ssDNA (referring to oligonucleotides without and with the protective groups form the oligonucleotide synthesis) will be compared. The layers are post-treated with various hydroxyalkyl substituted lipoamides and 6-mercapto-1-hexanol. The probes used were selected based on our previous observations that these gene loci were frequently methylated in cancer specimens [23]. The hybridization of PCR amplified real samples of various lengths will be reported. Almost all papers reporting on development of DNA hybridization sensors deal with model, relatively short, oligonucleotides and only a few authors have reported on hybridization with PCR amplified DNA of clinical interest [24–28]. We have used SPR for detection of the hybridization. SPR allows simultaneous real-time monitoring of the hybridization of immobilized

* Corresponding author. Tel.: +358 40 538 9484; fax: +358 20 722 3319.
E-mail address: Inger.Vikholm-Lundin@vtt.fi (I. Vikholm-Lundin).

0039-6028/$ - see front matter © 2009 Elsevier B.V. All rights reserved.
doi:10.1016/j.susc.2008.12.026

oligonucleotide probes [18]. Also the hybridization reaction takes time during a relatively short time of 10 min contrary to the long times of 2–24 h normally used [12,29].

2. Experimental

2.1. Chemicals

Tris(hydroxymethyl)aminomethane, ammonium hydroxide (28–30% NH_3) and bovine serum albumin (BSA), minimum 98% purity were purchased from Sigma Aldrich Finland Oy (Helsinki, Finland). α-Lipoic acid *N*-succinimidyl ester (Lipa-NHS) and *N,N*-bis(2-hydroxyethyl)-α-lipoamide (Lipa-DEA) were prepared as previously described [19]. The solvents (analytical grade), hydrogen peroxide (30%), EDTA and Na_2HPO_4 were purchased from Merck KGaA, sodium chloride and NaH_2PO_4 from J. T. Baker.

2.2. NMR and MS

The ^1H and ^{13}C NMR spectra were recorded with a 300 MHz Varian NMR spectrometer operating at frequencies given with the spectral data. The compounds were dissolved in $CDCl_3$ and the solvent was used as the internal reference standard. The mass spectrometric analyses were performed on an Agilent 1100 Series LC/MSD Trap system (Agilent Technologies, Espoo, Finland) equipped with an electro spray source and operated in the positive ion mode.

2.3. Chromatography

Thin-layer chromatography (TLC) was performed on silica gel 60 F_{254} TLC aluminium sheets (Merck KGaA). The spots were visualised by dipping the TLC plate in an alkaline aqueous solution of potassium permanganate. For column chromatography, silica gel 60 with a particle size of 0.04–0.063 mm (230–400 mesh) (Fluka, Sigma Aldrich Finland Oy, Helsinki, Finland) was used.

2.4. Preparation of 5-(1,2-dithiolan-3-yl)-N-[2-hydroxy-1,1-bis(hydroxymethyl)ethyl]pentanamide (Lipa-TRIS)

α-Lipoic acid *N*-succinimidyl ester (0.75 g, 2.48 mmol) was added to a stirred solution of tris(hydroxymethyl)aminomethane (0.33 g, 2.72 mmol) in *N,N*-dimethylformamide (25 mL) at 50 °C. The mixture was stirred at 50 °C, while the disappearance of α-lipoic acid *N*-succinimidyl ester was monitored by TLC (ethyl acetate). After 23 h, the solvent was removed by rotary evaporation. Purification of the residual oil by column chromatography [silica, elution with ethyl acetate/methanol (100/8 vol/vol)] and evaporation of the solvent yielded a yellow solid. Recrystallisation from 2-propanol gave the pure product (0.43 g, 56%). ^1H NMR (300 MHz, $CDCl_3$): δ 6.51 (s, 1H, NH), 4.68 (br, 3H, 3 × OH), 3.60 (m, 7H, 3 × CH_2OH, H-6), 3.15 (m, 2H, 2 × H-8), 2.47 (m, 1H, H-7_a), 2.26 (t, 2H, J = 7.3 Hz, 2 × H-2), 1.91 (m, 1H, H-7_b), 1.76–1.38 (m, 6H, 2 × H-3, 2 × H-4, 2 × H-5). ^{13}C NMR (75.4 MHz, $CDCl_3$): δ 175.0, 62.0, 61.6, 56.5, 40.4, 38.6, 36.8, 34.7, 28.8, 25.5. ESI-MS: *m/z* 332 (18, MNa^+), 310 (100, MH^+), 292 (1, MH^+–H_2O).

2.4.1. Oligonuceotide sequences

Single stranded, 16 to 27 bases long DNA (16–27-mer ssDNA) molecules with sequences according to Table 1 were used. The probes obtained from Metabion (Martinsried, Germany) were disulfide-modified in the 5′ end by a dimethoxytrityl-group (5′-DMT-S-S-$(CH_2)_6$-DNA). The probes are referred to as DMT-S-S-ssDNA. When the protective group was removed according to instructions from the supplier probes with a thiol-modification was obtained. These are referred to as SH-ssDNA. For clarity the base pair length of the probes is given as an extension of the probe name. The probes were designed to be completely complementary to the pairing DNA-strands as shown in Table 1.

2.5. Sample pre-treatment

One microgram of SssI (New England Biolabs, Hitchin, UK) treated human white blood cell DNA (heavily methylated) (Promega, Southampton, UK) was modified by sodium bisulphite using the EZ DNA Methylation-Gold Kit™ from Zymo Research (HiSS Diagnostics GmbH, Freiburg, Germany). The following oligo sets were used for the amplification of the dsDNA: PTGS2-27 Forward: 5′-TGTATGAGTGTGGGATTTGATTAGTATAAG, PTGS2-27 Reverse: 5′-CTATATCC AACCCCACTCCTAATAAAA, PTGS2-16 Forward: 5′PO_4-AGAGGGGGTAGTTTTTATTTTT, PTGS2-16 Reverse: AACA TATCAACCTTTCTTAACCTT, CALCA-25 Forward: 5′-TATA ATCCC TACCTAAATCAAACTCACACT, CALCA-25 Reverse: 5′-TGGGT ATATGTTGGGA GATA GTAATGG, CALCA-18 Forward: 5′PO_4-GTTTTGGAAGTATGAGGGTG, CALCA-18 Reverse: CCAAA TTCTAAACCAATTTCC. PCR reactions were performed using a GeneAmp 9700 thermal cycler (PE Applied Biosystems, Foster City, CA, USA) with a total volume of 25–50 μL reaction mixture containing 10–20 μL of bisulphite modified DNA, 0.2 μM dNTP Mix (Qiagen, Hilden, Germany), 1 Unit Hotstart Polymerase (Qiagen, Hilden, Germany), 1× PCR Buffer (Qiagen, Hilden, Germany) and 240 nM of each primer. An initial denaturation at 95 °C for 15 min was followed by 40 cycles of amplification. Each cycle consisted of denaturation at 95 °C for 60 s, annealing at 55–60 °C for 45 s, and extension at 72 °C for 60 s. A final extension for 10 min at 72 °C was performed. PCR products produced with CALCA and PTGS2 oligos, were used to obtain ssDNA for hybridization with the immobilized probe. The specific PCR products were purified using the QIAquick PCR purification Kit (Qiagen, Southampton, UK) and were treated with Strandase using the Novagen Strandase Kit (Darmstadt, Germany) according to the manufacturer's instructions. The Strandase-treated products were then further purified by MinElute PCR Qiagen purification Kit (Southampton, UK). Concentrations were determined with UV absorbance, after which the samples were diluted according to the requirements with nuclease free water. Purified ssDNA products for CALCA-25 and PTGS2-27 oligos were custom synthesized from Metabion (Martinsried, Germany).

The total base pair length of the PCR products generated and location of the complementary sequences in the target are given in Scheme 1. PTGS2-16 and CALCA-18 PCR products had a base pair length of 344 and 624 base pairs, respectively. Additional shorter PCR products with 92 and 123 base pairs were used for CALCA-25 and PTGS2-27 (see Scheme 1).

Table 1
Abbreviations, length and sequence of the probes are given. Sequence of complementary single stranded oligonucleotide and base pair (bp) length of PCR amplified DNA products. The number extension of the ssDNA refers the base pair length of the probes.

ssDNA	Probe sequence	Complementary strand	bp length
DMT-S-S-PTGS2-16	5′-DMT-S-S-C6-TAT CGT TTT AGG CGT A	5′-T ACG CCT AAA ACG ATA	344
SH-PTGS2-27	5′-SH-C6-CGA TTG TAT TCG GAT AGG ATT TTA TGG	5′-CCA TAA AAT CCT ATC CGA ATA CAA TCG	123
DMT-S-S-CALCA-18	5′-DMT-S-S-C6-GAG GGT GAC GTA ATT TAG	5′-CTA AAT TAC GTC ACC CTC	624
SH-CALCA-25	5′-SH-C6-GCT TCC GAT CAC ACT CAT TTA CAC A	5′-TGT GTA AAT GAG TGT GAT CGG AAG C	92

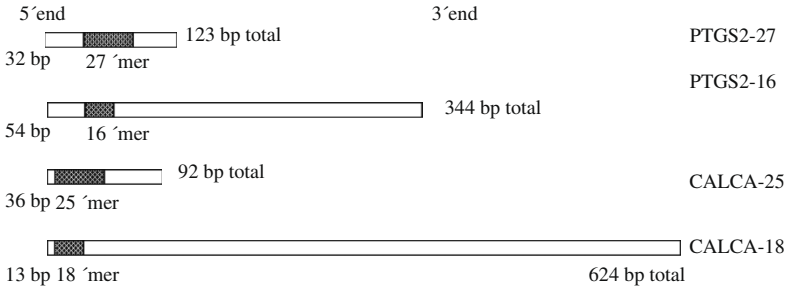

Scheme 1. Schematic presentation of the PCR products: PTGS2-27, PTGS2-16, CALCA-25 and CALCA-18. The location and length of the strand complementary to the surface probe (high-lighten in grey) and the total length of the amplicons are given. The number extension refers to the base pair length of the probe.

2.6. Immobilization procedure

Attachment of disulfide- or thiol-modified oligos and post-treatment with blocking agents on gold were carried out by a Biacore 3000 instrument (GE Healthcare, Uppsala, Sweden). Glass slides coated with a 50 nm thin film of gold by sputter coating (using an Edwards E306A sputter coater) were cleaned in a hot hydrogen peroxide/ammonium hydroxide/water solution (1/1/5) and rinsed with water. The slide was mounted in a plastic chip cassette by double-sided tape and inserted into the Biacore instrument. A phosphate-buffered saline (PBS) pH 7.5 composed of 20 mM Na_2HPO_4/NaH_2PO_4, 300 mM NaCl, 1 mM EDTA pH 7.5 was used. Stock solutions (10 mg/mL) of the blocking agents were prepared in methanol (Lipa-DEA) and DMSO (Lipa-TRIS). Before the immobilization, the stock solutions were diluted in the buffer solution to 1 mM. The immobilization procedure was started by rinsing the slide with buffer at a constant flow rate of 20 μL/min for 1 min. The probes at a concentration between 4 and 20 μM were allowed to adsorb on the gold surface for 10–15 min. The surface was rinsed with buffer and then post-treated with the blocking molecules for an additional time of 10–15 min.

The Biacore 3000 device was also used to determine binding of bovine serum albumin (1.5 μM concentration) and non-complementary strands (non-compDNA, 1 nM concentration). Hybridization of complementary strands (comp ssDNA), or PCR amplified double stranded (ds), or single stranded (ss) target oligonucleotides were determined all at a temperature of 25 °C. The oligonucleotides were dissolved in MilliQ-H_2O and diluted in the running buffer and applied by titration on the surface when studying the hybridization interaction. The oligonucleotide sample was added at a flow rate of 20 μL/min for 10–15 min, after which the surface was flushed with buffer for 10–15 min. As proteins and nucleotides have similar refractive indices a SPR response of 1000 RU was estimated to correspond to a surface coverage of about 100 ng/cm^2 [30]. Regeneration of the surface was performed with 10 mM NaOH-0.1% SDS-solution.

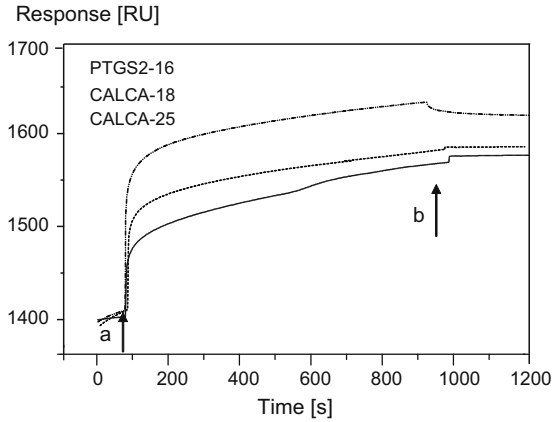

Fig. 1. Adsorption of (a) DMT-S-S-ssDNA PTGS2-16, CALCA-18, CALCA-25 probes on gold in the order of up to down. Rinsing with buffer is denoted by (b).

3. Results and discussion

3.1. Adsorption of ssDNA and post-treatment with blocking agent

Oligonucleotide surfaces are normally produced by adsorbing the probes for 12–16 h and post-treating the layer with MCH [8,11,15]. SPR shows that adsorption of DMT-S-S-ssDNA on gold is very fast (Fig. 1). Saturation coverage was obtained within a measuring time of 10–15 min. Thiol-modified probes had the same kinetics. When DMT-S-S-PTGS2-16 ssDNA was adsorbed on the gold surface a response of 1850 ± 100 RU was observed (Table 2). This corresponds to $2.2 \pm 0.1 \times 10^{13}$ probes/cm^2, which is half of the value reported for the maximum probe coverage of a 20-mer probe adsorbed for 5 h from a 1 μM solution [31]. Post-treatment of the surface with lipoamide (Lipa-DEA or Lipa-TRIS, Scheme 2)

Table 2
The response and probe density when adsorbing ssDNA of various probe-length on the gold surface and post-treating the surface with blocking agent. Non-specific binding of 1.5 μM BSA and 0.1 μM complementary DNA binding. Number of replicas is at least 4.

ssDNA	ssDNA (RU)	Probe density (10^{13} probes/cm^2)	Blocker (RU)	BSA (RU)	Comp-DNA (RU)	Comp-DNA density (10^{12} molecules/cm^2)
DMT-S-S-CALCA-18	2200 ± 100	2.6 ± 0.1	1500 ± 120	20 ± 5	270 ± 10	3.0 ± 0.1
DMT-S-S-CALCA-25	1920 ± 200	1.5 ± 0.2	980 ± 110	10 ± 5	430 ± 10	3.0 ± 0.1
SH-CALCA-25	1460 ± 50	1.1 ± 0.05	1260 ± 150	70 ± 80	300 ± 20	2.2 ± 0.2
DMT-S-S-PTGS2-16	1850 ± 100	2.2 ± 0.1	1350 ± 120	150 ± 70	230 ± 20	2.9 ± 0.2
DMT-S-S-PTGS2-27	1430 ± 50	1.0 ± 0.1	1450 ± 60	110 ± 20	360 ± 30	2.7 ± 0.2
SH-PTSG2-27	1400 ± 200	1.0 ± 0.2	1475 ± 70	110 ± 30	410 ± 30	3.0 ± 0.2

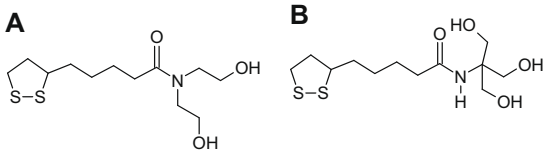

Scheme 2. Structures of the lipoamide blocking agents: (A) Lipa-DEA and (B) Lipa-TRIS.

caused an additional increase in response of 1350 ± 120 RU (Table 2). There was no remarkable difference between the lipoamides. The disulfide-modified and thiol-modified PTGS2-27 ssDNA gave a response of 1400 ± 200 RU ($1.0 \pm 0.2 \times 10^{13}$ probes/cm^2). This value was much lower than that observed for the other probes, but is in agreement with the probe density of 1.1×10^{13} probes/cm^2 reported by Peterson et al. [11]. Post-treatment of the thiol-modified PTGS2-27 ssDNA-surface with Lipa-DEA gave an additional response of 1475 ± 70 RU. The amount was thus only slightly larger than that adsorbed on the DMT-S-S-PTGS2-16 surface. Post-treatment with blocking agents replaces ssDNA probe molecules gradually. After 5 h about half of the probes are displaced [31]. In our case the post-treatment time was only 15 min and much fewer probes are to be displaced. The surface density of closely-packed ssDNA strands with an estimated cross-sectional radius of 0.6–0.7 nm/strand oriented normal to the surface is about 8×10^{13} probes/cm^2, excluding effects of counter ions and hydration [14]. The PTGS2-27 probes take up 12.5% of a monolayer if the displacement due to blocking agent is not taken into account.

The DMT-S-S-CALCA-18 probe showed a response of 2200 ± 100 RU, with a probe density ($2.6 \pm 0.1 \times 10^{13}$ probes/cm^2) somewhat higher than that of PTGS2-16 ssDNA ($2.2 \pm 0.1 \times 10^{13}$ probes/cm^2). The CALCA-25 ssDNA showed a much lower response corresponding 1.5 ± 0.2 and $1.1 \pm 0.05 \times 10^{13}$ probes/cm^2 for the disulfide-modified and thiol-modified probes, respectively (Table 2). The additional response on post-treatment of the layers with lipoamide gave a response between 980 and 1260 ± 50 RU. There seems to be a clear difference in surface coverage between the shorter (16–18 mer) probes compared to the longer (25–27 mer) probes. The longer probes showed a much lower surface coverage ($1.0–1.5 \pm 0.2 \times 10^{13}$ probes/cm^2) than the shorter probes ($2.2–2.6 \pm 0.1 \times 10^{13}$ probes/cm^2). Thus the longer probes seem to be adsorbed on the surface through several base groups with a less-efficient surface coverage.

3.2. Non specific binding of BSA and non-complementary DNA binding

Only low amounts of BSA adsorbed onto disulfide-modified 18 and 25 mer CALCA layers. Non specific binding (NSB) of BSA was higher to the SH-CALCA-25 (70 ± 80 RU) layer and even higher to the disulfide- and thiol-modified 16–27 mer PTGS2 surfaces (Table 2). This might be due to the longer probe-length. There was a very low non-complementary DNA binding to the layers. Somewhat higher non-specific binding was observed to the Lipa-TRIS layer than to the Lipa-DEA for which even a negative response was observed (data not shown).

3.3. Hybridization of 16–27 mer probe surfaces with complementary strands

Binding of complementary DNA at a concentration of 0.1 μM to a surface functionalized with DMT-S-S-CALCA-25 ssDNA and post-treated with Lipa-DEA gave a response of 430 ± 10 RU that is $3.0 \pm 0.1 \times 10^{12}$ strands/cm^2 (Table 2). This response is comparable with that of complementary binding to DMT-S-S-CALCA-18 and DMT-S-S-PTGS2-16 probe surfaces post-treated with the blocking molecules. After regeneration of the layer complementary DNA could be bound with a slightly higher response (470 ± 20 RU). The higher response was most probably due to NSB as an additional subsequent regeneration of the layer and a binding of BSA gave a response of 60 ± 30 RU. There was also a higher binding of non-comp DNA to the regenerated layer (20 ± 5 RU).

A DMT-S-S-PTGS2-16 ssDNA layer post-treated with blocking agent showed a response of 260 ± 20 RU when hybridized with the complementary strand at a concentration of 0.2 μM. After two subsequent regenerations of the layer the response was somewhat higher and remained at 300 ± 15 RU after several regeneration/hybridization cycles. Hybridization of the corresponding DMT-S-S-CALCA-18 ssDNA and Lipa-DEA layer showed a hybridization response of 300 ± 10 RU. Complementary CALCA have a sequence longer than that of DMT-S-S-PTGS2-16 and consequently a higher hybridization would be expected. There was only a minor difference between the blocking molecules with Lipa-TRIS giving a somewhat higher response (320 ± 10 RU). The difference in hybridization response agrees exactly with the length of the strands. The response is also comparable with that of comp DNA previously studied if the length of the complementary strand is taken into account [18]. The complementary hybridization corresponds to $3.0 \pm 0.1 \times 10^{12}$ strands/cm^2. This accounts for a hybridization efficiency of about 10% if the displacement of probes from the surface is not taken into account.

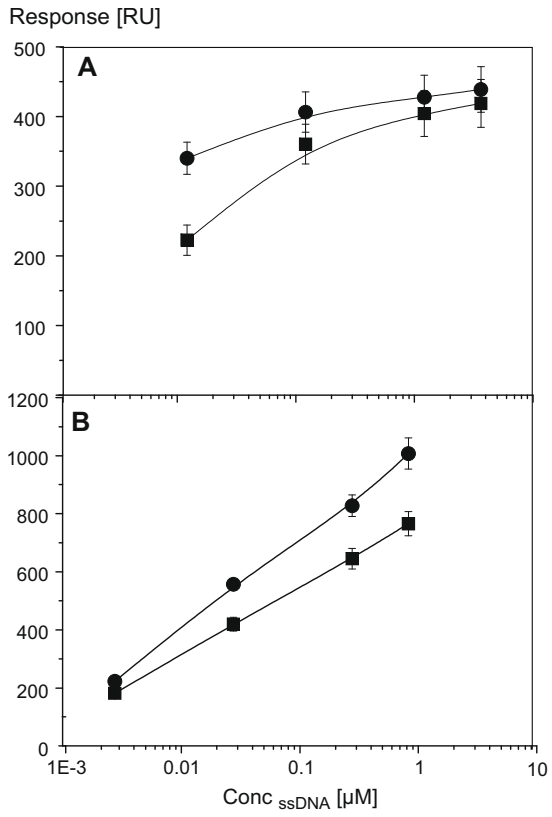

Fig. 2. Binding of (A) complementary DNA and (B) ssDNA PCR amplicons to monolayers composed of PTGS2-27 SH-ssDNA (●) and DMT-S-S-PTGS2-27 ssDNA (■) post-treated Lipa-DEA. The layers were tested for NSB of BSA and non-complementary binding of DNA. Number of replicas = 4.

Fig. 2A shows complementary DNA binding to monolayers of disulfide-modified and thiol-modified PTGS2-27 ssDNA formed by post-treatment with Lipa-DEA. At a concentration of 10 nM the PTGS2-27 DMT-S-S-ssDNA layer gave a response of 210 ± 20 RU whereas the response for the PTGS2-27 SH-ssDNA was 320 ± 20 RU. The higher response of the thiol-modified oligos indicates that they have a more end-on orientation on the surface offering better binding of complementary oligos. When the analyte concentration rises and the surface reaches saturation the effect is diminished showing not much difference in the maximal binding capacity of the surface. The response increased with concentration to about 425 ± 30 RU at saturation for both the surfaces, which corresponds to $3.1 \pm 0.1 \times 10^{12}$ strands/cm^2.

3.4. Hybridization with double and single stranded PCR products

The binding of single stranded PCR amplified products with a base pair length of 344–624 to layers of CALCA-18 and PTGS2-16 ssDNA was very low and in the range of 10 ± 5 RU even if the concentration was raised to 10 nM (data not shown). The low response was most probably due to the length of the amplicons forming the secondary structures. Long strands of DNA might coil into blobs in non-denaturing conditions like in this study and make hybridization very difficult and energetically unfavourable.

In order to study the influence on the length of the PCR product, amplicons with a shorter base length was applied (92–123 base pairs). The response of normal double stranded product was studied as a reference to that of hybridization with a single stranded product. When running the normal double stranded PCR product on a thiol- or disulfide modified surface the responses were very small (data not shown). Hybridization of ds PCR products of PTGS2 up to 40 nM with the thiol-modified PTGS2-27-oligo layer resulted in a response of only 33 ± 4 RU. The corresponding surface composed of the disulfide-modified PTGS2-27-probe showed a response of 130 ± 25 RU.

Hybridization of the CALCA-25 SH-ssDNA layer post-treated with Lipa-DEA with a single stranded PCR product with a length of 92 base pairs at a concentration of 0.8 μM resulted in a response of 820 ± 150 RU that is $1.7 \pm 0.1 \times 10^{12}$ strands/cm^2. After regeneration of the layer an amount corresponding to 610 ± 100 RU could be re-hybridized. Saturation of the hybridization was not reached at this ssDNA concentration. The CALCA-25 single stranded PCR product showed a response of 1270 ± 20 RU on hybridization to a DMT-S-S-ssDNA layer at a concentration of 1.5 μM. This response corresponds to $2.7 \pm 0.1 \times 10^{12}$ strands/cm^2 and is comparable to that of the complementary strand.

The binding of the single stranded PCR product to the disulfide-modified and thiol-modified PTGS2-27 surface was in the same range at lower concentrations but increased to 780 and 1000 ± 20 RU, respectively at higher concentrations (Fig. 2B). Thus also very high responses could be obtained with probes adsorbed on the surface through the disulfide-group. The amount of strands hybridized was 1.2 and $1.6 \pm 0.1 \times 10^{12}$ strands/cm^2 for the disulfide-modified and thiol-modified PTGS2 probes, respectively. This agrees with the amount obtained for the CALCA-25 SH-ssDNA surface. A 30% higher degree of hybridization could thus be obtained with the thiol-modified compared to the disulfide-modified probes.

4. Conclusions

Single-stranded oligonucleotides adsorb within 15 min on the gold surface. The adsorption is related to the length of the probe. Short probes with a base pair length of 16–18-mer show a higher surface coverage and are thus standing more end-on than probes with a length of 25–27-mer. Longer probes seem to be adsorbed through several base pairs. The shorter probes take a more end-on orientation. A somewhat higher non-specific binding was observed to the Lipa-TRIS than to the Lipa-DEA layer. No non-complementary binding was observed to the layers. Several regeneration/hybridization cycles could be performed. A very low response was obtained for hybridization with PCR amplified products above 300 base pairs long. If amplicons with a length about 100 base pairs was used the hybridization response was much higher and in agreement with that of the complementary binding. Thiol-modified oligos showed a 30% higher hybridization response to the PCR amplified products than the DMT disulfide-modified.

Our results clearly demonstrate that short, single stranded PCR products might serve as exact and sensitive analytes in label-free diagnostics. The selectivity in the measurement and the markeŕs identity can be obtained through the amplified sequence and the sensitivity in the measurement comes from the efficient pairing of the single stranded product with the chosen probe on the surface. These results could be useful for example in faster label-free cancer diagnostics.

Acknowledgment

The research has been funded by the European Community FP6 program (Biognosis No. 016467). We thank Dr. Leif Kronberg from Åbo Akademi University, Turku, Finland for the mass spectra.

References

[1] M. Ferrari, L. Cremonesi, P. Carrera, P.A. Bonini, Clin. Biochem. 29 (1996) 201.
[2] M.J. Morales, D.I. Gottlieb, Anal. Biochem. 210 (1993) 188.
[3] J.A. Schumacher, K.S.J. Elenitoba-Johnson, M.S. Lim, J. Clin. Pathol. 61 (2008) 109.
[4] F. Foulet, F. Botterel, P. Buffet, G. Morizot, D. Rivollet, M. Deniau, F. Pratlong, S. Bretagne, J. Clin. Microbiol. 45 (2007) 2110.
[5] T.T. Nikiforov, Y.H. Rogers, Anal. Biochem. 227 (1995) 201.
[6] F.N. Rehman, M. Audeh, E.S. Abrama, P.W. Hammond, M. Kenney, T.C. Boles, Nucleic Acids Res. 27 (1999) 649.
[7] C.M. Nimyer, L. Boldt, B. Ceyhan, D. Blohm, Anal. Biochem. 268 (1999) 54.
[8] T. Herne, M. Tarlov, J. Am. Chem. Soc. 119 (1997) 8916.
[9] J.H. Kim, J. Hong, M. Yoon, M.Y. Yoon, H.S. Juong, H. Hwang, J. Biotechnol. 96 (2002) 213.
[10] Y.H. Rogers, P. Jiang-Baucom, Z.J. Huang, V. Bogdanov, S. Anderson, M. Boyce-Jacino, Anal. Biochem. 266 (1999) 23.
[11] A.W. Peterson, L.K. Wolf, R.M. Georgiadis, J. Am. Chem. Soc. 124 (2002) 14601.
[12] F. Lucarelli, G. Marrazza, A. Turner, M. Mascini, Biosens. Bioelectron. 19 (2004) 515.
[13] V. Dugas, G. Depret, Y. Chevalier, X. Nesme, E. Souteyrand, Sens. Actuators B Chem. 101 (2004) 112.
[14] A. Steel, R. Levicky, T. Herne, M. Tarlov, Biophys. J. 79 (2000) 975.
[15] A. Steel, T. Herne, M. Tarlov, Bioconjug. Chem. 10 (1999) 419.
[16] A. Opdahl, D.Y. Petrovykh, H. Kimura-Suda, M. Tarlov, L. Whitman, Proc. Natl. Acad. Sci. USA 104 (2007) 9.
[17] I. Vikholm-Lundin, R. Piskonen, W.M. Albers, Biosens. Bioelectron. 22 (2007) 1323.
[18] I. Vikholm-Lundin, R. Piskonen, R. Sens. Actuators B Chem. 134 (2008) 189.
[19] K. Tappura, I. Vikholm-Lundin, W.M. Albers, Biosens. Bioelectron. 22 (2007) 912.
[20] I. Vikholm, Sens. Actuators B Chem. 106 (2005) 311.
[21] I. Vikholm-Lundin, Langmuir 21 (2005) 6473.
[22] I. Vikholm-Lundin, W.M. Albers, Biosens. Bioelectron. 21 (2006) 1141.
[23] M. Widschwendter, H. Fiegl, D. Egle, E. Mueller-Holzner, G. Spizzo, C. Marth, D.J. Weisenberger, M. Campan, J. Young, I. Jacobs, P.W. Laird, Nat. Genet. 39 (2007) 157.
[24] B. Meric, K. Kerman, G. Marrazza, I. Palchetti, M. Mascini, M. Ozsoz, Food Control 15 (2004) 621.
[25] Y.K. Ye, J.H. Zhao, F. Yan, Y.L. Zhu, H.X. Ju, Biosens. Bioelectron. 18 (2003) 1501.
[26] F. Azek, C. Grossiord, M. Joannes, B. Limoges, P. Brossier, Anal. Biochem. 284 (2000) 107.
[27] I. Mannelli, M. Minunni, S. Tombelli, M. Mascini, Biosens. Bioelectron. 18 (2003) 129.
[28] T. Jiang, M. Minunni, P. Wilson, J. Zhang, A.P.F. Turner, M. Mascini, Biosens. Bioelectron. 20 (2005) 1939.
[29] M.F. Hagan, A.K. Chakraborty, J. Chem. Phys. 120 (2004) 4958.
[30] <http://www.biacore.com>.
[31] P. Gong, C. Lee, L.J. Gamble, D.G. Castner, D.W. Grainger, Anal. Chem. 78 (2006) 3326.

Series title and number
VTT Science 33

Title	**Biofunctionalised surfaces for molecular sensing**
Author(s)	Sanna Auer
Abstract	In many application fields, like in biosensors, the sensing biomolecules are immobilized on solid surfaces to enable measuring of very small concentrations of molecules to be analysed. Such application fields are, for example, diagnostics, detection of abused drugs, environmental monitoring of toxins and tissue engineering. This thesis studies the immobilization of biomolecules (antibodies and Fab'-fragments, avidins and oligonucleotide sequences) on gold surfaces in biosensors. In order to achieve high nanomolar sensitivity even in difficult sample matrices, the effect of the sensing molecule immobilization type and concentration within these biomolecular surfaces were studied in detail. The suitability of these surfaces for neuronal stem cell attachment was also one of the topics. Real-time label-free detection was performed with surface plasmon resonance (SPR). The molecular surfaces in this study were constructed of biomolecules and repellent molecules, which formed self-assembled monolayers on gold. The molecules were immobilized on surfaces via reactive thiol- or disulphide groups. On surfaces assembled of proteins, the non-specific binding was minimized by hydrophilic polymer molecules and on surfaces assembled of oligonucleotides by means of lipoate molecules embedded on the surface in between the biomolecules, respectively. With these highly sensitive biomolecular surfaces, a nanomolar detection of small sized molecules such as the 3,4-methylenedioxymethamphetamine (MDMA) drug was achieved. MDMA was analysed from a difficult sample matrix of diluted saliva. Improved orientation of surface immobilized Fab'-fragments leading to a higher sensitivity was shown with surfaces constructed of cys-tagged avidins: Fab'-fragments immobilized via thiol-biotinylation to a surface constructed of cys-tagged avidins bound almost ten times the amount of antigen when compared to a conventional surface constructed of non-oriented wild-type avidins. Polymer molecules embedded in between the biomolecules efficiently reduced non-specific binding. Selective neuronal cell attachment was also shown with polymer and neuronal-specific antibody molecules physisorbed on cell culture plates. Only the differentiated neuronal cells attached to surfaces physisorbed with neuronal-specific antibodies, while the non-differentiated neurospheres did not. Selective surfaces were also developed for oligonucleotide sequences. Lipoate-based molecules efficiently reduced the non-specific binding of proteins and non-complementary DNA. A nanomolar detection range was achieved for single-stranded, breast cancer-specific polymerase chain reaction (PCR) products. First, the shorter single-stranded PCR-products were analysed and a nanomolar detection range was achieved in buffer. In the following study, the DNA-surfaces were analysed in the presence of diluted serum. Even in diluted serum matrix, nanomolar concentrations of longer single- stranded sequences could be analysed due to the efficient blocking of non-specific binding of serum proteins. It was found that sensitive detection surfaces for biomolecular recognition can be achieved, when optimal function of the biomolecules is ensured by immobilizing the molecules on surfaces in an oriented manner towards the analyte. Efficient reduction of non-specific binding is also important in reaching highly sensitive label-free detection. The surfaces were also found to be effective in selective neuronal stem cell attachment.
ISBN, ISSN	ISBN 978-951-38-8001-9 (Soft back ed.) ISBN 978-951-38-8002-6 (URL: http://www.vtt.fi/publications/index.jsp) ISSN-L 2242-119X ISSN 2242-119X (Print) ISSN 2242-1203 (Online)
Date	June 2013
Language	English, Finnish abstract
Pages	76 p. + app. 46 p.
Keywords	Antibody, Fab´-fragment, cysteine tagged avidin, neuronal cells, DNA hybridisation, gold surface, immobilisation, surface plasmon resonance, non-specific binding
Publisher	VTT Technical Research Centre of Finland P.O. Box 1000, FI-02044 VTT, Finland, Tel. 020 722 111

Julkaisun sarja ja numero
VTT Science 33

Nimeke	**Biofunktionalisoidut pinnat molekyylien määrityksessä**
Tekijä(t)	Sanna Auer
Tiivistelmä	Monilla sovellusalueilla, kuten bioantureissa, tietylle analyytille herkät biomolekyylit kiinnitetään kiinteälle pinnalle, mikä mahdollistaa hyvin pienten analyyttipitoisuuksien määrittämisen. Tällaisia sovellusalueita ovat esimerkiksi sairauksien merkkiaineiden määritys, huumausaineiden tai ympäristömyrkkyjen määritys ja kudosteknologia. Tämä väitöskirja käsittelee biomolekyylien (vasta-aineiden ja Fab´-fragmenttien, avidiinien ja deoksiribonukleiinihappo (DNA) -koettimien) kiinnittämistä kultapinnoille bioantureissa. Tunnistavien molekyylien kiinnittämistapaa ja pitoisuutta biomolekulaarisilla pinnoilla tutkittiin yksityiskohtaisesti nanomolaarisen herkkyyden saavuttamiseksi myös vaikeista lähtömateriaaleista. Lisäksi tutkittiin, miten nämä pinnat soveltuvat kantasoluista erilaistettujen hermosolujen tartuttamiseen. Reaaliaikainen määritys ilman leima-aineita tehtiin pintaplasmoniresonanssin (SPR) avulla. Tutkimuksessa käytetyt itseasettuvat kalvot muodostettiin biomolekyyleistä ja hylkivistä molekyyleistä kultapinnoille. Molekyylit kiinnitettiin pinnoille tioli- tai disulfidiryhmien kautta. Proteiinipinnoilla epäspesifistä sitoutumista vähennettiin hydrofiilisten polymeerien avulla ja DNA-koetinpinnoilla vastaavasti lipoaattipohjaisten molekyylien avulla, jotka oli asetettu pinnoilla biomolekyylien väliin. Biomolekulaaristen pintarakenteiden avulla pystyttiin mittaamaan myös pienikokoinen 3,4-dimetyleenidioksimetyyliamfetamiini (MDMA) -huumausaine nanomolaarisessa pitoisuudessa. MDMA pystyttiin määrittämään myös laimennetusta sylkinäytteestä. Kysteiinimuokattujen avidiinipintojen avulla pystyttiin parantamaan Fab´-fragmenttien orientaatiota pinnoilla, mikä johti tavoiteltuihin, korkeampiin antigeenivasteisiin. Tioli-ryhmiin biotinyloituja Fab´-fragmentteja pystyttiin kiinnittämään kysteiinimuokattuihin avidiinipintoihin kymmenkertainen määrä verrattuna villityypin ei-orientoituihin avidiinipintoihin. Biomolekyylien väliin pinnoille kiinnitetyt polymeerimolekyylit ehkäisivät tehokkaasti epäspesifistä sitoutumista. Kun hermosolujen kasvatuslevyille kiinnitettiin polymeeriä ja hermosoluille spesifisiä vasta-ainemolekyylejä, levyille saatiin tarttumaan valikoidusti vain kantasoluista erilaistuneita hermosoluja. Kantasoluista erilaistumattomat solut eivät kiinnittyneet vasta-ainepolymeeripinnoille. Valikoivia pintoja kehitettiin myös DNA-koettimille. Proteiinien ja ei-pariutuvan DNA:n epäspesifinen sitoutuminen DNA-koetinpinnoille pystyttiin ehkäisemään tehokkaasti lipoaattipohjaisten molekyylien avulla. Yksijuosteiset rintasyöpä-spesifiset DNA-juosteet pystyttiin tunnistamaan nanomolaarisella herkkyydellä. Ensin tutkittiin lyhyiden yksijuosteisten DNA-näytteiden tunnistusta puskuri-liuoksessa saavuttaen nanomolaarinen herkkyys. Seuraavaksi DNA-pintojen toiminnallisuutta tutkittiin seerumiin laimennetuilla näytteillä. Myös pidempiä yksijuosteisia DNA-näytteitä pystyttiin määrittämään nanomolaarisina pitoisuuksina seerumilaimennoksesta, koska lipoaattipohjaiset molekyylit estivät tehokkaasti seerumin proteiinien epäspesifisen sitoutumisen pinnoille. Biomolekyylien määritykseen pystytään tekemään herkästi tunnistavia pintoja, kunhan biomolekyylien optimaalinen toiminta varmistetaan kiinnittämällä biomolekyylit pinnoille siten, että analyytin tunnistavat osat ovat orientoituneet analyyttiä kohden. Myös epäspesifisen sitoutumisen estäminen pinnoille on tärkeää korkean herkkyyden saavuttamiseksi leimavapaissa mittauksissa. Vasta-aine-polymeeripinnat todettiin hyvin toiminnallisiksi myös haluttaessa tartuttaa pinnoille valikoiden vain hermosoluja.
ISBN, ISSN	ISBN 978-951-38-8001-9 (nid.) ISBN 978-951-38-8002-6 (URL: http://www.vtt.fi/publications/index.jsp) ISSN-L 2242-119X ISSN 2242-119X (painettu) ISSN 2242-1203 (verkkojulkaisu)
Julkaisuaika	Kesäkuu 2013
Kieli	Englanti, suomenkielinen tiivistelmä
Sivumäärä	76 s. + liitt. 46 s.
Avainsanat	Antibody, Fab´-fragment, cysteine tagged avidin, neuronal cells, DNA hybridisation, gold surface, immobilisation, surface plasmon resonance, non-specific binding
Julkaisija	VTT PL 1000, 02044 VTT, Puh. 020 722 111

Biofunctionalised surfaces for molecular sensing

This thesis studies the immobilization of biomolecules (antibodies and Fab'-fragments, avidins and oligonucleotide sequences) on gold surfaces in biosensors. The effect of the sensing molecule immobilization type and concentration within these biomolecular surfaces were studied in detail. Real-time label-free detection was performed with surface plasmon resonance (SPR).

The results of this thesis can be applied (apart from in SPR biosensors) in diagnostics, environmental monitoring of toxins, tissue engineering and in detection of abused drugs: with these highly sensitive biomolecular surfaces, a nanomolar detection of small sized molecules such as the 3,4-methylenedioxymethamphetamine (MDMA) drug was achieved and detected in diluted saliva. Selective neuronal cell attachment was also shown with surfaces physisorbed with polymer and neuronal-specific antibody molecules. Sensitive surfaces were also developed for oligonucleotide sequences and a nanomolar detection range was achieved for single-stranded, breast cancer-specific DNA products in diluted serum matrix.

It was found that sensitive detection surfaces for biomolecular recognition can be achieved, when optimal function of the biomolecules is ensured by immobilizing the molecules on surfaces in an oriented manner towards the analyte. Efficient reduction of non-specific binding is also important in reaching highly sensitive label-free detection.

ISBN 978-951-38-8001-9 (Soft back ed.)
ISBN 978-951-38-8002-6 (URL: http://www.vtt.fi/publications/index.jsp)
ISSN-L 2242-119X
ISSN 2242-119X (Print)
ISSN 2242-1203 (Online)